LINKING SULFUR METABOLISM TO THE CELL DIVISION MACHINERY IN YEAST

A Dissertation

by

HEIDI MARIE BLANK

Submitted to the Office of Graduate Studies of
Texas A&M University
in partial fulfillment of the requirements for the degree of

DOCTOR OF PHILOSOPHY

December 2009

Major Subject: Biochemistry

LINKING SULFUR METABOLISM TO THE CELL DIVISION MACHINERY IN YEAST

A Dissertation

by

HEIDI MARIE BLANK

Submitted to the Office of Graduate Studies of
Texas A&M University
in partial fulfillment of the requirements for the degree of

DOCTOR OF PHILOSOPHY

Approved by:

Chair of Committee,	Michael Polymenis
Committee Members,	Mary Bryk
	Sumana Datta
	Donald Pettigrew
Head of Department,	Gregory Reinhart

December 2009

Major Subject: Biochemistry

ABSTRACT

Linking Sulfur Metabolism to the Cell Division Machinery in Yeast. (December 2009)

Heidi Marie Blank, B.S., Southern Methodist University

Chair of Advisory Committee: Dr. Michael Polymenis

The longstanding view has been that metabolism allows for cell division to take place, but that metabolic processes do not actively promote cell division. I have recently challenged this notion by identifying a unique gain-of-function metabolic mutant in the budding yeast *Saccharomyces cerevisiae*. Moderate over-expression of Abf2p, a conserved mitochondrial DNA (mtDNA) maintenance protein, increases the amount of mtDNA by 100-150%. I have shown that cells moderately over-expressing Abf2p can out-proliferate their wild type (WT) counterparts, initiate DNA replication sooner, and increase in size faster than WT cells.

Yeast grown under certain conditions in continuous cultures become synchronized with respect to their oxygen consumption, displaying distinctive oxidative and reductive phases. In cells over-expressing Abf2p, the reductive phase is expanded compared to that of WT cells. Since glutathione, the cell's main redox buffer and sulfur containing metabolite, peaks during this phase, I asked if sulfur metabolism was altered in cells with more mtDNA.

Sulfur metabolite levels are *increased* ~40% in cells over-expressing Abf2p. Furthermore, exogenous addition of various sulfur containing compounds, which is

known to increase sulfur metabolic flux, caused WT cells to increase in size faster and initiate DNA replication sooner, mimicking the phenotype seen in cells moderately over-expressing Abf2p.

I then investigated possible interactions between sulfur metabolism enzymes and the yeast Cdk, Cdc28p. Performing co-immunoprecipitation experiments, two enzymes of the sulfur metabolic pathway were found to bind Cdc28p. One of these, Cys4p, lies at the critical junction point between the pathways leading to the formation of glutathione versus one carbon metabolism. The interaction of the enzymes with Cdc28p appears to be dependent on progression through the cell cycle, and preliminary evidence suggests that Cdc28p/Cys4p binding may peak at the G1/S transition of the cell cycle.

In summary, I have identified a unique gain-of-function metabolic mutant in *S. cerevisiae* that leads to accelerated initiation of DNA replication. Sulfur metabolic flux is up-regulated in cells over-expressing Abf2p, and exogenous sulfur sources added to WT cultures phenocopied cells over-expressing Abf2p. Most importantly, I have shown a physical interaction between sulfur metabolic enzymes and the Cdk driving the cell cycle in yeast.

DEDICATION

I dedicate this dissertation to my parents, Jack and Margaret Finke, who have always been supportive throughout my life, and to the many other family and friends who have given me guidance over the years. A special thanks to my husband, Jason, and son, Connor, who have been very patient and understanding throughout this process. I also dedicate this dissertation to my undergraduate advisor and professor, Dr. Edward Forest, without whose encouragement and teaching I would have never pursued a research career.

ACKNOWLEDGEMENTS

I would like to thank my committee members, Dr. Mary Bryk, Dr. Suma Datta, and Dr. Don Pettigrew, for their guidance and support throughout my tenure as a graduate student at Texas A&M. I would especially like to thank my committee chair, Dr. Michael Polymenis, for all of his help and guidance and being an exceptional mentor over the past several years.

I wish to thank members of the Polymenis lab, both past and present, for their help and friendship. I wish to thank the Bryk lab for always being willing to help me with technical questions and experiments, and the Young lab for repeated use of their equipment. Thanks also go to my friends and colleagues and the department faculty and staff for making my time at Texas A&M University a great experience. The staff in this department have always been friendly and more than willing to help out in whatever way they can. My friends in the department have been not only a source of information for research but have been vital to making my experience here both memorable and enjoyable.

Finally, thanks to my husband for his encouragement, patience, and love.

Additionally, I wish to acknowledge the following people and organizations for specific chapters of this dissertation.

Chapter II: This paper is dedicated to the memory of Ron Butow. We thank R. Butow and G. Shadel for strains and plasmids, R. Butow and B. Kennedy for

discussions, D. Pettigrew for advice and encouragement, and J. Kapler and D. Pettigrew for comments on the manuscript.

Chapter III: We thank B. Tu for strains, J. Mueller for help with metabolite analysis, M. Bryk for help with tetrad dissections, and D. Pettigrew for advice and encouragement. We also thank B. Baxter, S. Joseph, C. Vargas, and A. Rife for technical assistance. This work was supported by grants from the National Institutes of Health and the National Science Foundation to M. Polymenis.

TABLE OF CONTENTS

Page

ABSTRACT iii

DEDICATION v

ACKNOWLEDGEMENTS vi

TABLE OF CONTENTS viii

LIST OF FIGURES x

CHAPTER

I INTRODUCTION 1

Historical Perspective on Cell Division 1
Coordination of Cell Growth and Division 10
Chemostats and Metabolic Oscillations 16
Mitochondrial DNA Maintenance 24

II AN INCREASE IN MITOCHONDRIAL DNA PROMOTES NUCLEAR DNA REPLICATION IN YEAST 28

Overview 28
Introduction 29
Results and Discussion 32
Materials and Methods 50

III SULFUR METABOLISM ACTIVELY PROMOTES INITIATION OF CELL DIVISION IN YEAST 55

Overview 55
Introduction 55
Results and Discussion 57
Materials and Methods 68

CHAPTER Page

IV SULFUR ENZYMES AND PHYSICAL INTERACTION WITH THE CELL DIVISION MACHINERY 71

Overview 71
Introduction 72
Results and Discussion 74
Materials and Methods 86

V CONCLUSION 91

REFERENCES 98

APPENDIX A 108

APPENDIX B 115

APPENDIX C 122

VITA 125

LIST OF FIGURES

FIGURE		Page
1.1	General schematic of cell cycle progression	3
1.2	G1/S gene transcription is controlled by two regulatory complexes, SBF and MBF	14
1.3	Yeast metabolic oscillation	17
1.4	Key enzymes and metabolites of sulfur metabolism	21
2.1	Cells moderately over-expressing *ABF2* proliferate faster, and have altered cell cycle progression in chemostat cultures.	31
2.2	*3xABF2*$^{+}$ cells do not have altered cell size in chemostat cultures.	33
2.3	Moderate over-expression of *ABF2* does not trigger the RTG response	34
2.4	Over-expression of *ABF2*, or loss of *SIR2*, accelerates DNA replication	37
2.5	Sic1p stability and Abf2p	38
2.6	mtDNA is required for the accelerated DNA replication in *3xABF2*$^{+}$ cells	40
2.7	Loss of *SIR2* in cells over-expressing *ABF2* dramatically accelerates DNA replication when NADH is depleted	43
2.8	Loss of Sir2p does not accelerate overall cell proliferation	45
2.9	Cells over-expressing *ABF2* have less Sir2p and higher levels of K9, K14 acetylated histone H3 at the rDNA ARS elements	46
2.10	A schematic of the model suggested by our data: An increase of mtDNA by moderate over-expression of Abf2p promotes mitochondrial functions, which in turn accelerate cell proliferation and DNA replication	47

FIGURE Page

3.1 An increase in mtDNA levels expands the Yeast Metabolic Cycle 59

3.2 Sulfur metabolite levels are increased in cells with more mtDNA 60

3.3 An increase in sulfur metabolic flux accelerates initiation of cell division 63

3.4 Cys4p(1-353) accelerates initiation of cell division 66

4.1 *CYS4(1-353)* is recessive to *CYS4*$^{+}$ regarding START 75

4.2 Cdc28p binds Cys4p *in vivo* 77

4.3 Cys4p(1-353) binds Cdc28p *in vitro* 78

4.4 hCBS and yeast Cys4p(1-353) interact with human Cdk2/cyclin E complex *in vitro* 81

4.5 Regulation of the Cys4p/Cdc28p interaction 83

4.6 Both subunits of sulfite reductase, Met10p and Ecm17p, interact with Cdc28p *in vivo* 85

CHAPTER I

INTRODUCTION

Historical Perspective on Cell Division

In 1858, Rudolph Virchow formally denounced the idea of spontaneous generation of life by stating that all cells come from pre-existing cells, a tenant that became accepted as part of the Cell Theory. Life on earth is thereby dependent on cellular division, as new organisms could not be formed in the absence of the transmittance of genetic information and cellular components that occurs at each cell division. Depending on the situation, one cell division could lead to the formation of a new single-celled organism, or to the production of tissues and organs that will develop into a new multi-cellular organism. Even in the case of adult plants or animals, cell division is necessary for certain types of tissues to replace dead or damaged cells to maintain the viability of the organism. Aberrant cell division is implicated in a range of diseases, most notably cancer, but also more lately in neurodegenerative diseases such as Alzheimer's (1). Cell division also holds the key to several medical therapies. Normally non-dividing cells might be induced to divide and regenerate damaged tissue which generally has minimal ability to repair itself, such as neuronal or cardiac tissue.

This dissertation follows the style of *Proceedings of the National Academy of Sciences*.

The overall goal of a cell when it undergoes division is to replicate its contents, and then divide these contents equally between the two newly formed daughter cells. It does so in a series of tightly regulated and coordinated events known as the cell cycle. Briefly, the cycle can be divided into distinct phases: S phase, where DNA replication occurs, M phase, where mitosis and cytokinesis occur, and often additional gap phases, known as G1 and G2, which occur between M and S phase and S and M phase, respectively. Progression through the cell cycle is controlled by cyclin-dependent kinases (CDKs), whose activity is regulated by association with proteins called cyclins (Fig. 1.1*A*).

While the cyclin/CDK concept of controlling transitions through the cell cycle phases is well established today, many important discoveries paved the way to provide this understanding. Much of our understanding of the cell cycle stems from different avenues of research, spanning roughly the past forty years, which have propelled the study of the cell cycle to reach the level of understanding that is has today.

The advent of the modern study of how the cell cycle is regulated began primarily with two distinctive lines of work. One utilized the genetic manipulation of various types of yeast, and the other began in oocytes of frogs and marine organisms. Eventually the two would tie back together to make significant progress in the field of cell cycle study.

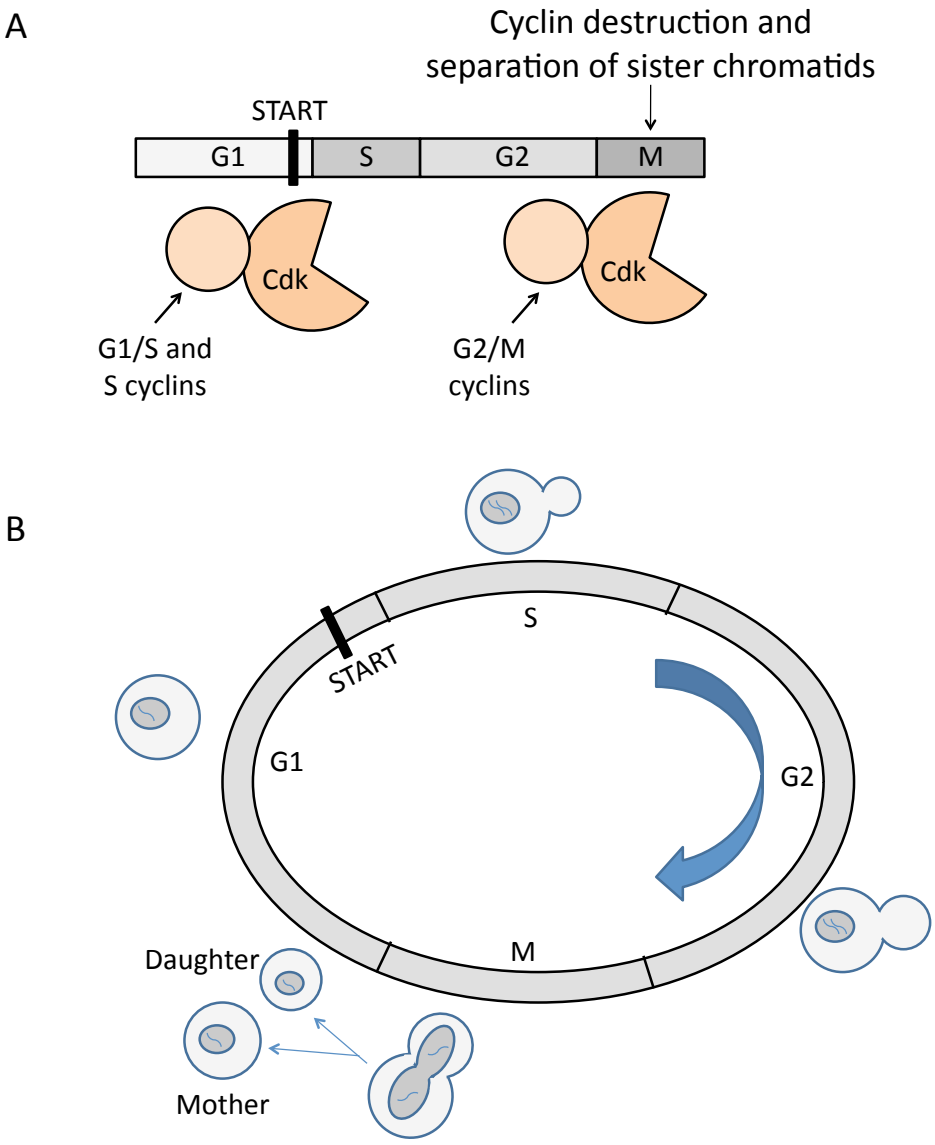

Fig. 1.1. General schematic of cell cycle progression. *(A)* Progression through the cell cycle is controlled by the association of cyclin-dependent kinases (Cdks) with their regulatory subunits called cyclins. Three different transitions are controlled by cyclin/Cdk complexes: the G1 to S transition, the G2 to M transition, and the metaphase to anaphase transition of mitosis, where the destruction of cyclins occurs and Cdk activity drops. *(B)* Progression through the cell cycle as it relates to the morphology of the budding yeast *S. cerevisiae*. Growth of the unbudded cell occurs during G1. Budding and DNA synthesis are initiated, and growth of the bud continues throughout G2 until mitosis and cytokinesis occur. *S. cerevisiae* undergoes an asymmetrical division, resulting in the original, larger mother cell and a new, smaller daughter cell.

Interested in the proliferation of cancer cells, Lee Hartwell picked the budding yeast *S. cerevisiae* as his model organism of choice to study cell division. Not only is it a single celled organism that lends itself to genetic techniques, but it also displays the same cell cycle patterns of higher eukaryotes. In addition, morphological examination of yeast cells provides information as to what phase the cell resides. Cells are initially small and un-budded, grow in size until a bud forms, then growth of the bud continues until it reaches a size close to that of the original cell, and the cell divides into two cells (Fig. 1.1*B*).

In 1970, Hartwell began publishing his work with temperature sensitive yeast mutants used to dissect the gene products required for progression through various stages of the cell cycle. Beginning with a mutagenesis screen, Hartwell identified yeast strains capable of growing at a lower, permissive temperature, but blocked at a higher, non-permissive temperature (2). A small fraction of the temperature sensitive mutants had the characteristic trait that all the cells in the colony were stopped in their growth at the restrictive temperature at the same cellular morphology. Because the shape and size of a yeast cell can be used to determine where it is in the cell cycle, Hartwell postulated that the strains exhibiting this phenotype likely acquired a mutation in a gene involved in the cell division cycle (*cdc*). Examination of the *cdc* mutants under the microscope allowed for the characterization of each cell cycle gene identified in the screen, both the timing of where in the cell cycle the defect first occurred, and at what phase of the cell cycle the cells reached their terminal phenotype.

Further study of his cell division cycle (*cdc*) mutants identified the gene product *cdc28* as a necessary requirement for both bud emergence and initiation of DNA replication. The event START was defined as the early event(s) of the cell cycle required for the two aforementioned pathways to commence (3). Cells passing through START are committed to another round of division and are insensitive to mating factor arrest (4). With the exception of cdc mutants that undergo multiple rounds of the cell cycle, only *cdc28* mutants arrested at a point where they are still able to mate with cells of the opposite mating type (3). Passage through START also required some growth and nutrient conditions be fulfilled, as cells in stationary phase arrest prior to bud emergence and initiation of DNA replication. Stationary phase cells are also still sensitive to mating factor and will arrest if switched to fresh media with mating factor, meaning their arrest is prior to START. Additionally, in chemostat cultures under glucose limiting conditions, generation time correlates with the budding index of the culture population, suggesting that cells delay START under conditions where growth and/or nutrients are limiting (3).

Around the same time that Hartwell began publishing the results of his budding yeast cell cycle screen, Paul Nurse was beginning his postdoctoral work in the United Kingdom to address the question of how cellular reproduction is controlled. Influenced by Hartwell's genetic experiments in *S. cerevisiae*, Nurse spent several months learning fission yeast genetics in Urs Leupold's lab, then joined Murdoch Mitchison's cell cycle lab. Nurse employed a mutagenesis screen tactic similar to that of Hartwell to isolate cdc^- mutants in *S. pombe*, a fission yeast. Using this fungus, he identified cdc^- mutants

as those that were blocked for division at the restrictive temperature and whose shape was abnormally elongated (5).

Twenty-seven recessive temperature sensitive mutants were identified, corresponding to 14 different genes (5). One of these genes, *cdc2*, was also identified as *wee2-1* in a screen designed to identify mutants undergoing mitosis and cell division at a reduced size compared to wild type (6). Because the *wee2-1* mutation affected the timing of mitosis, but the other *cdc* mutants of the same allele were blocked at mitosis, it was now clear that *cdc2* encoded for a protein that was not only required for mitosis, but was also involved in regulation (6).

S. cerevisiae cdc28 and *S. pombe cdc2* both block cells before the completion of START. Because they act at similar phases of the cell cycle, it was thought the gene products might be performing the same function. *CDC28* functionally complemented the *cdc2* mutation in *S. pombe* (7), providing the first evidence that START and regulation of mitosis might be conserved, as they were from two highly diverged fungi. When the human homolog of *cdc2* was cloned by complementation (8), this finding confirmed what scientists had been hoping—that the mechanisms controlling the cell cycle are likely conserved in all eukaryotes, from single celled organisms to humans.

In a scientific world far from yeast, consisting of frogs and sea creatures, important discoveries were also being made that would eventually tie back in with the specific cell cycle work done in yeast. In the 1960s, the idea that some cytoplasmic factor controlled the status of the nucleus during mitosis had been investigated both by nuclear transplantation and cell fusion experiments, which showed that the nucleus

tended to conform to the mitotic state of the host cell. However, a direct experimental approach showing this had not been done until Masui and Markert (9) published their work in 1971. They transferred cytoplasm from stimulated frog oocytes into unstimulated oocytes and saw this was sufficient to cause the resumption of meiosis in the recipient eggs. The resumption of meiosis in the eggs, similar to the G2 to M transition in somatic cells, is also called oocyte maturation. Thus, the cytoplasmic factor responsible for this process was called "maturation promoting factor" or MPF, although its identity as a dimer of cyclin B and cdc2 would remain elusive for seventeen more years.

By the late 1970s, it was well established that upon stimulation of starfish or amphibian oocytes, simulating a G2 to M transition, protein kinase activity and protein phosphorylation is increased (10, 11). In starfish, the phosphorylation levels were shown to be correlated with MPF activity (12). Around the same time, protein synthesis was shown to be required for chromosome condensation and nuclear envelope breakdown to occur, again simulating a G2 to M transition, in sea urchins (13) and for the reappearance of MPF activity in the second meiotic cycle in frog oocytes (14). Then, in 1985, the coordinate oscillation of both MPF and a cAMP-independent histone kinase was shown to depend on protein synthesis and degradation during meiotic maturation of starfish oocytes. From this work, scientists proposed that proteolysis might be responsible for the inactivation of the kinase activity and concomitant drop in MPF activity at the exit from mitosis (15). These types of features showed a notable similarity to the cyclins that Tim Hunt discovered (see below) in 1983.

Tim Hunt, who coined the term "cyclin," discovered cyclin proteins when he was examining protein synthesis patterns in sea urchin eggs that were fertilized by sperm or activated with a calcium ionophore. Surprisingly, levels of one protein oscillated reproducibly upon fertilization. Further investigation of another type of sea urchin and a surf clam showed each had two proteins with reproducible oscillations upon fertilization. The proteins were also shown to be continuously synthesized but degraded rapidly and periodically. They also noted that the degradation seemed to depend on cell division, but had no evidence to say if the converse was also true (16). Hunt commented on the parallels between MPF and the cyclins he discovered, but did not go so far as to claim cyclins were actually a component of MPF.

The link between cyclins, MPF, and kinase activity was strengthened by experiments in clams showing that expressing cyclin A could induce oocyte maturation in the absence of hormonal stimulation, experiments performed in frog eggs, where it was shown that exogenous cyclin mRNA could produce multiple cell cycles and that the new cyclin was degraded at the end of each mitosis, and experiments in cell free extract, where it was shown that destroying cyclin mRNA blocked entry into mitosis (17). These types of experiments provided solid evidence that cyclins were necessary and sufficient for the appearance of MPF activity, and cyclin degradation was required for the disappearance of MPF activity. The kinase activity seemed to have the same requirements as MPF, as kinase activity was always strongly linked with MPF activity.

Purification eventually led to detection of one of the components of MPF to be a homolog of fission yeast Cdc2, a protein kinase required for mitosis in this species, and

conserved from yeast to humans. Cyclins from clams and fission yeast were shown to co-immunoprecipitate with Cdc2, and it was proposed that cyclins could control MPF activity by controlling the phosphorylation status of Cdc2. Finally, in 1989, Labbe et al. (18) purified the M-phase specific kinase activity from starfish oocytes and showed that the activity (and thus MPF) was a heterodimer of one molecule of Cdc2 and one molecule of cyclin B. The fundamental discovery of Cdc2 bound to a cyclin was found to hold true in vertebrates, including mammals. The components of MPF, cyclin B and Cdc2, were later shown to be part of a larger family of cyclins and cdc2-related-kinases that associated with each other at various cell cycle transitions, similar to the function of cyclin B and Cdc2. The discovery of MPF and cyclins paved the way for determining the basic regulation of the cell cycle that exists in all eukaryotes.

While the aforementioned experiments highlight key discoveries that paved the way for cell cycle research, there are many more details that are known about how cells divide. While control of all the cell cycle transitions is important, the G1 to S transition is particularly unusual in that once cells reach the point called START in yeast and the restriction point in animals, the cells are generally committed to another round of division. The commitment to division determines when cells divide, as opposed to how, and determines overall rates of proliferation. The question of when cells divide also addresses the issue of coordinating division with growth and metabolism, a subject where there is currently a lack of understanding of how cells couple these two processes.

Coordination of Cell Growth and Division

Maintaining size homeostasis

While the topics thus far have centered on cell division with a focus on replication of DNA, it is important not to overlook that the entire mass of the cell must double on average every cell cycle in order for the cell to maintain size homeostasis, otherwise the cell would become progressively larger or smaller with each successive division. Cell growth determines not only the size of the individual cell or organism, it also controls body shape, proportioning, and symmetry.

Cell growth is thought to be a continuous process, while DNA synthesis is a discontinuous process (19). Yet cells must obviously coordinate the two processes—this is shown by the narrow size distribution of a particular cell type and the fact that cells disturbed for cell size quickly revert back to their normal size upon removal of the perturbing agent (20). More than 100 years ago, Theodor Boveri and colleagues noted a correlation between cell ploidy and volume (20). Indeed this correlation seems to hold true—in murine and human liver cells, cell ploidy and size are directly correlated (21) and the relationship between ploidy and size of 159 species of vertebrate erythrocytes show a positive allometric relationship (22).

On the most basic level, this coordination could be achieved by cell cycle progression depending on growth, growth depending on cell cycle progression, or a combination of the two. The first mechanism seems to be utilized by most proliferating cells. Blocking growth by limiting nutrients or depleting growth factors typically causes a block in G1 of the cell cycle. Conversely, the second mechanism, where growth would

depend on cell cycle progression, does not seem to be utilized, as cells that are blocked in a particular phase of the cell cycle will often continue to grow to abnormally large sizes. While existing evidence points to the first mechanism as a means of coordinating the two processes of growth and division, evidence of interactions between growth and cell cycle regulators suggests some interconnection of the two processes (20).

As mentioned previously, the question of "when" cells divide determines overall rates of cell division. The fate of a cell in determining if it will undergo a subsequent round of cell division or not is primarily determined at a cell-cycle checkpoint in late G1 known as START in yeast (3) and the restriction point in animals (23). The decision to pass through START commits the cell to irreversible entry into the cell cycle; the entire cycle will be completed even if conditions become unfavorable.

Coordination of growth and division has been best characterized in yeast, which will be the focus of much of the introduction. Yeast cell proliferation is primarily limited by nutrient availability, while animal cells typically have a constant nutrient availability and the decision to divide comes from developmental signals and mitogens. In either cell type, however, the cell must assess its environment in order to make the decision to divide or not. Adding complexity to the issue is the concept of size homeostasis mentioned earlier. A proliferating population must maintain a constant cell size, on average. Thus, growth and division must be coordinated such that when a cell decides to proceed through another round of division, it must also ensure that it has synthesized enough macromolecules and cells do not become progressively larger or smaller as multiple divisions ensue.

START and G1/S gene expression

The commitment to irreversible entry into the cell cycle, START or the restriction point, depends on the activation of the G1/S cyclin-Cdk complexes, which are responsible for initiating early cell cycle events such as spindle pole body (SBP) or centrosome duplication, budding (in yeast), and initiation of DNA replication. Once cells have activated their G1/S cyclin-Cdk complexes and initiated DNA replication, they have already passed through START. What signals bring about the activation of this process? The answer lies in the G1 cyclins, specifically Cln3p in budding yeast and cyclin D in vertebrates. The G1 cyclins do not oscillate in a regular pattern during the cell cycle; instead they increase steadily in response to growth and regulatory signals. Thus, the G1 cyclins are ideally poised to respond to the environment and help cells coordinate growth with the decision to pass through START and commit to another cell division cycle.

In order for cells to initiate DNA replication, a program of approximately 200 G1/S genes must be turned on (Fig. 1.2*A*), providing for expression of both regulatory components (G1/S cyclins Cln1p and Cln2p, and the S cyclins Clb5p and Clb6p) and cell-cycle machinery responsible for carrying out early cell cycle events. Two gene regulatory protein complexes, SBF (SCB-binding factor) and MBF (MCB-binding factor) are responsible for controlling most of this gene expression. SBF and MBF are both heterodimers composed of a distinct DNA-binding protein recognizing distinctive DNA sequences in the promoter region and a regulatory subunit that is the same in both proteins. Outside of G1, expression of these genes must be silenced. For SBF, this

occurs as a result of being bound to an inhibitory protein Whi5p in early G1 to cause transcriptional repression. This inhibition is relieved when Cln3p-Cdc28p activity reaches a high enough level to phosphorylate Whi5p and cause its dissociation from SBF. MBF is thought to repress transcription, with the inhibition being relieved to allow for transcription during G1, and repression occurring again at the G1/S transition due to the binding of the co-repressor Nrm1p (24).

Once MBF and SBF are activated, they trigger the expression of *CLN1* and *CLN2*, the G1/S cyclins, among other genes. Cln1,2p-Cdc28p complexes act in a positive feedback mechanism to further stimulate G1/S gene expression and commit the cells to pass irreversibly through START. Cln1,2p-Cdc28p also acts to trigger the destruction of the Cdc28p inhibitor Sic1p. Sic1p binds to and inhibits Clbp-Cdc28p complexes, thus preventing the activation of the S-cylins, Clb5p and Clb6p. Once Cln1,2p-Cdc28p activity reaches some threshold level, Sic1p is phosphorylated at multiple sites and destroyed, allowing the accumulated Clb5,6p-Cdc28p complexes to become activated and initiate chromosome duplication (Fig. 1.2*B*).

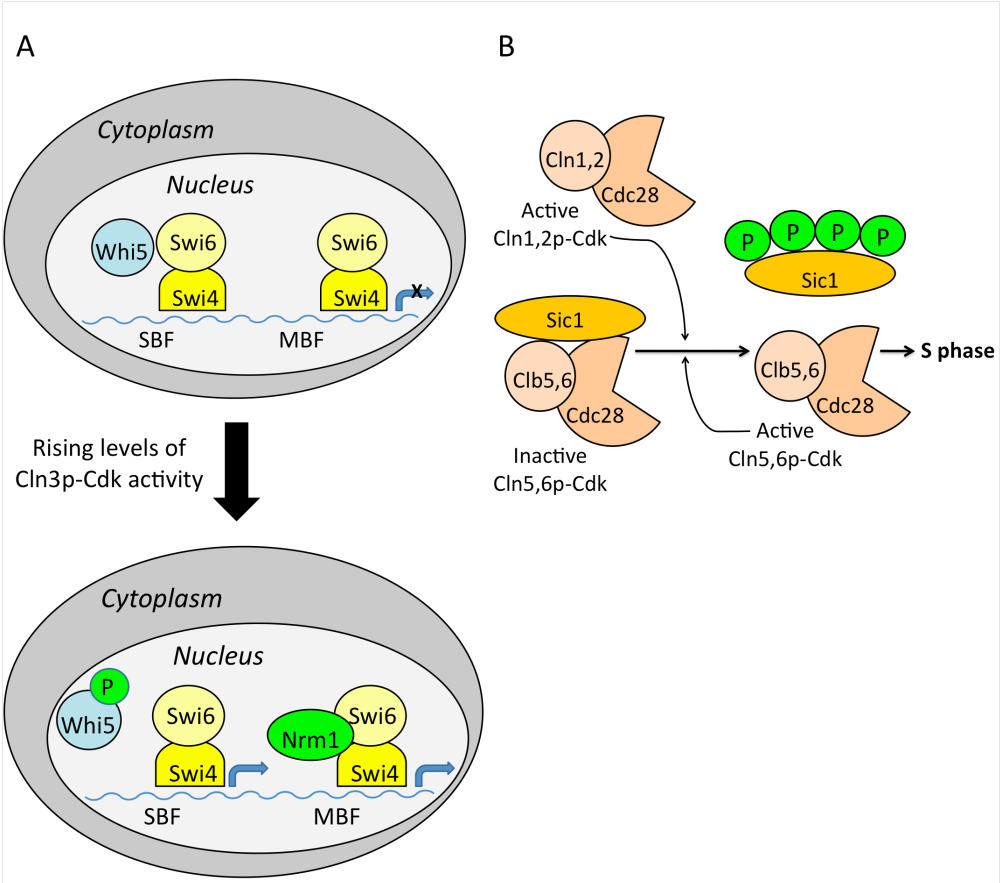

Fig. 1.2. G1/S gene transcription is controlled by two regulatory complexes, SBF and MBF. *(A)* G1/S gene transcription is initially repressed. MBF is transcriptionally repressive, and SBF is inhibited by Whi5p. Rising levels of Cln3p-Cdk activity cause phosphorylation and release of Whi5p inhibition from SBF. Nrm1 binds to and inactivates the repressive activity of MBF. The active transcription factors initiate expression of over 200 G1/S genes, of which two are Cln1p and Cln2p. *(B)* Active Cln1,2p-Cdk complexes phosphorylate Sic1p, an inhibitor of the S cyclins, Clb5p and Clb6p. Phosphorylation of Sic1p causes its release from Clb5,6p-Cdk complexes, which also initiates a positive feedback loop to further activate Clb5,6p-Cdk complexes. Their activation brings about progression into S phase of the cell cycle.

Knowing when to commit to DNA replication

A wealth of information is known about the sequence of events that takes place once Cln3p-Cdk activation leads to eventual G1/S gene expression and DNA replication, yet how a cell knows the correct time to trigger the events that commit it to another round of cell division remains unclear. In order to maintain size homeostasis, growth and division must be coupled. Cells must also reach a threshold size before entering START, yet it remains unclear how cells measure size, be it volume, mass, and/or biosynthetic capacity.

Since Cln3p acts upstream of all known activators of START, it is one likely candidate for being involved in the coordination of growth and division. Multiple mechanisms control Cln3p levels. The 5'-untranslated region of *CLN3* contains an upstream open reading frame, which provides translational control and prevents the accumulation of Cln3p when growth conditions are not favorable (25). Cellular localization is also used to control the levels of Cln3p in the nucleus, as it is retained in the ER until sufficient chaperone production occurs to trigger release from the ER and entry into the nucleus. Since chaperone availability is limiting for Cln3p release, but chaperones are also required for biosynthetic processes, this competition provides the cells an additional way to coordinate nuclear Cln3p levels with growth capacity (26).

Despite playing a role in coordination of growth and division, *CLN3* itself can not fully explain the coordination. Cells lacking *CLN3* are still viable despite an increased G1 duration and critical size. Other signals relaying information about growth

and nutrients must exist that feed into the cell cycle machinery during G1 to tell the cell to commit to another round of division.

Chemostats and Metabolic Oscillations

General principles and background

Yeast and other microorganisms can be grown in continuous cultures called chemostats. Using this type of experimental setup, steady state growth can be maintained by fixing the rate of input of a rate-limiting nutrient. Not only does biomass in the reactor remain constant, but also nutrient availability, metabolites, enzyme activity, etc. Dilution rate, D, the fraction of the cell culture that is displaced per unit of time, can be varied as a function of the flow rate of fresh media pumped into the reactor. Dilution rate and doubling time, T_d, of the culture are related by $D = \ln 2/T_d$. Thus, the doubling time, or growth rate, of the culture can be controlled by simply changing the flow rate of fresh media pumped into the chemostat, up to a point where the dilution rate would exceed the growth rate of the organism and washout would occur.

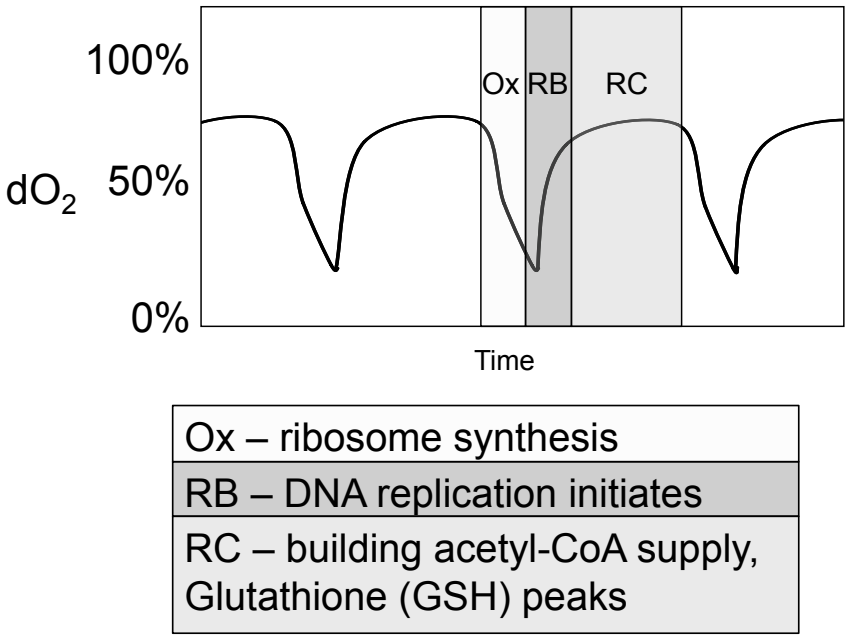

Fig. 1.3. Yeast metabolic oscillation. The graph depicts a typical yeast metabolic cycle (YMC) as measured by the percent oxygen saturation in the media. It can be divided into three phases, Ox, RB, and RC, during which each particular cellular functions occur.

Besides being amenable to steady metabolic growth in this experimental setup, yeast have another unique feature of chemostat growth that makes them very useful for studying the coordination of growth and cellular division. When grown in a continuous culture under particular conditions, generally D less than 0.2 hr^{-1} and dissolved oxygen (DO) percent saturation less than 80% (27), yeast can display metabolic oscillations involving the alternation between glycolytic and respiratory metabolism (Fig. 1.3). These types of oscillations give distinctive metabolic landmarks which challenge the notion that metabolism is a continuous process operating in the background of the cell. By providing ordered metabolic phases, similar to the successive phases of the DNA division cycle, it allows for a more thorough investigation of the coupling of the two processes.

Depending on the growth conditions used, these oscillations occur with a periodicity from approximately 0.5 hr to over 24 hr (28). While the shorter oscillations have been classified as short period oscillations with no dependency on the cell cycle, the longer oscillations are coupled to varying extent to the cell cycle, with budding index generally fluctuating between 10% and 60% (28). It should be noted that experiments documenting short period respiratory oscillations may also be coupled to the cell cycle, despite not being classified as such. Murray *et al*. studied yeast cultures oscillating with an approximate 40 minute metabolic cycle and found distinct bursts of DNA replication gated by the metabolic cycle, albeit less than 10% of the population initiated DNA replication at a given interval (29). It is possible that low levels of synchrony related to the cell cycle have caused observers to miss cell cycle dependency in experiments

involving short period oscillations, and these might be a variation of the longer respiratory oscillations with known cell cycle dependence. The mechanism for the synchrony of the oscillations is unknown, although it likely depends on easily diffusible chemicals such as H_2S and acetaldehyde, which can cause shifts in the oscillations when added exogenously (30).

Expression of 6,209 genes was examined throughout robust yeast metabolic cycles (YMC) of approximately 4 to 5 hr of cells grown under glucose limiting conditions. Microarray data showed that 3,552 genes were expressed periodically throughout the metabolic cycle (31). By clustering their array data, three superclusters of periodically expressed genes were revealed and these clusters were expressed at distinct phases of the YMC, called the oxidative (Ox), reductive/building (RB), and reductive charging (RC) phases (31). Cell division was restricted to the reductive phases, probably as a means to maintain genomic integrity (31, 32), and if forced to take place in the oxidative phase, the spontaneous mutation rate was significantly enhanced (32). This group also looked at cell division cycle mutants and found that those with a decreased growth rate had a *shortened* YMC, perhaps giving these slower growing mutants more windows in which to initiate DNA replication (32). While their data provides evidence for what happens with a loss-of-function metabolic mutant, no evidence exists for how the YMC and its coupling with cell division might be altered in a gain-of-function mutation.

Because of the large fluctuations in oxygen consumption throughout the YMC, one would hypothesize that the intracellular redox status of the cell also varies with the

YMC. This is the case, as shown by a *YAP1*-green fluorescent protein (GFP) fusion which localizes to the nucleus under conditions of oxidative stress. During the Ox phase, the GFP signal was enhanced in the nucleus and throughout other phases was primarily cytosolic (31). Other metabolites involved in maintaining redox status also showed distinctive peaks, corresponding to particular phases of the YMC, including NADP(H), NAD(H), and glutathione (GSH) (33).

Sulfur metabolism as a function of the YMC

A metabolite profile for the same duration YMC used for the *YAP1*-GFP fusion protein showed that more than 60 metabolites had distinctive peaks in at least one phase of the YMC (33). Interestingly, several sulfur metabolites displayed robust peaks as a function of the YMC, including cystathionine, homocysteine, homoserine, serine, S-adenosylhomocysteine (SAH), and GSH (33).

Sulfur metabolism is a very important aspect of the overall physiology for nearly all organisms and cells. For example, cysteine is critical in protein structure and function for its ability to exist in an oxidized disulfide bond or reduced sulfhydryl state, methionine is required to initiate protein synthesis, glutathione supplies the cell's main redox buffering capacity, and S-adenosylmethionine (SAM) supplies methyl groups for a variety of methyl transferase reactions. The biological sulfur cycle involves the reduction and oxidation of sulfur over a range of oxidation states from –2 to +6. Yeast, bacteria, and fungi are capable of sulfur assimilation, or the reduction of sulfur to sulfite and eventually sulfide. Mammals are only capable of sulfur oxidation, so ingesting

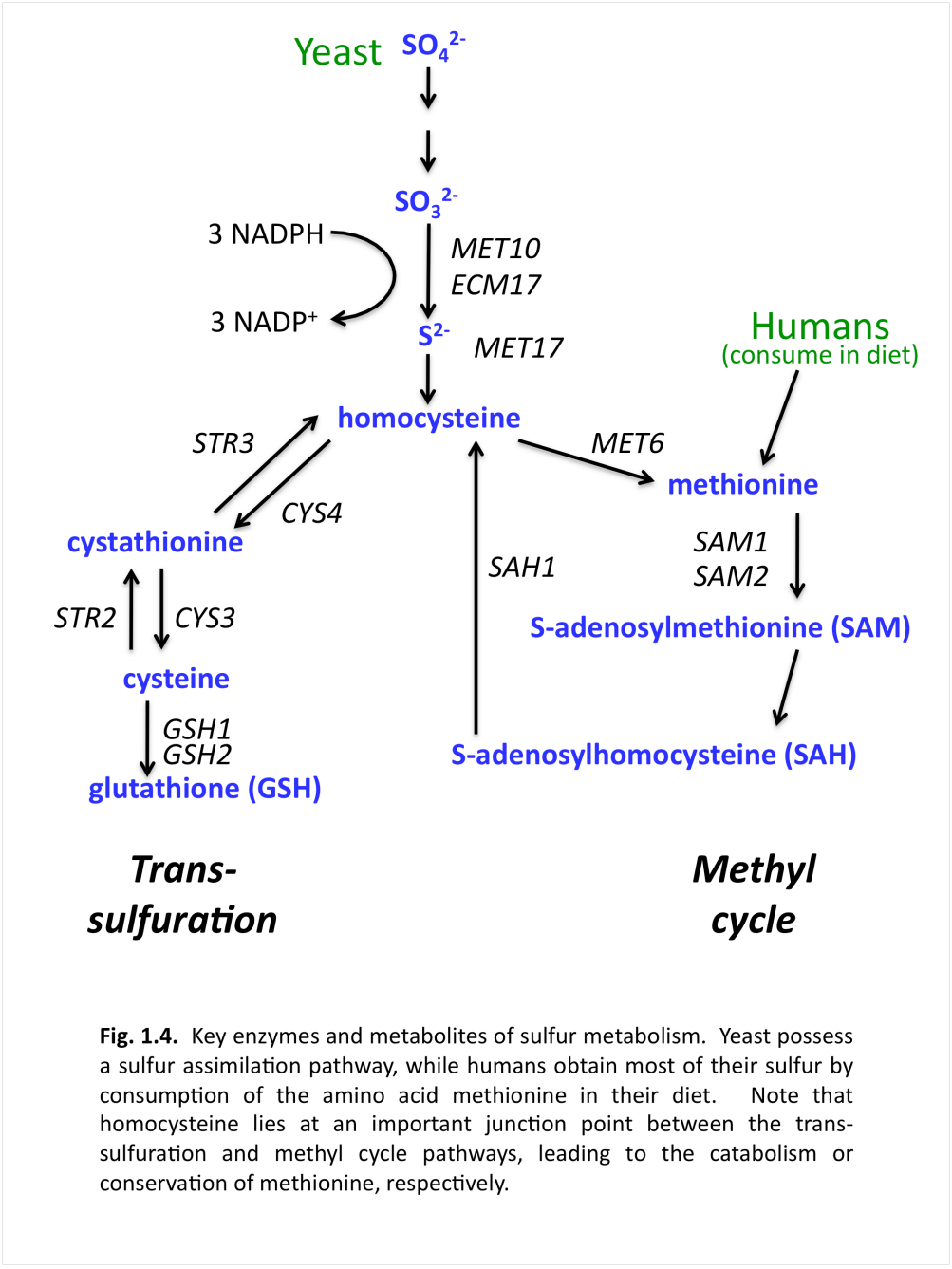

Fig. 1.4. Key enzymes and metabolites of sulfur metabolism. Yeast possess a sulfur assimilation pathway, while humans obtain most of their sulfur by consumption of the amino acid methionine in their diet. Note that homocysteine lies at an important junction point between the trans-sulfuration and methyl cycle pathways, leading to the catabolism or conservation of methionine, respectively.

sulfur at its reduced state of -2 is a dietary requirement, usually met by the consumption of the essential and semi-essential amino acids methionine and cysteine, respectively (34). Aside from a mammalian lack of ability to reduce sulfur, most of the sulfur metabolism pathways are conserved from yeast to humans.

The sulfur assimilation pathway of yeast reaches a critical junction point at the metabolite homocysteine (Fig. 1.4). The cell must then determine its fate as it enters one of two pathways—the trans-sulfuration branch leading to the net catabolism of methionine and eventual production of cysteine, a precursor to GSH, or the methyl cycle branch, where methionine is conserved, involving SAM and SAH (33). This same junction point is reached in mammals via methionine (consumed in the diet) entering the conserved transmethylation pathway and eventually forming the products homocysteine and adenosine (35).

During the RB phase, when DNA replication is taking place, SAH levels are increased, indicating increased flux thru the methyl cycle pathway, possibly due to the increased need for methylation of newly synthesized DNA and other macromolecules. However, during the RC phase, GSH levels peak, likely to provide the cell with enough redox buffer to protect against damage during the upcoming Ox phase (33). Because of the dynamic switch that occurred in sulfur metabolism at distinctive phases of the YMC, it was postulated that oscillations in sulfur metabolism were crucial to the respiratory oscillations. To test this hypothesis, eight loss-of-function enzymes of the sulfur pathways were created and tested for their ability to undergo oscillations of the YMC. Surprisingly, only disruption of *CYS4*, the gene encoding the enzyme cystathionine-β-

synthase, which lies at the junction point for determining the fate of homocysteine, abolished metabolic oscillations (33). Whether the loss of oscillations is due to diminished H_2S, altered flux through the SAM versus GSH pathways, or some unknown mechanism remains to be seen, but clearly, the temporal oscillations of various sulfur compounds are vital to the yeast metabolic oscillations.

Sulfur metabolism and cell division

The existing chemostat data provide evidence for a possible role, though not conclusive, of sulfur metabolism having an effect on cell division, since altering sulfur metabolism in *cys4Δ* cells leads to a loss of respiratory oscillations in which a large fraction of the cells are normally synchronized with respect to cell division. Other, more direct data exists as well. By limiting cells for various sulfur metabolites at different steps of the sulfur assimilation pathway, it was shown that at least one nutrient signal the cells were sensing occurred at or subsequently to methionyl-tRNA synthesis (36). While sulfur limiting conditions have been studied, the effects of adding endogenous sulfur compounds on the cell cycle have not previously been examined.

A very exciting yet unexplored link between sulfur and the cell cycle presents itself in the results of large scale mass spectrometry studies revealing Cdc28p, the main cell division kinase for yeast, found in separate complexes with both cystathionine-β-synthase (Cys4p) and sulfite reductase (Met10p/Ecm17p) (37, 38). The possible interaction of either of these enzymes and its significance is currently unknown and is the focus of a portion of the work presented in this thesis.

Mitochondrial DNA Maintenance

Mitochondria play an essential role in nearly all eukaryotes. They are responsible for the production of the majority of ATP via oxidative phosphorylation, maintaining calcium homeostasis, iron-sulfur cluster biosynthesis, and acting as a source and sink for reactive oxygen species. The number of physiological roles the mitochondrion plays in the cell continues to expand as knowledge of the organelle increases. Understanding mitochondrial function becomes increasingly more important as research implicates dysfunctional mitochondria in not only traditional mitochondrial diseases, but also in more common diseases such as diabetes, cancer, and neurodegenerative disorders.

The mitochondria derive from an endosymbiotic α-Proteobacterium over one billion years ago, thus making the organelle unique along with chloroplasts in that it maintains its own genome separate from the nuclear genome. While comparatively few genes are encoded for by the mitochondrial genome as a percent of the total mitochondrial proteome, maintenance of mitochondrial DNA (mtDNA) is vital for proper functioning of a cell.

The architecture and size of the mtDNA varies from species to species. For example, humans have an approximate 16kbp genome while the *S. cerevisiae* mitochondrial genome consists of approximately 80kbp. While total genome size shows considerable variation, the total genes encoded by the mtDNA averages roughly 35 and shows much less variation across species.

mtDNA was once thought to be naked since the mitochondria do not contain histones as does the nucleus, but this notion has been superceded by the existence of mtDNA being packaged into protein structures called mtDNA nucleoids. The architecture of the mitochondrial nucleoids also varies by species as does total genome size. Humans contain 46-806 nucleoids per cell, with the number of genomes per nucleoid ranging from 2-10. *S. cerevisiae* contain 40-60 nucleoids in aerobically growing cells and approximately 7.6 in anaerobic cells. In these cells, the number of genomes per nucleoid varies from 1-2 in aerobically and approximately 20 in anaerobically growing cells (39).

Despite differences in nucleoid composition, the core DNA packaging proteins are conserved from yeast to humans. These proteins contain two high motility group (HMG) boxes and have properties of DNA binding and bending. Known as Abf2p (Ars binding factor 2) in yeast and TFAM (Transcription factor A, mitochondria) in vertebrates, the levels of Abf2p in yeast and TFAM in certain cell types is enough to completely coat mtDNA. Yeast cells lacking *ABF2* lose mtDNA when grown on a fermentable carbon source (40), possibly as a result of increased deletions of repetitive mtDNA in these mutant cells (41). Conversely, moderate over-expression of *ABF2* increases mtDNA levels by 100%-150% (40). A correlation between levels of TFAM and mtDNA are also seen in mice and chickens (42). While yeast *ABF2* lacks the C-terminal tail responsible for transcriptional activation in mammals, the packaging and transcriptional activities are separable. Over-expressing human TFAM rescued the mtDNA instability of *abf2Δ* cells (43), showing these core packaging proteins are

conserved from single celled to higher eukaryotes. Homologs of Abf2p are known to exist not only in mammals, but *Xenopus*, *Drosophila*, and *Physarum*.

Nucleoids undergo remodeling in response to different metabolic conditions. In yeast cells, mt nucleoids are more compact when grown in glucose medium, with an increased ratio of Abf2p to mtDNA. When grown under respiratory conditions, as in glycerol medium, the nucleoids are more open and the ratio of Abf2p to mtDNA decreased (44). The significance of nucleoid remodeling under different metabolic growth conditions is still unknown, but it is hypothesized that Abf2p plays a role in the access of various proteins to the mtDNA.

We have used *ABF2* not to study mitochondrial morphology and dynamics, but instead to address the question of how metabolism affects cell division. In particular, we wanted to address the hypothesis that upregulated metabolism could promote cell division. To answer this question, we needed a yeast cell cycle mutant that grew better than wild type cells. All known cell cycle mutants either have no effect or a deleterious effect on growth, which would not allow us to address our question. One clue to finding the type of mutant we were looking for came from a previous study which showed that yeast cells cultivated for many generations under glucose limiting conditions in a chemostat "evolved" into a more fit strain (45). This "evolved" strain, which could out compete the original parental strain, contained higher levels of TCA cycle enzymes, utilized more oxidative means of metabolism, and contained more mtDNA (45). Using their findings, we hypothesized that cells over-expressing Abf2p, leading to increased

amounts of mtDNA, would mimic the over-proliferation phenotype seen in the chemostat evolution experiment described above.

Our detailed analysis of cells over-expressing Abf2p, called *3xABF2*$^{+}$ cells, showed both an enhanced growth rate and accelerated nuclear DNA replication (46). This unique metabolic gain-of-function cell cycle mutant has allowed us to further dissect specific metabolic pathways affecting DNA replication. We have found that sulfur metabolism is altered in *3xABF2*$^{+}$ cells and provides at least one metabolic link between growth and DNA replication. Even more importantly, we have found direct physical interactions via co-immunoprecipitation experiments between sulfur pathway enzymes and cyclin dependent kinases. These physical interactions may prove to be key in how the cell transmits metabolic signals and coordinates growth with the decision to commit to another round of cell division.

CHAPTER II

AN INCREASE IN MITOCHONDRIAL DNA PROMOTES NUCLEAR DNA REPLICATION IN YEAST*

Overview

Coordination between cellular metabolism and DNA replication determines when cells initiate division. It has been assumed that metabolism only plays a permissive role in cell division. While blocking metabolism arrests cell division, it is not known whether an up-regulation of metabolic reactions accelerates cell cycle transitions. Here we show that increasing the amount of mitochondrial DNA accelerates overall cell proliferation and promotes nuclear DNA replication, in a nutrient-dependent manner. The Sir2p NAD^+-dependent de-acetylase antagonizes this mitochondrial role. We found that cells with increased mitochondrial DNA have reduced Sir2p levels bound at origins of DNA replication in the nucleus, accompanied with increased levels of K9, K14-acetylated histone H3 at those origins. Our results demonstrate an active role of mitochondrial processes in the control of cell division. They also suggest that cellular metabolism may impact on chromatin modifications to regulate the activity of origins of DNA replication.

Introduction

Without cellular metabolism there is no cell division (47), but the key question is whether metabolism only allows for division to happen, or can it actively promote cell cycle progression. To determine if metabolism can actively promote cell division it is important to identify gain-of-function mutations in metabolic pathways that also accelerate cell proliferation. Such mutations have not been described in the yeast *Saccharomyces cerevisiae*. It is known, however, that yeast populations evolved in continuous chemostat cultures can proliferate faster than the parent population, and they have higher levels of tricarboxylic acid cycle (TCA) enzymes and mitochondrial (mt) DNA (45). The mitochondrial genome is transmitted as a "nucleoid" DNA/protein complex. The number of mtDNA molecules per nucleoid varies, but there are usually more genome equivalents than nucleoids (48, 49). Abf2p is a conserved mtDNA maintenance protein (50, 51), which directly binds to, bends and compacts mtDNA (52, 53). Moderate over-expression of Abf2p by 2-3 fold elevates the amount of mtDNA by 50-150% (40). The consequences of an increase in mtDNA in cell proliferation have not been explored.

Sir2p is an evolutionarily conserved NAD^+-dependent de-acetylase (54, 55). Loss of Sir2p leads to loss of transcriptional silencing, genome instability and a decrease in replicative life span. In yeast, silent chromatin is formed at three regions: the rDNA, the *HML* and *HMR* mating type loci, and telomeres (56). Sir2p is required for silencing at all of these regions, and it is the only Sir protein required for silencing at the rDNA (57-59). Sir2p also appears to negatively impact on rDNA replication, because in *sir2Δ*

cells twice as many origins are activated within the rDNA array (60). The inhibitory effects of Sir2p on DNA replication extend beyond rDNA. Loss of Sir2p suppresses replication defects of mutants that can not assemble a pre-replicative complex of proteins (Pre-RC) at origins of DNA replication in the G1 phase of the cell cycle (61). These results may be linked to a general positive role of histone acetylation for origin activity (62). Indeed, loss of the Rpd3p de-acetylase globally accelerated DNA replication, and targeted acetylation of a late origin advanced its activation (63), demonstrating a clear causal role of histone acetylation and activation of DNA replication. However, whether such chromatin modifications may serve as a link between cellular metabolism and initiation of DNA replication is not known.

In this report we show that an increase in mtDNA in cells over-expressing Abf2p, actively promotes initiation of cell division. Furthermore, we identify physical changes, such as Sir2p binding and histone acetylation, at an origin of DNA replication that result from an increase in mtDNA.

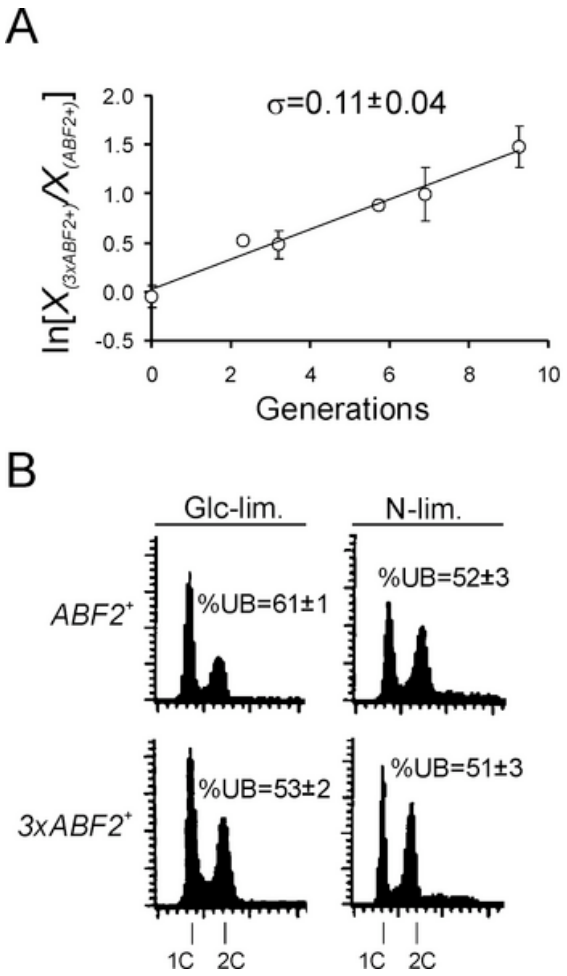

Fig. 2.1. Cells moderately over-expressing *ABF2* proliferate faster (*A*), and have altered cell cycle progression (*B*) in chemostat cultures. In *A*, a chemostat competition experiment done during glucose limitation at dilution rate D = 0.1 h^{-1} is shown. The specific growth differential (σ) between the two competing strains (64) is the average (± s.d.) of three independent competition experiments. In each experiment, and for each sampling point, the average (± s.d.) of at least three measurements was calculated. $X_{3xABF2}^{+}(t)$ and $X_{ABF2}^{+}(t)$ represent the relative proportion of the two strains at time t, in generations. In *B*, cell cycle progression of the indicated strains and nutrient limitations was evaluated by flow cytometry. Cell numbers are plotted on the y-axis and fluorescence on the x-axis. The DNA content of cells in G1 and G2/M is indicated as 1C and 2C, respectively. The percentage of unbudded cells (%UB) correlates with G1 cells. The values shown are the average (± s.d.) of at least three independent experiments.

Results and Discussion

Abf2p and cell proliferation in chemostats

We hypothesized that increasing the amount of mtDNA may mimic the situation of "evolved" yeast populations, which can proliferate faster than the parent population (45), allowing us to examine effects on cell division. We evaluated a strain (*3xABF2*$^+$), which carries two additional copies of *ABF2*, because in this strain the amount of mtDNA is increased (40). The *3xABF2*$^+$ strain proliferated faster than the wild type strain in glucose-limiting (0.08% glucose) conditions (Fig. 2.1*A*), mimicking "evolved" strains (45). We next examined cell cycle progression in defined chemostat cultures under glucose (Glc) or nitrogen (N) limitation at 0.2h^{-1} dilution rate, *D*, comparing *ABF2*$^+$ to *3xABF2*$^+$ cells (Fig. 2.1*B*). Under Glc-limitation, the fraction of *3xABF2*$^+$ cells in G1 was reduced (Fig. 2.1*B*, cells in G1, 53% *3xABF2*$^+$ compared to 61% *ABF2*$^+$). In contrast, under N-limitation, extra copies of *ABF2* did not affect the DNA content distribution in anabolically-restricted cells (Fig. 2.1*B*, cells in G1, 52% *3xABF2*$^+$ compared to 51% *ABF2*$^+$). These data suggest a connection between mitochondrial function and cell cycle progression that is evident under glucose limitation in cells over-expressing *ABF2*. Interestingly, *3xABF2*$^+$ cells are the same size as wild type cells (Fig. 2.2*A*), possibly explaining why *ABF2* mutations were not identified previously in size-based mutant screens for cell cycle regulators.

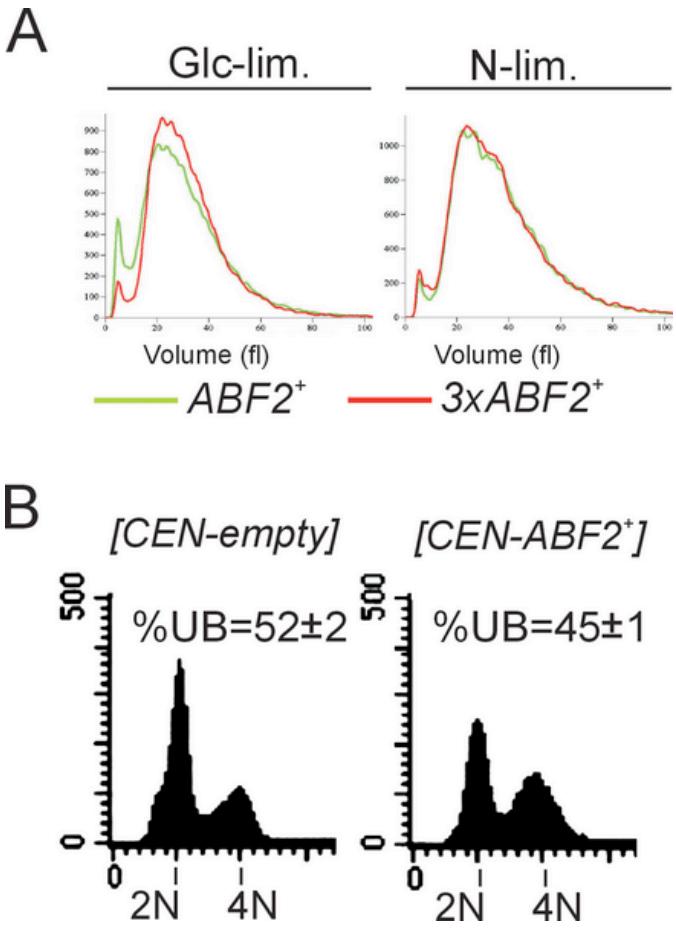

Fig. 2.2. (*A) 3xABF2*$^{+}$ cells do not have altered cell size in chemostat cultures. The cell size of the indicated cell populations was measured from the same chemostat experiments described in Fig. 2.1*B*, using a channelyzer. Cell numbers are plotted on the y-axis and the x-axis indicates size (in fl). (*B*) Moderate over-expression of *ABF2* from a low-copy CEN plasmid promotes cell cycle progression. The DNA content of the indicated strains is shown.

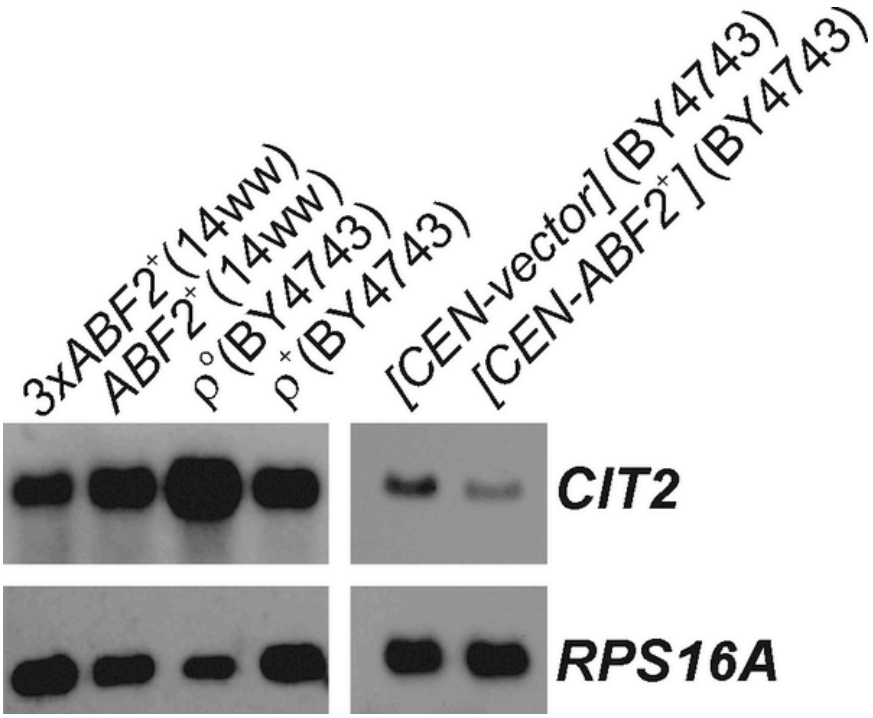

Fig. 2.3. Moderate over-expression of *ABF2* does not trigger the RTG response. RNA blots of *CIT2* steady-state levels, from cells grown under glucose limitation in chemostats. The relevant genotype and strain background are shown above each lane. *RPS16A* levels indicate loading.

To determine whether the effects observed in cell cycle progression are due to *ABF2* and not due to an unknown secondary mutation, we repeated the experiment shown in Fig. 2.1*B* using a different genetic background (BY4743). We used a low-copy centromeric plasmid carrying *ABF2* (*CEN-ABF2*$^{+}$) to achieve modest over-expression of Abf2p similar to *3xABF2*$^{+}$ cells (40, 65). Under glucose limitation, a lower fraction of *CEN-ABF2*$^{+}$ transformants (45±1%) was in the G1 phase of the cell cycle compared to the empty vector transformants (52±2%, Fig. 2.2*B*). Thus, the cell cycle effects we observed in *3xABF2*$^{+}$ cells are *ABF2*-linked.

Abf2p and the retrograde response

If mitochondria do not function properly a retrograde (RTG) response leads to elevated (~10-fold) *CIT2* levels (66, 67). As expected, in ρº cells, which lack mtDNA, the *CIT2* RNA level was increased ~5-fold over the level in ρ^{+} cells (Fig. 2.3). In contrast, we found that *CIT2* mRNA levels are not elevated in cells over-expressing *ABF2*. Instead, *CIT2* levels are reduced by ~2-fold (Fig. 2.3). Thus, the mitochondria of cells over-expressing *ABF2* are not dysfunctional. Using a colony sectoring assay (68), we also found that the frequency of chromosome loss was 1.66% (n=3,004) for *CEN-ABF2*$^{+}$ transformants, compared to 1.73% (n=2,657) for the empty vector transformants. Therefore, over-expression of *ABF2* does not cause gross genome instability.

Abf2p and the timing of START

Because *3xABF2*$^+$ populations proliferate faster (Fig. 2.1*A*) and have a reduced fraction of G1 cells (Fig. 2.1*B*), we hypothesized that DNA replication may be accelerated in *3xABF2*$^+$ cells. We examined cell cycle progression of *ABF2*$^+$ and *3xABF2*$^+$ cells from synchronous cultures obtained by centrifugal elutriation. We used standard (69) undefined medium (YPD) for these experiments, with lower glucose concentration (0.5%). A higher fraction of *3xABF2*$^+$ cells entered S phase sooner than *ABF2*$^+$ cells (Fig. 2.4, compare the top two rows). For example, at 60 min post-elutriation of *ABF2*$^+$ cells 10.7% were budded and 46.2% in G1, while of *3xABF2*$^+$ cells 40.2% were budded and 32% were in G1. In addition, the *3xABF2*$^+$ cells completed S phase sooner than *ABF2*$^+$ cells (see Fig. 2.4 compare the top two rows): At 80 min post elutriation, note the size of the G2/M peak relative to the G1 peak. More *3xABF2*$^+$ cells have completed DNA replication than *ABF2*$^+$ cells. Finally, although in asynchronous populations the overall cell size of *3xABF2*$^+$ cells was not different from *ABF2*$^+$ cells (Fig. 2.2*A*), the elutriated daughter *3xABF2*$^+$ G1 cells increased in size faster than their *ABF2*$^+$ counterparts (Fig. 2.4, compare the top two rows): at 60 min *3xABF2*$^+$ cells are 40.2 fl, while *ABF2*$^+$ cells are 37.1 fl, consistent with a growth-promoting role of Abf2p.

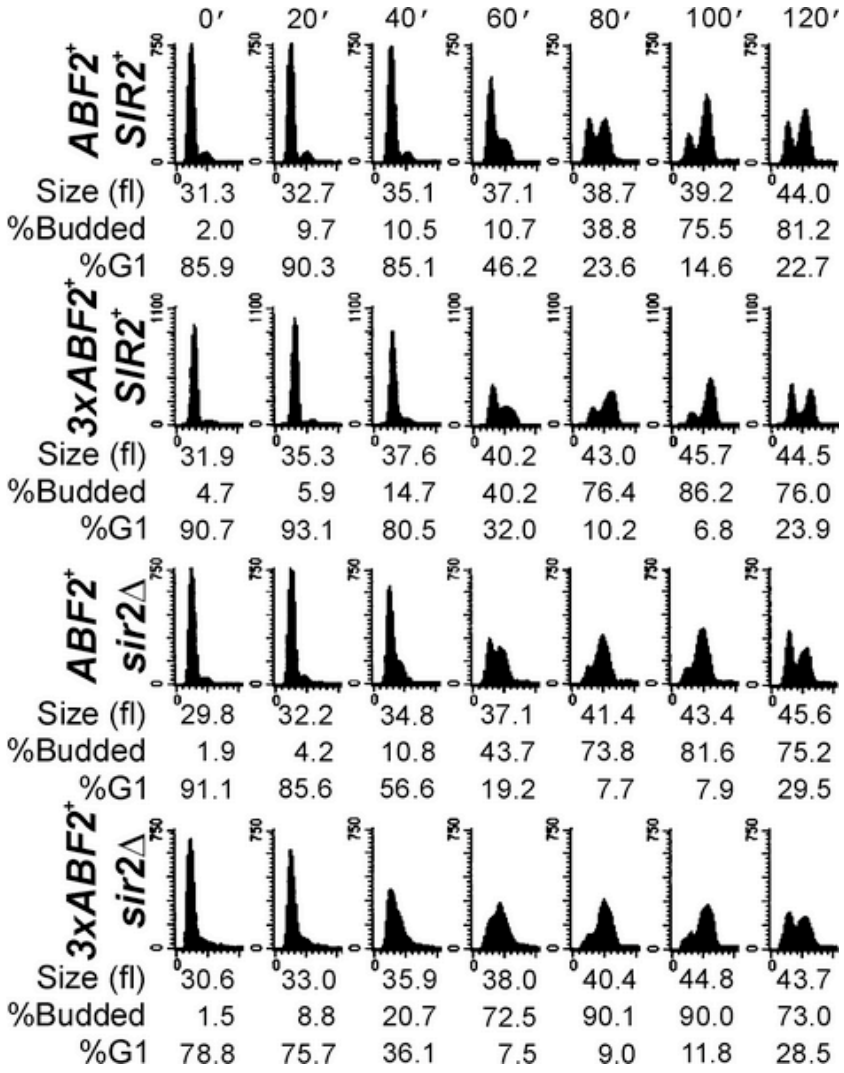

Fig. 2.4. Over-expression of *ABF2*, or loss of *SIR2*, accelerates DNA replication. Synchronous cultures of the indicated strains were obtained by centrifugal elutriation and the starting populations of each strain were of the same size. At the indicated times the DNA content was evaluated by flow cytometry.

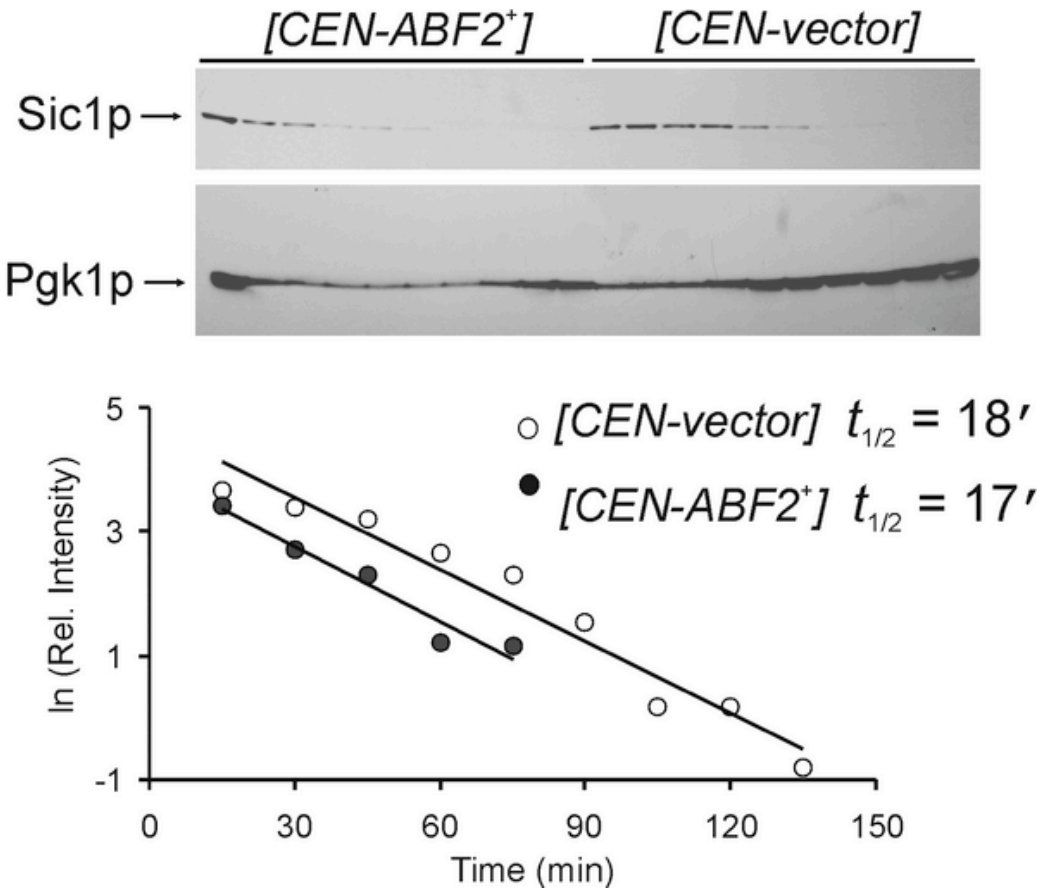

Fig. 2.5. Sic1p stability and Abf2p. The levels of galactose-induced Sic1p-TAG were monitored by immunoblotting from cells carrying the indicated plasmids after *SIC1-TAG* expression was turned off. The signal from Pgk1p was used to estimate loading.

To confirm these results, we repeated this analysis several times. In each case, *ABF2*$^+$ and *3xABF2*$^+$ cells were examined under identical conditions, using media from the same batch. We used two variables to compare the two strains across different experiments: the critical size for budding (at which 50% of the cells are budded); and the rate of cell size increase after elutriation. Interestingly, *3xABF2*$^+$ cells bud at a slightly larger size (41.2±1.1 fl, n=5, *P*=0.032, based on a 2-tailed Student's *t* test) than *ABF2*$^+$ cells (38.6±1.1 fl, n=6) (Fig. A-1*A,D*). We then plotted in each case cell size as a function of time, to estimate the rate of cell size increase (fl/min) after elutriation (Fig. A-1*B,C*). While these values can vary from experiment to experiment, in every case *3xABF2*$^+$ cells increased in size significantly faster (0.14±0.02 fl/min, n=5, *P*=0.013, based on a 2-tailed Student's *t* test) than *ABF2*$^+$ cells (0.11±0.01 fl/min, n=6) (Fig. A-1*E*). Thus, even though *3xABF2*$^+$ cells have a slightly larger critical size for budding than *ABF2*$^+$ cells, they reach that size significantly earlier than their *ABF2*$^+$ counterparts because they increase in size ~28% faster. For example, for *ABF2*$^+$ newborn daughter cells of 20 fl, it will take on average 169 min until they reach their critical size, but it will take 150 min for *3xABF2*$^+$ daughters. Together with our chemostat experiments (Figs. 2.1 and 2.2), our findings from these synchronous cultures (Figs. 2.4 and A-1) with standard YPD media strongly support the notion that Abf2p plays an active growth-promoting role and accelerates initiation of DNA replication.

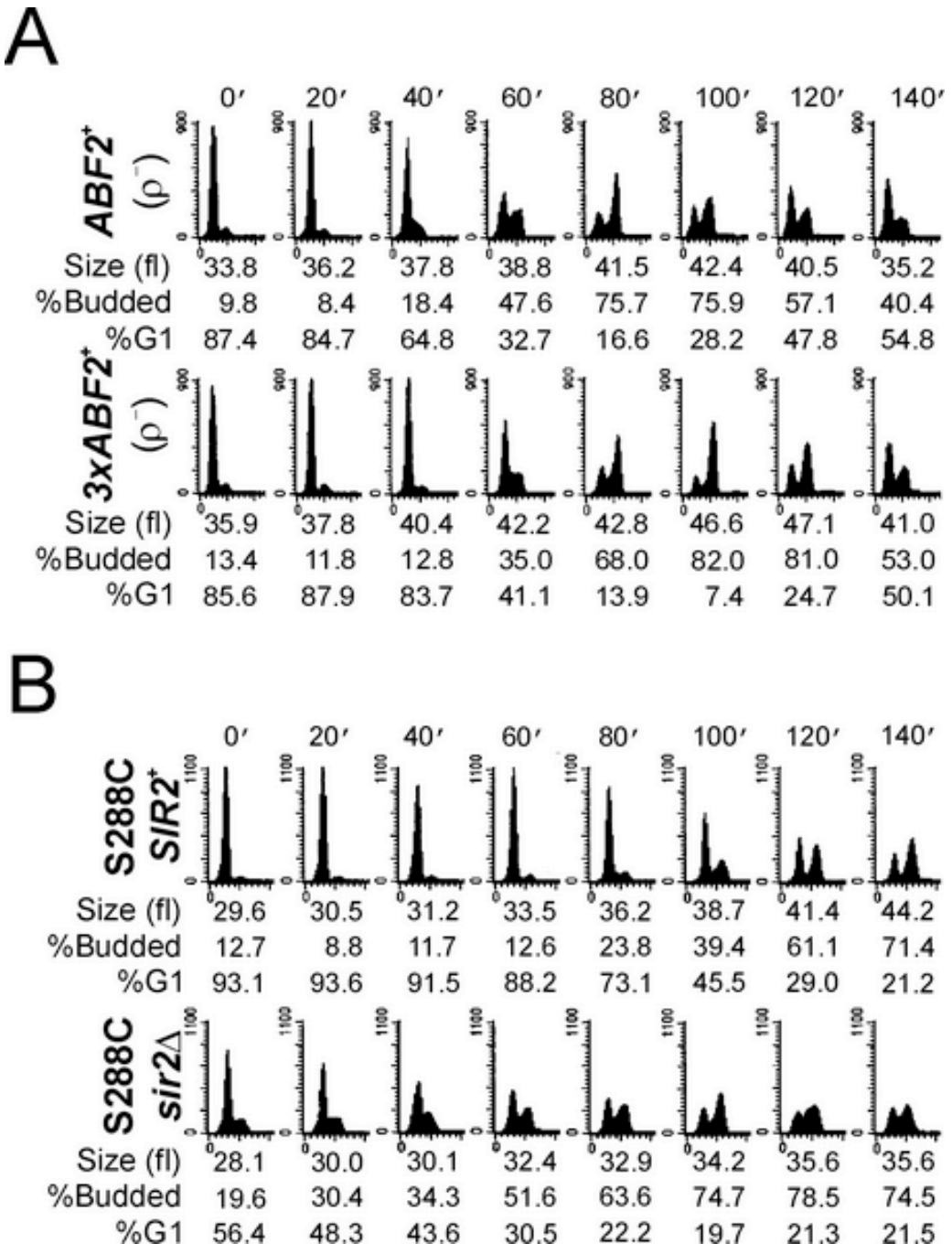

Fig. 2.6. *(A)* mtDNA is required for the accelerated DNA replication in *3xABF2*$^{+}$ cells. Cell cycle progression of elutriated cells was analyzed exactly as in Fig. 2.4, except that the strains used were made ρ^{-} as described in the Methods. (*B)* Loss of *SIR2* accelerates DNA replication in the S288C strain background. The elutriation experiment was done as in Fig. 2.4, except that the strains used were in a different strain background, described previously (57).

We also examined the levels of the cyclin-dependent kinase (Cdk) inhibitor Sic1p in cells over-expressing Abf2p. In late G1 rising levels of Cdk activity trigger the degradation of Sic1p and initiation of DNA replication (70). In cells over-expressing Abf2p degradation of Sic1p was initiated sooner than in the control cells (Fig. 2.5), consistent with a shortened G1 phase, but once triggered the rate of Sic1p degradationwas unaffected. We obtained identical results in separate repeats of this experiment (Fig. A-2).

We next generated the corresponding ρ^- strains to test whether over-expression of *ABF2*$^+$ requires mtDNA to promote DNA replication. These strains are respiratory incompetent (Fig. A-4*A*). DNA replication was not accelerated in *3xABF2*$^+$ (ρ^-) cells (Fig. 2.6*A*). Overall, in contrast to ρ^+ cells (see Figs. 2.4 and A-1) the critical budding size (Fig. A-4*B*), and the rate of cell size increase after elutriation (Fig. A-4*C*), were not significantly different between *ABF2*$^+$ (ρ^-) and *3xABF2*$^+$ (ρ^-) cells: P=0.43, and P=0.54, respectively (based on 2-tailed Student's t tests). In conclusion, our findings suggest that altered mitochondrial functions in *3xABF2*$^+$ cells impact on some factor(s) that affect DNA replication.

Functional interactions between Abf2p and Sir2p

A protein linked to both metabolism and DNA replication is the Sir2p sirtuin (54), which negatively impacts DNA replication (60-62). Consequently, we evaluated cell cycle progression of cells lacking Sir2p alone, or in combination with Abf2p over-expression (Fig. 2.4). Comparison of *ABF2*$^+$*, SIR2*$^+$ (Fig. 2.4, top row) to *ABF2*$^+$*, sir2Δ* (Fig 2.4, third row) cells at 60 min shows that cells lacking *SIR2* initiated and completed

S phase significantly sooner than wild type cells. Initiation of DNA replication was further accelerated in *3xABF2*$^{+}$*, sir2Δ* cells (Fig. 2.4, bottom row). We repeated this analysis several times, as we described earlier (Fig. A-1). Interestingly, *3xABF2*$^{+}$*, sir2Δ* cells bud at a smaller size (36.1±0.5 fl, n=5, *P*=0.0009, based on a 2-tailed Student's *t* test) than *ABF2*$^{+}$*, SIR2*$^{+}$ cells (38.6±1.1 fl, n=6) (Fig. A-1*D*). This explains the apparent additive acceleration of START we observed in *3xABF2*$^{+}$*, sir2Δ* cells (Fig. 2.4, compare at 40 min the *3xABF2*$^{+}$*, sir2Δ* strain to other strains, and see also Fig. 2.7, below). Taking into account the critical budding size and the rate of cell size increase for each strain, for *3xABF2*$^{+}$*, sir2Δ* newborn daughter cells of 20 fl, it will take on average 128 min to start budding, compared to 169 min for *ABF2*$^{+}$*, SIR2*$^{+}$ daughters. Finally, loss of Sir2p does not increase the amount of mtDNA in the cell (Fig. A-3).

We next generated the corresponding (ρ^{-}) strains lacking Sir2p (Fig. A-4*A*). These strains were examined after elutriation (Fig. A-4*B,C*), as we described above. Strains lacking Sir2p and mtDNA did not have a significant different rate of cell size increase after elutriation compared to the other (ρ^{-}) strains (Fig. A-4*C*). Finally, to ensure that the effects of Sir2p on cell cycle progression were not strain-specific, we also examined cell cycle progression of *sir2Δ* cells in a different strain background (an S288C derivative) (57). S phase entry was greatly accelerated in *sir2Δ* cells in that background, and cells spent very little time in G1 (Fig. 2.6*B*). For example, *SIR2*$^{+}$ cells initiate DNA replication at 80-100 min after elutriation, while *sir2Δ* cells do so at ~40 min.

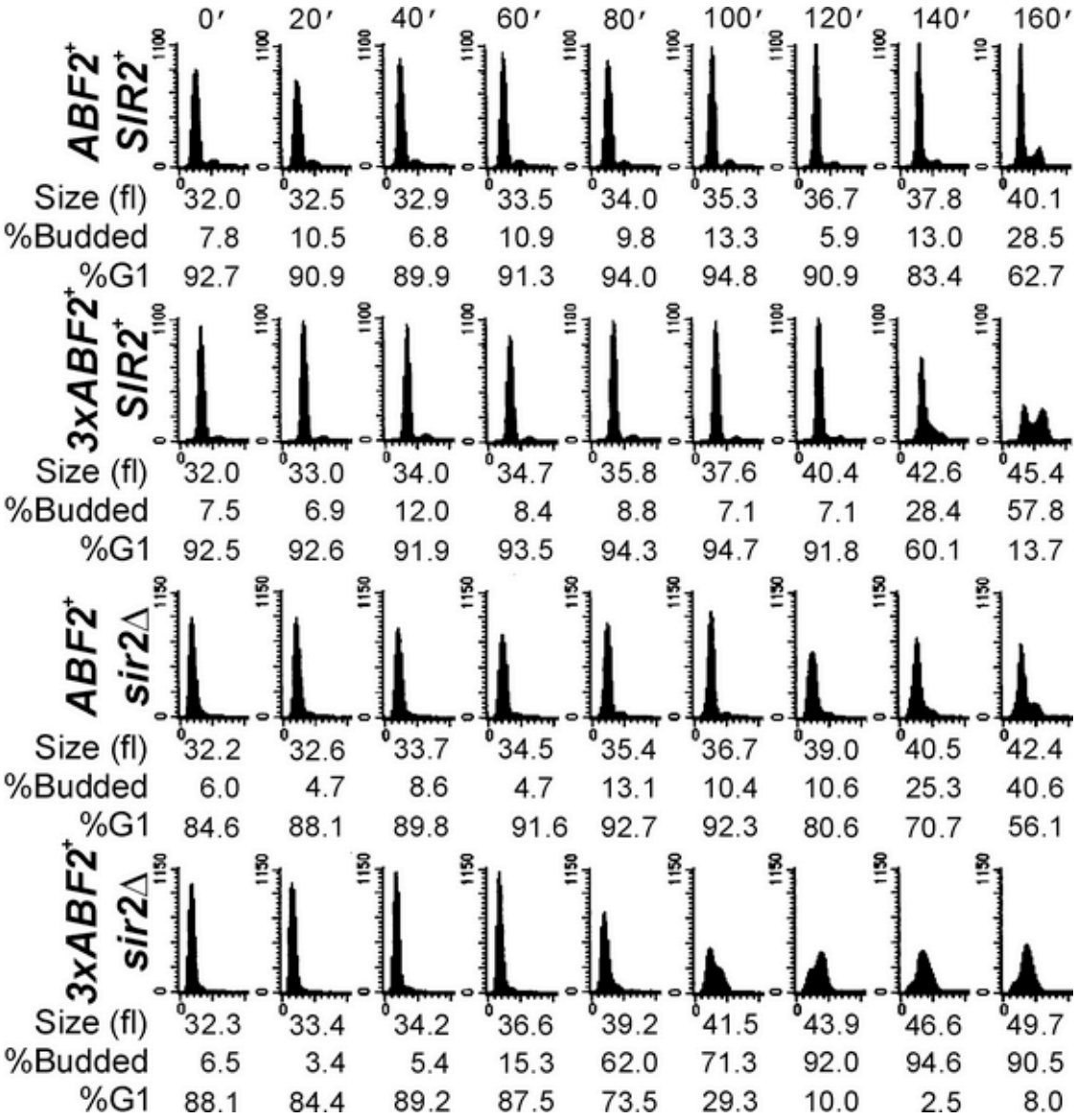

Fig. 2.7. Loss of *SIR2* in cells over-expressing *ABF2* dramatically accelerates DNA replication when NADH is depleted. Cell cycle progression was monitored after elutriation as in Fig. 2.4, except that 10 mM acetaldehyde was added to the starting samples.

We next tested if the acceleration of DNA replication in *3xABF2*$^{+}$ or *sir2Δ* cells depends on NADH. Yeast cells can display robust NAD(P)H oscillations, which are thought to gate metabolism with DNA replication, since DNA synthesis takes place when NAD(P)H levels are high (29, 31, 71). To deplete cellular NADH we added 10 mM acetaldehyde to the elutriated early-G1 cells (72). The G1 phase was greatly expanded (Fig. 2.7), compared to the untreated cells shown in Fig. 2.4, consistent with a requirement for NADH for initiation of DNA replication. G1 phase expansion was also evident in *3xABF2*$^{+}$, *SIR2*$^{+}$ or *ABF2*$^{+}$*, sir2Δ* cells, indicating that these cells still require NADH to progress through G1 into S phase. Nonetheless, *3xABF2*$^{+}$, *SIR2*$^{+}$ or *ABF2*$^{+}$*, sir2Δ* cells entered S phase sooner (~20 min) than wild type *ABF2*$^{+}$, *SIR2*$^{+}$ cells (Fig. 2.7, compare the top three rows at 140 min post-elutriation), consistent with our previous results shown in Fig. 2.4. Remarkably, 3x*ABF2*$^{+}$*, sir2Δ* cells entered and completed S phase with highly accelerated kinetics: they finished DNA replication before wild type cells even started (Fig. 2.7, compare the bottom row with the top row). These results are consistent with strong additive functional interactions between Abf2p and Sir2p, with Sir2p acting antagonistically to Abf2p's effects on DNA replication. How Abf2p over-expression impacts the metabolic status of the cell is unclear, but it may involve NAD/NADH metabolism because the functional interactions between Abf2p and Sir2p are quite prominent in the presence of acetaldehyde.

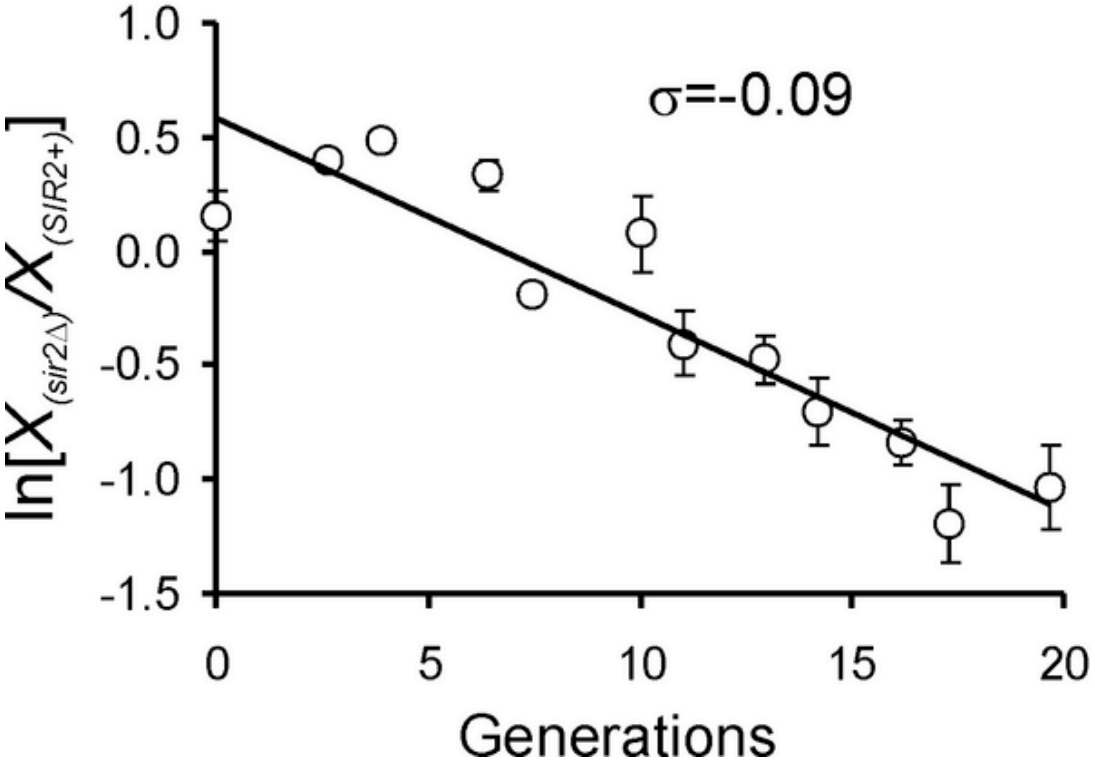

Fig. 2.8. Loss of Sir2p does not accelerate overall cell proliferation. Chemostat competition experiments between *SIR2*$^{+}$ and *sir2Δ* cells (in the 14ww strain background) were done during glucose limitation at dilution rate $D = 0.1\ h^{-1}$, as described in Fig. 2.1.

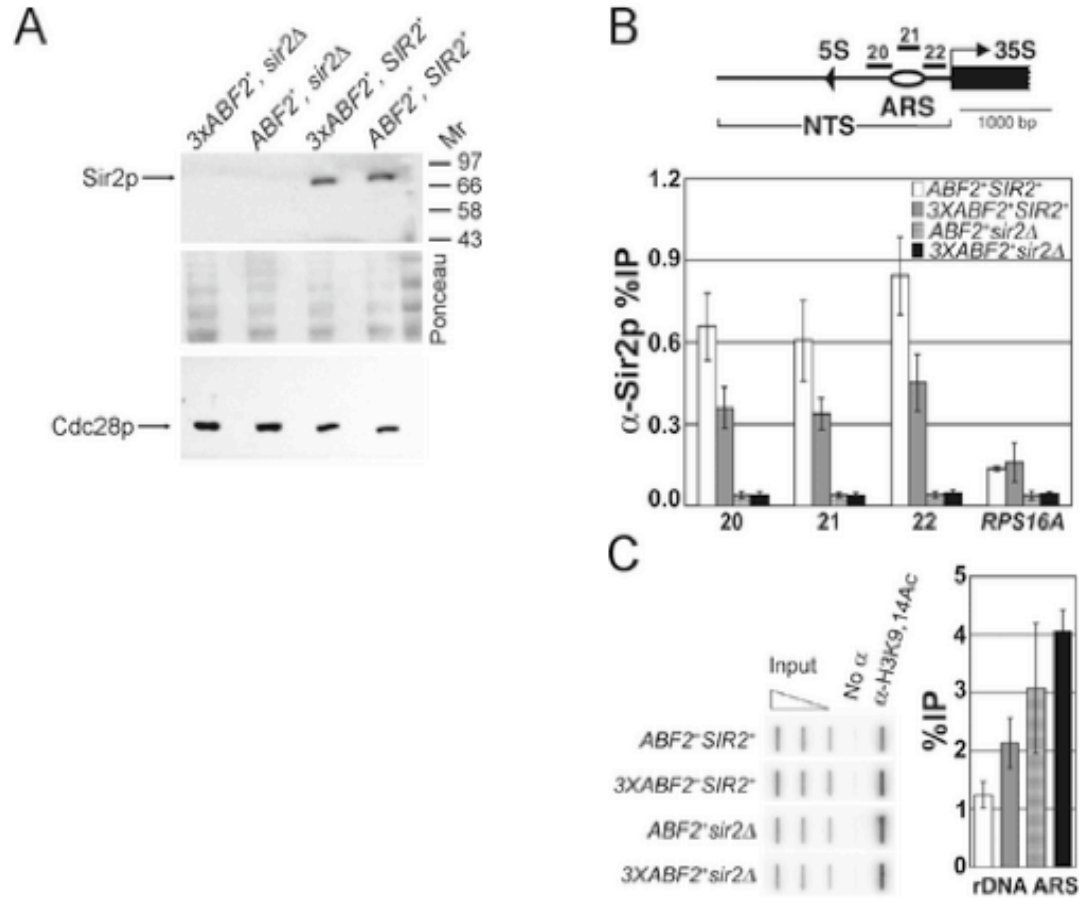

Fig. 2.9. Cells over-expressing *ABF2* have less Sir2p and higher levels of K9, K14 acetylated histone H3 at the rDNA ARS elements. (*A*) Immunoblot showing that the level of Sir2p is not altered in whole cell extracts from cells over-expressing *ABF2*. The same blot was stained with Ponceau, to indicate loading. Loading was also evaluated from the same samples, with an anti-Cdc28p antibody. (*B*) ChIP experiments analyzed by real-time PCR show that the level of Sir2p (%IP) at the rDNA ARS elements is reduced in *3XABF2*$^{+}$ cells. Part of one rDNA repeat is shown above indicating the location of the rDNA ARS elements, the primers used (primer pairs 20, 21, 22); the nontranscribed spacer (NTS); and the 35S and 5S rRNA genes. The values shown in the bar graph are the average %IPs (± s.d.) of three independent experiments. *(C)* ChIP experiments analyzed by slot blot show that the level of K9, K14 acetylated histone H3 is increased at the rDNA ARS elements in *3XABF2*$^{+}$ cells. In the graph, the average %IPs (+/- range) are shown for two independent experiments (Pearson coefficient = 0.95). The open triangle above the slot blot represents serial dilutions of input DNA to ensure linearity with respect to hybridization of the probe to the amount of DNA applied to the membrane. Other labels as in Fig. 2.9*B*. (Experiments shown in Fig. 2.9*B* and *C* performed by John Mueller and Chonghua Li.)

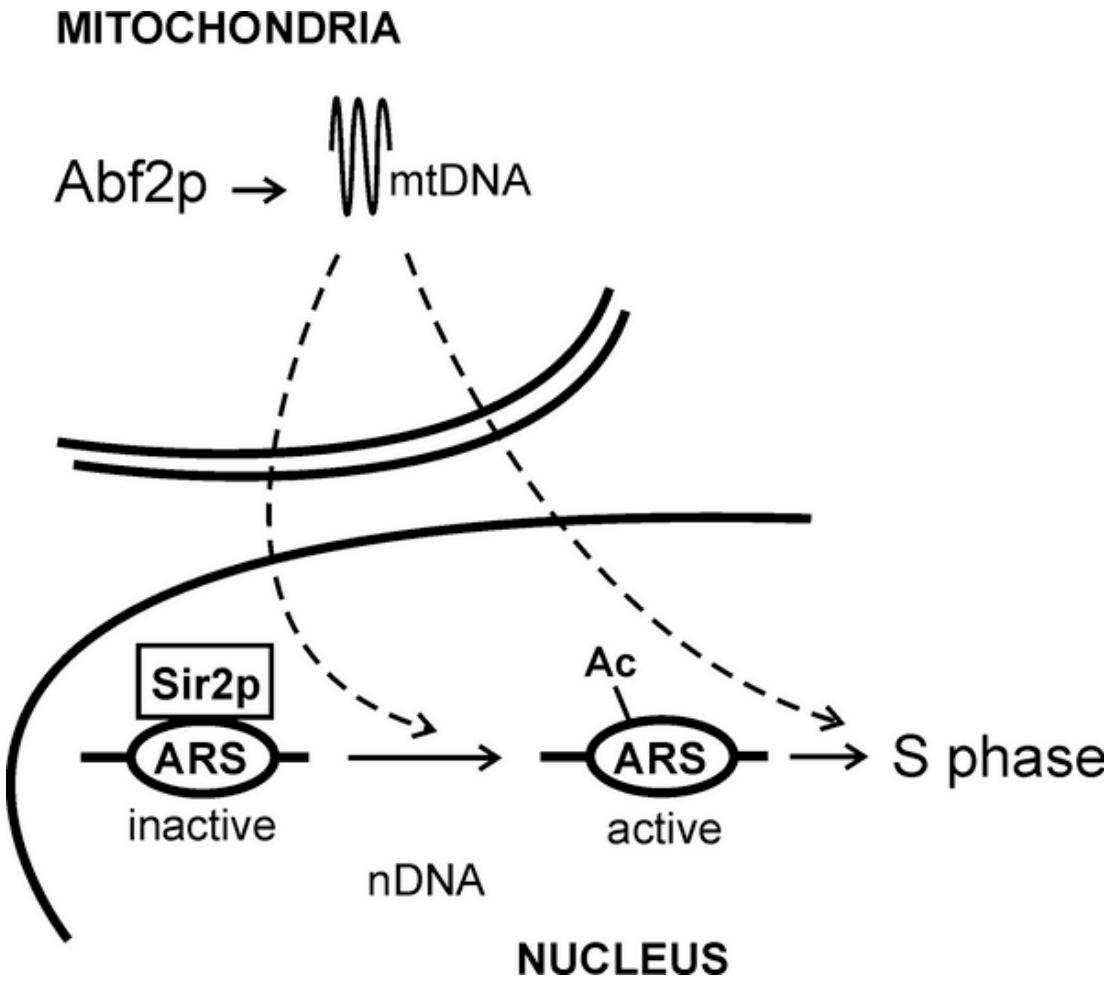

Fig. 2.10. A schematic of the model suggested by our data: An increase of mtDNA by moderate over-expression of Abf2p promotes mitochondrial functions, which in turn accelerate cell proliferation and DNA replication. The NAD^+-dependent de-acetylase Sir2p antagonizes initiation of DNA replication. Cells over-expressing Abf2p have decreased levels of Sir2p at origins of DNA replication (ARS), and higher levels of acetylated K9, K14 histone H3 residues (Ac). Additional mechanisms likely contribute to the overall positive effects on cell proliferation and DNA replication in cells with higher mtDNA levels.

We next asked if Sir2p negatively affects cellular metabolism to delay DNA replication. We found that *sir2Δ* cells did not proliferate faster than *SIR2*$^+$ cells under glucose limitation in chemostats (Fig. 2.8). Thus, loss of Sir2p does not up-regulate metabolic functions necessary to achieve the proliferation advantage evident in *3xABF2*$^+$ cells under the same conditions (Fig. 2.1*A*).

Abf2p and physical changes at origins of DNA replication

The overall levels of Sir2p are not altered in *3xABF2*$^+$ cells (Fig. 2.9*A*). In addition to its roles in silencing, Sir2p negatively affects the activity of origins of DNA replication throughout the genome (60, 61). Consequently, we next tested if the level of Sir2p at origins of DNA replication is altered in *3xABF2*$^+$ cells.

We examined the ARS elements in the rDNA tandem repeats, because the association of Sir2p with the rDNA (73) and the negative role of Sir2p in regulating these origins (60, 61) are well-characterized. Chromatin immunoprecipitation (ChIP) was performed with *ABF2*$^+$ or *3xABF2*$^+$ cells using antisera against Sir2p. *ABF2*$^+$, *sir2Δ* cells and *3xABF2*$^+$, *sir2Δ* cells were examined to provide a measurement of background. Immunoprecipitated DNA was analyzed by real-time PCR using primers that span the ARS elements in the rDNA. We found that the level of Sir2p at the rDNA ARS elements was reduced about two-fold in *3xABF2*$^+$ cells, compared to the level in *ABF2*$^+$ cells (Fig. 2.9*B*). The level of Sir2p at *RPS16A*, a locus that does not contain an ARS element, was not altered by over-expression of Abf2p. Consistent with the reduced level of Sir2p at the rDNA ARS elements, we also found that the level of K9, K14-acetylated histone H3 at the rDNA ARS elements was increased in cells over-expressing Abf2p

(Fig. 2.9*C*). In yeast and animals such chromatin modifications activate DNA replication (62, 63, 74). In addition to the rDNA ARS we also examined ARS315, which is a very active origin and fires in 90% of the cell cycles (75). Consistent with the high activity of ARS315, the level of K9, K14-acetylated histone H3 was also very high at that origin (data not shown). Since loss of Sir2p suppresses replication defects of ARS315 in *cdc6-4* cells (61), we then examined if Sir2p is present at ARS315. We did not detect Sir2p at ARS315 in $ABF2^{+}$ or $3xABF2^{+}$ cells (Fig. A-5), perhaps consistent with the already high activity of this origin. Thus, the previously observed (61) effects of Sir2p on MCM proteins binding at ARS315 maybe indirect.

To answer if binding of Sir2p at the rDNA origins depends on the presence of mtDNA, we then examined the corresponding ρ^{-} strains (Fig. A-6). Notably, in both $ABF2^{+}$ or $3xABF2^{+}$ ρ^{-} cells Sir2p levels are increased at the rDNA ARS by ~2-fold (Fig. A-6). Thus, the level of Sir2p bound at the rDNA ARS elements is inversely related to the amount of mtDNA in the cell. It appears that some mitochondrial function that depends on mtDNA limits the association of Sir2p with origins of replication. Together, these results identify physical changes associated with active origins of DNA replication in the nucleus, resulting from an increase in the amount of the mitochondrial genome (Fig. 2.10).

In conclusion, the control of DNA replication by an increase in mtDNA we describe here suggests that the mitochondrion does not simply provide the energy at the service of its larger cellular host, but it may actively dictate when cells initiate their

division. Furthermore, metabolic control of chromatin modifications may provide critical links between metabolism and cell division.

Materials and Methods

Strains and plasmids

The haploid *3xABF2*$^{+}$ strain and its wild-type counterpart (14ww) have been described elsewhere (40). Replacement of *SIR2* with a *sir2Δ*::KanMX6 cassette was done by standard methodology (76). BY4743 is a standard diploid strain (77). The strains used in Fig. 2.3 were made ρ^{o} after three passages of single colonies on plates containing 25 μg/ml ethidium bromide. A single colony from the final ethidium bromide passage was then plated on glucose and glycerol-containing plates to ensure the isolated colony was respiratory deficient and no growth occurred on the glycerol plates. Further PCR analysis failed to detect the presence of the *COX2* gene, which is mtDNA-encoded, in the ρ^{o} strains, but it detected the *CIT2* gene, which is nDNA-encoded. We similarly generated the ρ^{-} strains used in Figs 2.6*A*, A-4 and A-6.

For the Sic1p stability experiment described in Figs. 2.5 and A-2, the strains used were diploids, obtained from a cross of YSC3869-9515050 ([P_{GAL}-*SIC1-TAG*::*URA3* (78)], BY4741 (77) otherwise; purchased from Open Biosystems), with strain BY4742 (77) carrying (*CEN-ABF2*$^{+}$) (40, 65), or the empty vector (*CEN-vector*).

Yeast cultivation

For batch cultures we followed established yeast protocols (69). Conditions for chemostat cultures have been described previously (79, 80).

Elutriation

We followed previously described protocols to obtain cell cycle parameters (81) except that the cells were cultured and collected in YPD (0.5% glucose) medium. The percentage of cells in G1 from the flow cytometry panels was calculated from the DNA histograms using the ModFit® software (Verity Software House, ME). Cell cycle progression was also monitored microscopically, by the percentage of budded cells. Cell size (fl) was measured using a channelyzer.

From each elutriation experiment, we plotted the percent of budded cells as a function of cell size. To estimate the critical budding size, when ~50% cells are budded, we used data points from the linear portion of each graph, which were fit to a straight line using the regression function in Microsoft Excel. From the resulting equation [(%budded)=a(Cell size)-b; where a is the slope and b the y-intercept of the line] we calculated the critical budding size for each experiment. The average of all experiments for each strain was then calculated, along with the associated standard deviation.

From the same elutriations, to calculate the rate of cell size increase, we plotted the cell size as a function of time. The data were also fit to a straight line using the regression function in Microsoft Excel. From the slope of the line we obtained the rate of cell size increase. The average of all experiments for each strain was then calculated, along with the associated standard deviation.

RNA methods

Standard protocols (69) were used for RNA extraction and electrophoresis. The *CIT2* and *RPS16A* probes (see Fig. 2.3) were generated by PCR, and labeled using non-

radioactive reagents from the North2South® Biotin Random Prime Labeling Kit (Pierce), according to their instructions. Probe hybridization and detection were performed according to the North2South® Chemiluminescent Hybridization and Detection Kit (Pierce).

mtDNA abundance

We used PCR to estimate the relative amount of mtDNA (see Fig. A-3). The exponential range of amplification for the *COX2* (mtDNA-encoded) and *GID8* (nDNA-encoded) PCR products were determined by performing separate reactions for each of the two amplified products and removing them after 25, 30, or 35 cycles. The PCR products were run on a 2% agarose gel and the ethidium-stained signal intensities for the 30-cycle products (which were in the linear range of amplification) were quantified with Adobe Photoshop®. The ratio between the *COX2* and the *GID8* product was determined to normalize for differences in initial DNA concentration and reaction efficiencies. The ratio for each strain was then compared to $ABF2^{+}$ cells to determine the relative amounts of mtDNA.

Sic1p stability assays

Cultures were diluted 10-fold from an overnight culture in selective liquid synthetic complete medium containing raffinose as carbon source, to a total volume of 10 ml. Cells were grown at 30 °C, with shaking for 30-48 h to synchronize the cells in G1 by starvation. Galactose was then added to 2% (w/v) final concentration for 2 to 3 hours to induce expression of P_{GAL}-*SIC1*-*TAG*. After induction, the cells were pelleted, washed in water, and re-suspended in 20 ml fresh medium containing 2% (w/v) glucose,

to stop expression of P_{GAL}-*SIC1-TAG*. The cells were cultured at 30 °C and 1 ml was taken every 15 min, to monitor Sic1p-TAG levels. Proteins were extracted using TCA precipitation and resolved by SDS-PAGE. For immunoblotting, we used the PAP reagent (Sigma, used according to their instructions) to detect the Protein A epitope present in Sic1p-TAG. The same blot was also probed with an anti-Pgk1p antibody (from Molecular Probes, and used according to their instructions). Pgk1p is not cell cycle regulated, and it is widely used as a loading control in cell cycle experiments, including landmark studies that accurately quantified the levels of cell cycle proteins (82). The intensity of the bands was quantified using Adobe Photoshop, normalizing the levels of Sic1p-TAG to the loading control. Using Microsoft Excel, values were fit to a linear transformation of the exponential decay equation ($\ln X_t = -kt + \ln X_{t0}$, where X denotes the amount of Sic1p-TAG, k the degradation rate constant, and t time) to obtain k from the slope of the line. The half-life of Sic1p-TAG was then determined from $t_{1/2} = \ln 2/k$.

Chromatin immunoprecipitation

For these analyses, cells were cultured in YPD containing 0.5% glucose. The primers and protocols for ChIP experiments and analysis have been described previously (58, 83). ChIPs were performed with anti-Sir2p antisera (Santa Cruz Biotechnology, Cat#: sc-6666) or anti H3K9, K14Ac (Millipore, Cat#: 06-599). Percent immunoprecipitations (%IP) were determined by dividing IP signal by input signal. ChIP experiments were analyzed either by quantitative PCR (Fig. 2.9*B*, A-5), or by slot blot (Figs. 2.9*C*, A-6). For anti-Sir2p ChIPs, chromatin from *sir2D* cells was analyzed

to assess background signal. For anti H3K9, K14Ac ChIPs, "no antibody" controls were included to assess background signal. For slot blot analysis, samples were blotted to a membrane that was hybridized to a ^{32}P-labeled probe spanning the rDNA ARS region. Signals were quantified on a Storm 860 phosphorimager (Molecular Dynamics) using Imagequant software. Ethidium-stained gels were quantified using Quantity One software (BioRad).

Other

For Sir2p immunoblotting (Fig. 2.9*A*) we used anti-Sir2p antisera (Cat#: sc-6666) from Santa Cruz Biotechnology, and a secondary antibody from Pierce, at the recommended dilutions. The anti-Cdc28p antibody used to estimate loading was also from Santa Cruz Biotechnology (Cat#: sc-6708), and used according to their instructions. The immunoblots were processed with reagents from Pierce.

CHAPTER III

SULFUR METABOLISM ACTIVELY PROMOTES INITIATION OF CELL DIVISION IN YEAST

Overview

Sulfur metabolism is required for initiation of cell division, but whether or not it can actively promote cell division remains unknown. Here I show that yeast cells with more mtDNA have an expanded reductive phase of their metabolic cycle and an increased sulfur metabolic flux. I also show that in wild type cells manipulations of sulfur metabolic flux phenocopy the enhanced growth rate of cells with more mtDNA. Furthermore, introduction of a hyperactive cystathionine-β-synthase (CBS) allele in wild type cells accelerates initiation of DNA replication, revealing a novel connection between this sulfur metabolic enzyme and the cell cycle. Since the analogous allele in human CBS suppresses other disease-causing CBS mutations, these findings may be relevant for human pathology. Taken together, the results demonstrate the importance of sulfur metabolism in actively promoting initiation of cell division.

Introduction

Growth is rate limiting for cell division. It has been known for some time that growth and metabolism are required for cell division to take place (47). However, whether metabolism can actively promote cell division remains largely unaddressed due to the previous use of loss-of-function metabolic mutants when studying the

coordination of growth and division. The *S. cerevisiae* nuclear gene *ABF2*$^{+}$ encodes a highly conserved mitochondrial DNA maintenance protein, called TFAM in animals, which binds to and bends mitochondrial DNA (mtDNA) (52, 53). Moderate over-expression of Abf2p, from a low copy number plasmid or from two extra copies integrated in the genome, increases the amount of mtDNA by 50-150% (40). We have previously shown that moderate over-expression of Abf2p causes cells to increase in size faster and accelerate initiation of DNA replication in the nucleus (46). Furthermore, cells with more mtDNA proliferate faster than their wild type counterparts when cultured under carbon limiting conditions (46). These unique properties of cells over-expressing Abf2p represent an experimental system that allows for the eventual dissection of how metabolism can promote cell division.

Sulfur metabolism is critical for many cellular processes, and sulfur metabolic flux correlates with growth rate (35, 84). It has also been known for decades that cells with disrupted sulfur metabolism arrest before initiation of DNA replication (36). Homocysteine lies at a critical juncture between the transsulfuration pathway that leads to cysteine and glutathione (GSH) biosynthesis, and the branch that leads to S-adenosylmethionine (SAM) biosynthesis. Cystathionine-β-synthase (Cys4p in yeast, CBS in mammals) catalyzes pyridoxal 5'-phosphate-dependent (PLP) synthesis of cystathionine from serine and homocysteine (85). In yeast, loss of Cys4p leads to cysteine auxotrophy (86), while even in rich media cell proliferation is delayed by ~ 4-fold (87). Among natural yeast isolates *CYS4* polymorphisms are the most common cause of sensitivity to pharmacological compounds (88). In humans, mutations in CBS

cause homocystinuria, associated with vascular disease (89), with >130 CBS mutations identified in patients (90). Interestingly, a hyperactive CBS allele that encodes a truncated CBS suppresses other disease-causing mutations (91). CBS activity positively correlates with cell proliferation in humans and yeast (92). However, it is not known if CBS activity and sulfur metabolic flux are simply required for cell proliferation, or whether they can also actively promote initiation of cell division.

In this chapter, I show that cells with more mtDNA, which have an accelerated growth rate, also have an increased sulfur metabolic flux. Furthermore, an up-regulation of sulfur metabolism is sufficient to trigger initiation of DNA replication in wild type cells. Finally, I show that in the presence of a hyperactive CBS allele alone, initiation of cell division is accelerated.

Results and Discussion

An increase in mtDNA levels expands the yeast metabolic cycle (YMC)

We had previously shown that cells moderately over-expressing Abf2p proliferate faster than their wild type counterparts (46). Furthermore, we found that these cells accelerate initiation of DNA replication by increasing the rate of cell size increase, or their "growth rate" (see B-1 and (46)). In contrast, most known accelerators reduce the "critical size" for division, and they have no effect on growth rate. Thus, we reasoned that cells over-expressing Abf2p likely carry "gain-of-function" metabolic alterations that promote cell cycle progression. We then used this strain as a tool to

identify metabolic signatures that might impact on the timing of initiation of DNA replication.

To determine how metabolism differs in cells with more mtDNA, I first analyzed their metabolic cycle. When grown under carbon-limited steady-state conditions in a chemostat, yeast cells display robust oscillations in their oxygen consumption as they alternate between glycolytic and respiratory metabolism (28, 29, 31). Following the nomenclature of Tu et al (31), the metabolic cycle can be divided into three major phases: oxidative (Ox), reductive/building (RB), and reductive/charging (RC). DNA replication is restricted to the reductive phases, (29, 32). This dual metabolic and cell cycle synchrony provides a unique experimental approach for studying the coupling of metabolism and cell division.

I evaluated cells transformed with a low-copy centromeric plasmid containing *ABF2* (*CEN-ABF2*$^{+}$) versus empty vector transformants (*CEN-vector*). Cells with more mtDNA had a longer period of the metabolic cycle (5.9 hr vs. 5.3 hr), and specifically showed an expansion of the RC phase (Fig. 3.1). In both strains, the metabolic cycle gated cell division, and DNA replication was triggered only in the reductive phases of the metabolic cycles (Fig. 3.1*B*), as has been previously reported (29, 31, 93). Importantly, although the period of the metabolic cycles of numerous "loss-of-function" mutants is shorter than wild type (32), an expansion of the metabolic cycle I observed in cells with more mtDNA has not been previously described, and it is perhaps consistent with "gain-of-function" metabolic alterations in these cells.

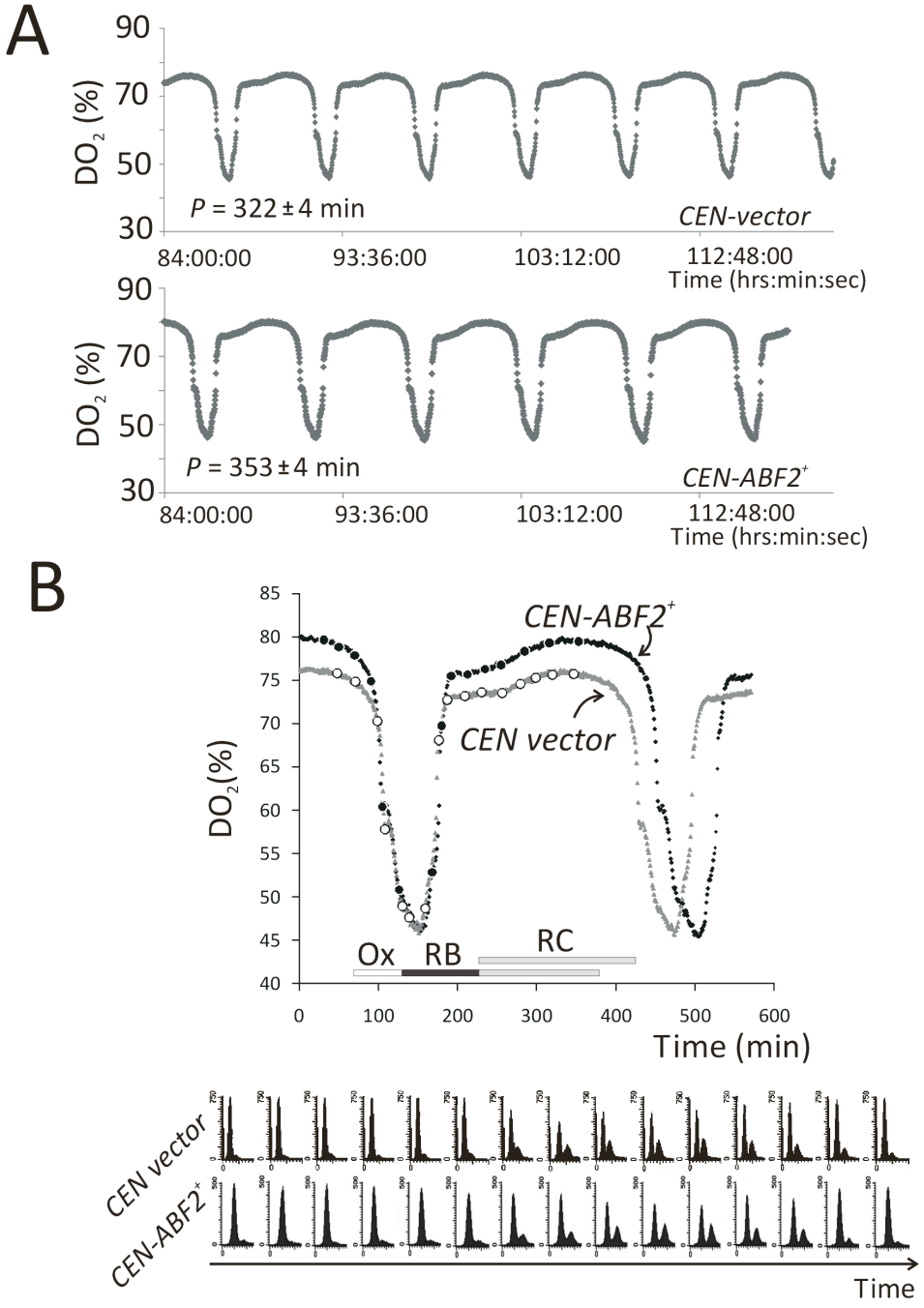

Fig. 3.1. An increase in mtDNA levels expands the Yeast Metabolic Cycle (YMC). **(***A)* Oscillations of dissolved oxygen concentrations (% saturation, DO_2) in continuous cultures of cells carrying either a control empty plasmid (*CEN-vector*), or a plasmid containing *ABF2* (*CEN-ABF2*$^+$). The average (± SD) period, *P*, calculated from the experiments shown is indicated. (*B)* The metabolic cycles of the two indicated strains were superimposed and shown in higher resolution. At regular intervals as indicated, samples were taken and analyzed for DNA content by flow cytometry (shown at the bottom). The corresponding oxidative (Ox), reductive/biosynthetic (RB), and reductive/charging (RC) phases, based on Tu et al. (31) are shown.

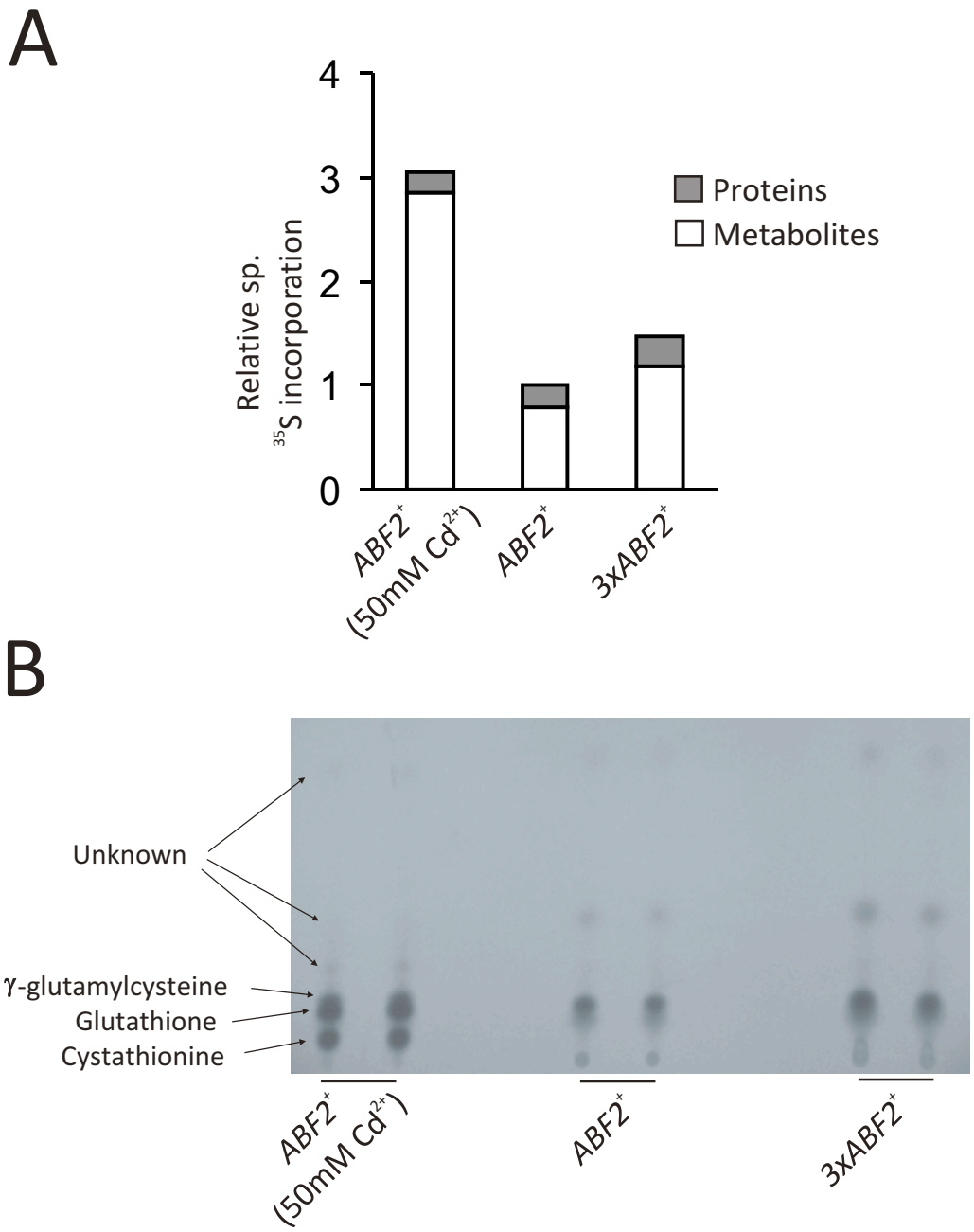

Fig. 3.2. Sulfur metabolite levels are increased in cells with more mtDNA. (*A)* Relative levels of ^{35}S incorporation into proteins and metabolites from ^{35}S -labeled cultures of the indicated strains. Incorporated radioactivity from each extract was quantified by liquid scintillation counting. Results shown are the average of two independent experiments. (*B)* The metabolites fractions from (*A*) were resolved by cellulose thin-layer chromatography. Due to the oxidation with performic acid during sample preparation (see Methods), "glutathione" includes both the oxidized and reduced forms.

Sulfur metabolic flux is increased in cells with more mtDNA

Sulfur metabolism is crucial to the metabolic cycle. Glutathione (GSH), the cell's main redox buffer, peaks during the RC phase (33), the same phase cells over-expressing Abf2p showed an expansion. Because of these links between sulfur metabolism and the RC phase of the metabolic cycle, we sought to determine if sulfur metabolism was altered in cells over-expressing Abf2p. No rate-limiting step exists in the sulfur metabolic pathway, and a change in sulfur metabolite and/or enzyme levels should affect the flux of the overall pathway (94).

To examine if sulfur metabolite levels were altered in *3xABF2*$^{+}$ cells, exponentially growing cells in batch cultures were radiolabeled with ^{35}S. Metabolites were water-extracted by boiling the cells and proteins were TCA-extracted from the cell pellet after removal of the metabolite fraction. As a control, we also treated wild type cells with cadmium sulfate, which is toxic. To cope with the toxicity, cells produce large amounts of glutathione to shuttle cadmium into the vacuoles, at the expense of protein synthesis (95). As expected, overall sulfur metabolites were increased in these cells (Fig. 3.2*A*), with a reduction of radioactivity in the protein fraction. Importantly, sulfur metabolite levels were increased significantly (>40%) in *3xABF2*$^{+}$ cells versus wild type (*ABF2*$^{+}$) cells, but this increase of sulfur metabolites was not at the expense of protein synthesis as in the Cd^{2+} treated cells (Fig. 3.2*A*). Metabolite fractions were further resolved by cellulose thin layer chromatography (TLC) after oxidation with performic acid. Sulfur metabolite levels, including total glutathione levels (reduced plus oxidized forms), were increased in cells with more mtDNA (Fig. 3.2*B*).

I also obtained a genome-wide gene expression profile from cells with increased mtDNA levels (Fig. B-2). I observed the expected higher levels of *ABF2* due to the two extra chromosomal copies of *ABF2*, and also the increased expression from the rDNA (*RDN*) locus, which we had shown to be de-repressed in *3xABF2*$^{+}$ cells (46). Otherwise, there were very few changes in the steady-state mRNA levels in *3xABF2*$^{+}$ cells (Fig. B-2). In retrospect, this is not surprising. Previous microarray experiments identified only 34 genes whose expression was up-regulated (>2-fold) in ρ° petite cells (which do not have mtDNA) compared to ρ^{+} cells (67). Interestingly, regarding mRNAs encoding sulfur metabolic enzymes, there were small (Fig. B-3), but concerted changes: the mRNA levels for most enzymes were slightly elevated, except for *STR2* and *STR3*, which encode enzymes that allow synthesis of homocysteine from cysteine away from glutathione. Thus, expression of sulfur metabolic enzymes from both the GSH and SAM branches is not reduced, and even perhaps slightly elevated. These results, together with the increased sulfur metabolite levels we found in cells with more mtDNA strongly suggest that overall sulfur metabolic flux is elevated, in accordance with the expansion of the RC phase of the metabolic cycle of these cells (Fig. 3.1). Our findings may have broader relevance, because over-expression of the animal ortholog of Abf2p, TFAM, has been recently shown to restore glucose secretion in a mouse model of maturity-onset diabetes (96) and protect from age-dependent impairment of brain performance (97).

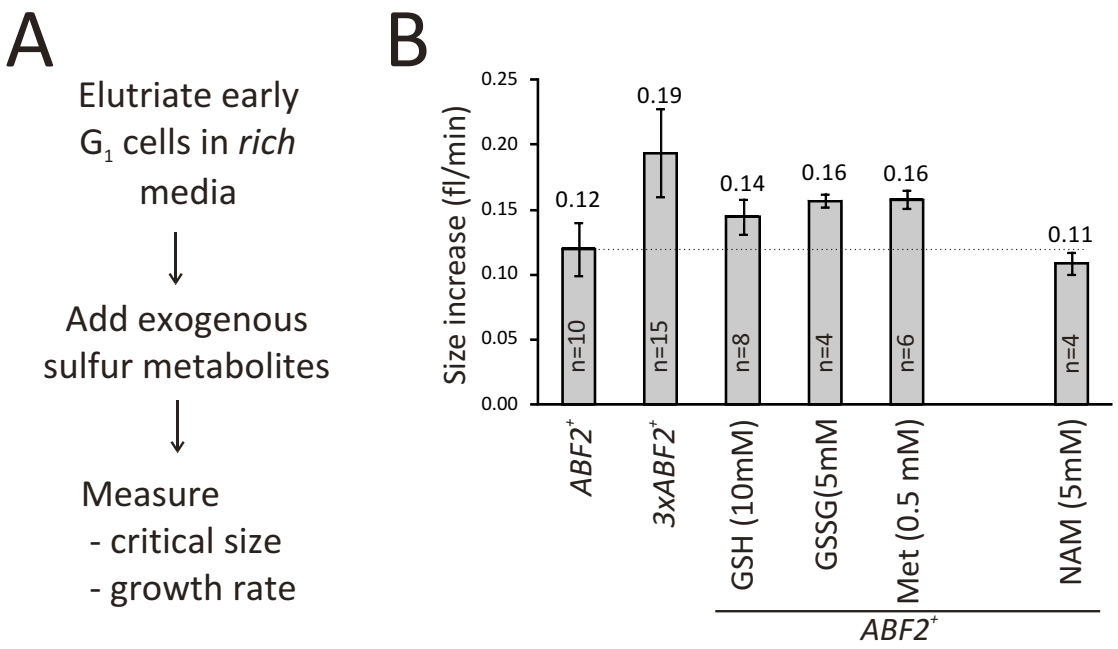

Fig. 3.3. An increase in sulfur metabolic flux accelerates initiation of cell division. (*A)* Schematic of our approach to measure cell cycle parameters after addition of exogenous metabolites. (*B)* The rate of cell size increase (fl/min) of the indicated strains and metabolites added are shown. Values shown are the average (± SD) of the indicated number of experiments.

An increase in sulfur metabolic flux accelerates initiation of cell division

Sulfur metabolism is required for cell division to take place (36), and transcription of certain genes involved in sulfur biosynthetic pathways is cell cycle regulated, peaking in S phase (98). Furthermore, our results that an increase in sulfur metabolic flux is associated with accelerated initiation of cell division in cells with more mtDNA is consistent with other data that sulfur metabolic flux correlates with growth rate (84). However, all these results do not necessarily point to a *causal* role of sulfur metabolism in the control of cell division.

I reasoned that if the increase in sulfur metabolic flux we observed in cells with more mtDNA is responsible for the accelerated growth rate and initiation of cell division in these cells, then an increase in sulfur metabolic flux in wild type cells might lead to similar effects. It has been previously shown that exogenous addition of sulfur metabolites is sufficient to increase the flux of the overall pathway, because there is no rate-limiting step in the sulfur metabolic pathway (94). Consequently, I then examined if adding exogenous sulfur metabolites to wild type cells would phenocopy the enhanced growth rate seen in cells over-expressing Abf2p. Cells were centrifugally elutriated to collect a synchronous population of small, un-budded cells in G1. Note that budding marks initiation of cell division, and serves as a convenient morphological landmark for the G1/S transition. Cells were then re-suspended in fresh, rich media containing extra sulfur metabolites and their cell cycle progression was monitored. The reported growth rates (Fig. 3.3*B*) are the summary of many repeats of individual experiments (Fig. B-1). Remarkably, adding either reduced (GSH) or oxidized (GSSG) forms of glutathione

significantly increased the growth rate of wild type cells, as did the addition of methionine. Adding additional GSH to *3xABF2*$^{+}$ cells did not further enhance their growth rate (not shown). I also tested the effect of nicotinamide (NAM) because it inhibits NAD^{+}-dependent enzymes, including the deacetylase Sir2p (99, 100). Sir2p and similar enzymes are thought to couple energy status with many cellular processes, and we have previously shown that Sir2p acts antagonistically to Abf2p (46). Interestingly, however, NAM did not alter the rate of cell size increase (Fig. 3.3*B*). Overall, although the rich media (YPD) used in this experiment were thought to set an upper limit to how fast cells can grow, addition of sulfur metabolites further increased growth rate.

In all the above experiments I also measured the cell size at which cells trigger a new round of cell division (Fig. B-1). I did not find significant cell size decreases that could explain the accelerated initiation of cell division (Fig. B-1). Thus, from a detailed analysis of both "growth rate" and "critical size" I conclude that an up-regulation of sulfur metabolic flux in wild type cells is sufficient to significantly accelerate initiation of cell division, which can be largely attributed to an increase in growth rate. This is a surprising and important finding, because there is no reason to expect that the growth rate of a fast-proliferating unicellular eukaryote grown in rich medium that is not limited for any particular nutrient, including sulfur, can be further increased by up-regulating sulfur metabolic flux.

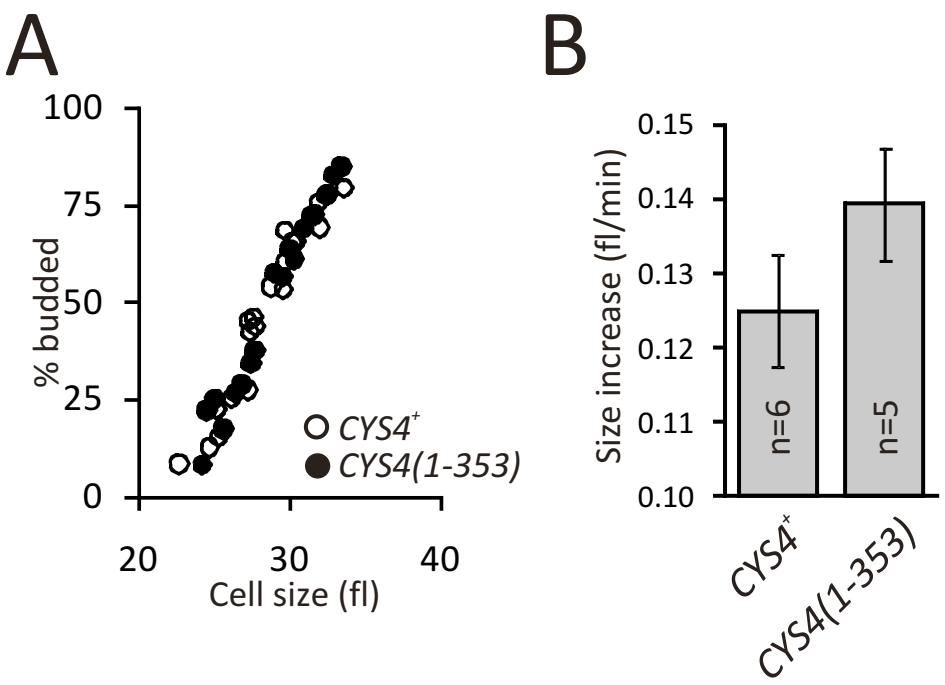

Fig. 3.4. Cys4p(1-353) accelerates initiation of cell division. (*A)* The "critical size" for division is unchanged in *CYS4(1-353)* cells. The raw data points showing the percent of budded cells as a function of cell size, from separate independent elutriation experiments with *CYS4*$^{+}$ and *CYS4(1-353)* strains. The data points shown were from the linear portion of each experiment, when the percentage of budded cells began to increase. (*B)* The rate of cell size increase is elevated in *CYS4(1-353)* cells. The rate of cell size increase was determined from the same elutriation experiments shown in (*A*), as described in Fig. B-1. The raw data for these calculations are shown in Fig. B-5.

Cystathionine-β-synthase and cell cycle progression

Among several sulfur metabolic enzymes examined, only reducing the expression of *CYS4*, the gene encoding cystathionine β-synthase, abolished the yeast metabolic cycles (33). Consequently, I decided to study the effects of cystathionine β-synthase perturbations on cell cycle progression. It was known that in the absence of Cys4p cell proliferation is delayed by ~ 4-fold (87), but I asked the opposite question: Can Cys4p positively affect cell division? To answer this I needed a gain-of-function *CYS4* allele. The C-terminal domain (~145 amino acid residues) is thought to participate in protein-protein interactions (101), and this domain interferes with catalytic activity, because its truncation elevates activity in the human (91) and yeast (102) enzymes. We confirmed these observations by expressing and purifying the full-length (Cys4p) and the truncated (Cys4p(1-353)) yeast enzymes from bacteria, and comparing their kinetic properties (Fig. B-4). The truncated Cys4p(1-353) is a more efficient enzyme, with a k_{cat}/K_M ~ 3-fold higher than that of the full-length enzyme. We then generated a strain that carried only a truncated Cys4p(1-353) instead of the full-length Cys4p, and examined cell cycle progression from synchronous cultures as described above (Figs. B-1 and 3.4).

I found that *CYS4(1-353)* cells have a shorter G1 than their otherwise isogenic wild type (*CYS4*$^+$) counterparts (Fig. 3.4). *CYS4(1-353)* cells bud at the same size (28.9±0.2 fl, n=5) as (*CYS4*$^+$) cells (28.6±0.5 fl, n=6; *P*=0.25, based on a 2-tailed Student's *t* test) (Fig. 3.4*A*). However, *CYS4(1-353)* cells increased in size faster (0.14±0.01 fl/min, n=5) than *CYS4*$^+$ cells (0.12±0.01 fl/min, n=6; *P*=0.01, based on a 2-

tailed Student's *t* test) (Figs. 3.4*B* and B-5). Thus, even though *CYS4(1-353)* cells do not bud at a smaller size, they reach that size ~15% faster than their *CYS4*$^{+}$ counterparts. In conclusion, introduction of a single hypermorphic allele of a sulfur metabolic enzyme, cystathionine-β-synthase, is sufficient to accelerate growth rate and initiation of cell division (Fig. 3.4). Together with our sulfur metabolite analysis, these results reveal a critical role of sulfur metabolism in actively controlling cell division. Perhaps the nature of sulfur metabolism, lacking any rate-limiting steps, allows for adjustments in the overall flux that cannot be easily achieved in other pathways.

Finally, although the most common cause of human disorders in sulfur metabolism is mutations in CBS (89, 90), a role for CBS in cell cycle progression in humans has not been examined. There is a very high degree of conservation between Cys4p and human CBS. Importantly, human CBS can complement yeast cells lacking Cys4p (103). Thus, findings from our yeast studies might be relevant to studies of the human CBS ortholog and sulfur metabolism in general.

Materials and Methods

Strains and plasmids

The haploid *3xABF2*$^{+}$ strain and its wild type counterpart (14ww) have been described elsewhere (40). For the yeast metabolic oscillations we used the CEN.PK strain described in (31). From this strain we generated a Ura^{-} auxotroph (strain SCMSP202) by plating on solid media containing 5-Fluoroorotic Acid (5-FOA). This strain was then transformed with a *URA3*-marked plasmid containing *ABF2* (*CEN*-

ABF2^{+}) (40, 65), or the empty vector (*CEN-vector*). To introduce a *CYS4(1-353)-13MYC::KANMX* allele in the standard BY4742 (*MATα; his3Δ; leu2Δ; lys2Δ; ura3Δ*); strain, we followed a single-step PCR replacement protocol as described (76), to generate strain SCMSP179. The corresponding wild-type isogenic strain carrying a full-length *CYS4-13MYC::KANMX* was also constructed (strain SCMSP178). Both strains were genotyped by PCR and tested for protein expression of the corresponding alleles.

For recombinant expression of Cys4p and Cys4p(1-353) as N-terminal 6xHis fusions, DNA fragments encoding these proteins were generated by PCR and inserted into the NheI and XhoI sites of pET-28 (Novagen), to allow for T7-driven protein expression in *E.coli*. The proteins of interest were purified using TALON® Co^{2+} beads according to the manufacturer's instructions (Clontech), and analyzed for their kinetic parameters as described in (104).

Yeast cultivation and cell cycle analysis

For batch cultures we followed established yeast protocols (69). Conditions for yeast metabolic oscillations in chemostat cultures were identical to previously published methods (31). Centrifugal elutriation conditions, DNA content, "growth rate" and "critical size" analyses were done as we have described (46).

Metabolite levels and cellulose TLC

^{35}S metabolic labeling was done as in (95). Cadmium treated cells were supplemented with 50 mM Cd^{2+} sulfate for one hour prior to labeling. Metabolites were extracted and separated by TLC according to (105), with the exception that cells were quenched with cycloheximide (50 μg/ml) and sodium azide (0.1%) just prior to

harvesting. After 4 hours of labeling with ^{35}S, cells were quenched, harvested, washed in 200 µl ice-cold water, and re-suspended in 50 µl ice-cold water. Metabolites were extracted by boiling for 5 minutes followed by centrifugation to obtain the labeled metabolites in the supernatant. Performic acid was added in a 1:1 ratio to the supernatant to oxidize the metabolites for analysis. 10 µl of sample was applied on cellulose thin layer chromatography using the solvent system butanol-1/acetic acid/water (90:15:33). Along with metabolite extraction, ^{35}S-labeled proteins in the cell pellet were TCA extracted, washed in acetone, and re-suspended in 1M Na_2CO_3, following the protocol of (95). Liquid scintillation counting was used to quantify incorporated radioactivity of the metabolite and TCA fractions.

Microarray analysis

We prepared total RNA from *ABF2*$^+$ and *3xABF2*$^+$ cells grown in chemostats under glucose limitation at a dilution rate of 0.2 h^{-1}, as we have described (46). Microarray hybridizations using Affymetrix methodology were done at a UT Southwestern Medical Center core facility. To facilitate the visualization of the data, the *ABF2*$^+$ and *3xABF2*$^+$ signals were first normalized against the signals for TFIID (*YER148W*), *SRB4* (*YER022W), WBP1* (*YEL002C*) and *TDH1* (*YJL052W*), which were linear in both datasets, taking the average for each control and averaging those ratios. We then calculated the $\log_2$(*3xABF2*$^+$/*ABF2*$^+$) values shown in Figs. B-2 and B-3.

CHAPTER IV

SULFUR ENZYMES AND PHYSICAL INTERACTION WITH THE CELL DIVISION MACHINERY

Overview

We have previously shown that cells over-expressing Abf2p (*3xABF2*$^{+}$) proliferate faster than their wild type counterparts and have accelerated initiation of DNA replication. We know metabolism, and particularly sulfur metabolism, is altered in *3xABF2*$^{+}$ cells. Expression of a truncated, hypermorphic form of a key sulfur metabolic enzyme, Cys4p, accelerates initiation of DNA replication in haploid cells. Here I address the question of how sulfur metabolism impinges on the cell division machinery on a molecular basis. I show that expression of the hypermorphic allele of Cys4p acts recessively to the wild type protein, indicating that Cys4p's effect on initiation of DNA replication is independent of its catalytic activity. We show a physical interaction of Cys4p with the cyclin-dependent kinase Cdc28p *in vivo* and *in vitro*, and show the conservation of Cys4p/Cdk complex *in vitro* using recombinant human proteins. The complex appears to be regulated, as it requires actively dividing cells for formation. Because of the conservation of the complex in yeast and humans and the fact that this type of metabolic enzyme/Cdk binding is not just limited to Cys4, our results suggest a broader phenomenon of metabolic enzymes relaying signals to the cell division machinery to affect cell cycle progression.

Introduction

Sulfur metabolism is well conserved over a wide range of organisms. The transsulfuration pathway, involving the interconversion of homocysteine to cysteine (Fig. 1.1), is found in archaebacteria, yeast, humans, tetrahymena, (86, 106) etc., although differences do exist in the directionality of the pathway for certain organisms. The methyl, or methionine cycle (Fig. 1.1) is also widespread, found in both eukaryotic and prokaryotic cells, (107, 108). The methyl cycle generates *S*-adenosylmethionine (SAM), a methyl donor that is second only to ATP in its frequency of use in a variety of biochemical reactions (109).

Cystathionine-β-synthase is an important enzyme of the sulfur metabolic pathways, catalyzing the pyridoxal 5'-phosphate-dependent (PLP) synthesis of cystathionine from serine and homocysteine (85). It lies at a critical juncture point between the methyl cycle and conservation of methionine and the transsulfuration pathway, leading to the catabolism of methionine and eventual production of glutathione. Cys4p is an evolutionarily conserved protein. Human CBS, when expressed in yeast cells lacking Cys4p, can fully complement the cysteine auxotrophy of *cys4*Δ cells (103). CBS deficiency has implications for human health and disease; deficiencies in this enzyme are the most common cause of homocystinuria (elevated plasma levels of homocysteine). The disease affects the ocular, cardiovascular, skeletal, and nervous systems to varying degrees in afflicted individuals (103). Even individuals with milder forms of the disease are shown to be at increased risk of vascular disease, stroke, heart attack, and dementia (110).

We have previously shown that cells with more mitochondrial DNA have accelerated initiation of DNA replication. These cells increase in size faster than their wild type counterparts, and thus are a unique metabolic gain-of-function cell cycle mutant serving as a tool to determine how metabolism affects the cell cycle. An expanded RC phase (Fig. 3.1) and increase in total sulfur metabolites (Fig. 3.2) show that metabolism, and particularly sulfur metabolism, is altered in *3xABF2*$^{+}$ cells. Adding exogenous sulfur sources to wild type cells, which is known to increase sulfur metabolic flux, caused them to phenocopy *3xABF2*$^{+}$ cells and accelerate START. Furthermore, expressing a truncated hypermorphic allele of Cys4p in yeast cells also caused accelerated initiation of DNA replication (Fig. 3.4). While this data strongly points to a causative role of sulfur metabolism in the initiation of DNA replication, the question of how, on a molecular basis, sulfur metabolism impinges upon the cell division machinery remains unanswered.

Results and Discussion

CYS4(1-353) is recessive to CYS4 regarding START

The C-terminal domain serves as a negative regulatory domain for CBS, and its removal increases the activity of the enzyme in the human (91) and yeast (102) enzymes. Introducing a C-terminal truncated form of human CBS in *cis* with different mutant CBS alleles into *cys4*Δ yeast cells rescued their cysteine auxotrophy (91). The result from (91) highlights the obvious importance of the catalytic activity of cystathionine-β-synthase. Our previously reported data (Fig. 3.4) using *haploid* cells expressing the hyperactive, C-terminal truncated Cys4p(1-353) showed a significant acceleration of initiation of DNA replication. I hypothesized that in *diploid* cells expressing one wild type $CYS4^{+}$ allele and one *CYS4(1-353)* hypermorphic allele, the more active, truncated version of the enzyme would be dominant.

To test this, we repeated the same elutriation experiment as in Fig. 3.4 but instead used a diploid strain, collecting small, unbudded G1 cells and then following their size and progression through the cell cycle. Surprisingly, we found that diploid cells expressing one wild type $CYS4^{+}$ allele and one *CYS4(1-353)* allele grew at the same rate as diploid cells expressing two wild type $CYS4^{+}$ alleles (Fig. 4.1*C*) with nearly identical growth rates of 0.21 fl/min and 0.20 fl/min, respectively, and no significant difference in critical budding size (Fig. 4.1*A*, P=0.64 for growth rates and P=0.08 for critical budding size, 2 tail student's t-test).

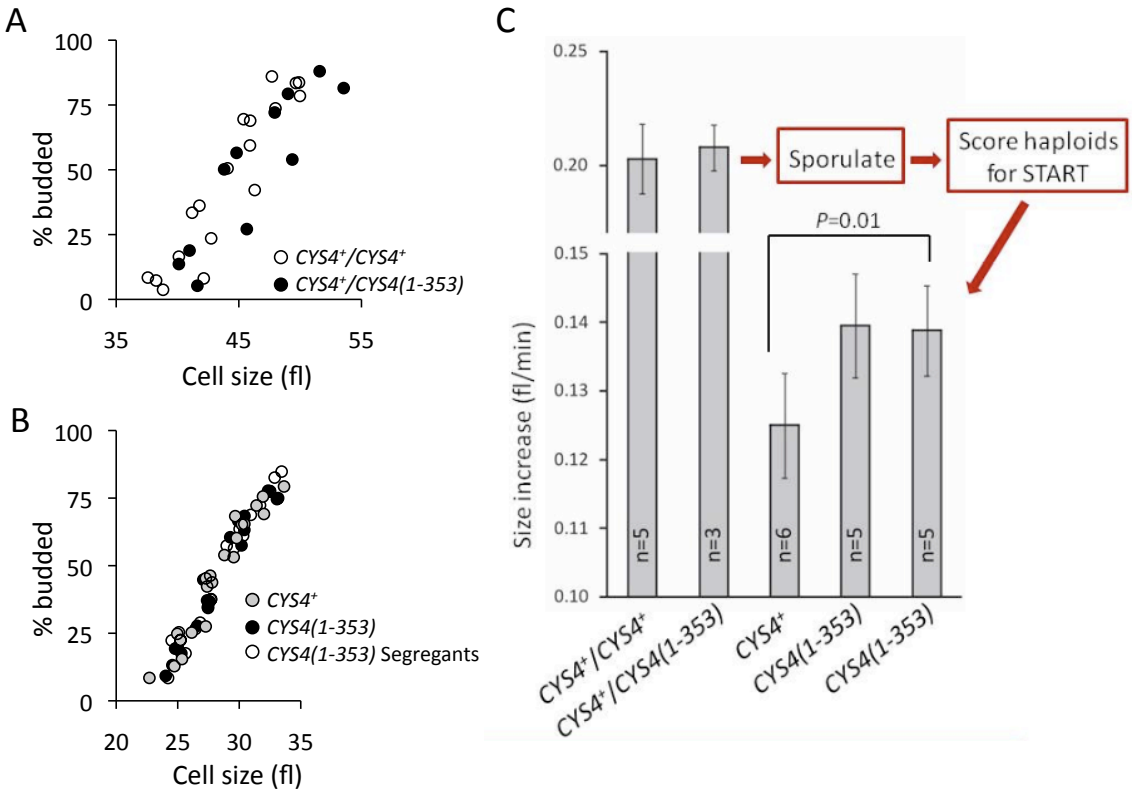

Fig. 4.1. *CYS4(1-353)* is recessive to *CYS4*$^+$ regarding START. *A*, The "critical size" for division is unchanged in *CYS4*$^+$/*CYS4*$^+$ versus *CYS4*$^+$/*CYS4(1-353)* cells and (*B*) *CYS4*$^+$, *CYS4(1-353)*, and *CYS4(1-353)* cells dissected from tetrads in (*A*). *A, B,* The raw data points showing the percent of budded cells as a function of cell size, from separate independent elutriation experiments with the indicated strains. The data points shown were from the linear portion of each experiment, when the percentage of budded cells began to increase. *C*, The rate of cell size increase is unchanged in *CYS4*$^+$/*CYS4*$^+$ versus *CYS4*$^+$/*CYS4(1-353*) cells. A significant increase in growth rate exists for *CYS4*$^+$ versus *CYS4(1-353)* cells. The rate of cell size increase was determined from the same elutriation experiments shown in *A* and *B*. The raw data for these calculations are shown in Figs. B-5, C-1 and C-2.

To ensure that our initial results in Fig. 3.4 were not the result of an unknown mutation occurring during construction of the strains, we sporulated diploid *CYS4*$^{+}$*/ CYS4(1-353)-13MYC* cells and dissected tetrads to segregate away any additional mutation that may have led to the accelerated initiation of cell division in our original haploid cells. We again repeated elutriation experiments identical to that in Fig. 3.4 using haploid cells expressing Cys4p(1-353) and saw the same enhanced growth rate with no difference in critical budding size (Fig 4.1*C*, compare *CYS4*$^{+}$ to the sporulated *CYS4(1-353)* cells, growth rates of 0.125 fl/min versus 0.139 fl/min, respectively, P=0.01 for growth rate, P=0.56 for size, 2 tail student's t-test). This result not only confirmed the results of our initial experiment, but because the diploid cells showed no significant difference in growth rate or critical budding size, we conclude that the *CYS4(1-353)* allele is recessive to *CYS4*$^{+}$ and caused no accelerated initiation of DNA replication. Since increased enzymatic activity did not appear to be responsible for the acceleration of initiation of DNA replication, we decided to investigate other possibilities for how Cys4p might be exerting its effect on START.

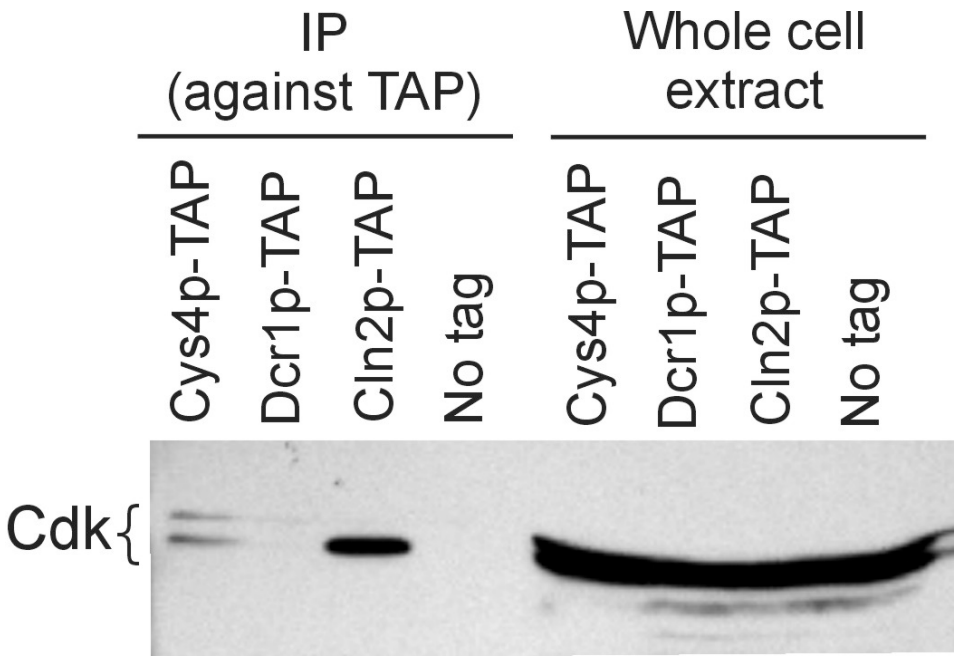

Fig. 4.2. Cdc28p binds Cys4p *in vivo*. A western blot of co-immunoprecipitation experiments was performed on whole cell extracts of cells containing the indicated TAP tagged protein or an untagged control strain. Rabbit IgG agarose beads were used to pull down the TAP tag. The membrane was probed with an antibody against a conserved motif of Cdc28p to see if the yeast Cdk was pulled down along with the TAP tagged protein. Whole cell extracts were run in parallel with the IP lanes to use as a loading control.

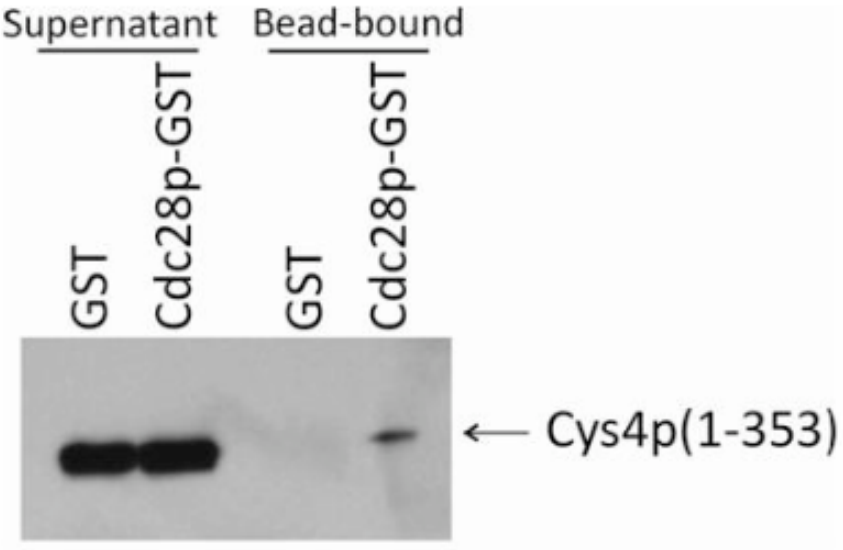

Fig. 4.3. Cys4p(1-353) binds Cdc28p *in vitro*. Western blots of co-immunoprecipitation experiments using recombinant Cdc28p and Cys4p(1-353) were performed by pulling down the GST tagged Cdc28p and probing the bead bound and supernatant fractions to detect the presence of Cys4p(1-353) using an antibody against hCBS which also detects yeast Cys4p. As a negative control free GST was added to the beads along with the Cys4p(1-353).

Cys4p and Cdc28p physical interaction

While most of the work done on cystathionine-β-synthase focuses on its catalytic role in sulfur metabolism, evidence exists suggesting that CBS has additional functions in the cell not directly related to its β-synthase activity. Expressing a nearly inactive mutant of human CBS in CBS knockout mice rescued their neonatal lethality even though the animals still retained elevated levels of homocysteine (111). A genome wide proteomics study using mass spectrometry revealed Cys4p to be part of a large protein complex containing Cdc28p (37), the Cdk controlling cell cycle progression in yeast. I decided to test if we could detect a physical interaction of Cys4p with Cdc28p by performing co-immunoprecipitation experiments.

For this experiment I pulled down TAP-tagged Cys4p from whole cell extracts using rabbit IgG agarose beads, then washed the beads and separated the immunoprecipitated proteins via SDS PAGE. The membrane was probed with the PSTAIR antibody, which recognizes a conserved region of Cdks involved in cyclin binding (112, 113), to detect Cdc28p. I used Cln2p-TAP as a positive control, and Dcr1p-TAP and cells without a TAP tag as negative controls. I was able to detect Cdc28p in the IP lane for both Cln2p-TAP and Cys4p-TAP, while little to no signal was present in the two negative control lanes (Fig. 4.2).

For a variety of technical reasons I was unable to perform the reverse IP *in vivo*, *i.e.*, pulling down Cdc28p and seeing if Cys4p was also present. We were, however, able to detect *in vitro* binding using recombinant semi-pure Cdc28p and a purified, truncated form of Cys4p. For this experiment, Cdc28p containing a GST tag and

purified Cys4p(1-353)-6xHIS were mixed and added to glutathione beads. The beads were then washed and the proteins analyzed by SDS-PAGE to determine if Cys4p(1-353) was pulled down along with the GST tagged Cdc28p. As a negative control to ensure Cys4p(1-353) was not simply binding to the GST tag, we added purified GST protein alone with Cys4p(1-353). The results show a very strong signal for Cys4p(1-353) in the pulldown from the glutathione beads and no detectable signal in the negative control lane (Fig. 4.3). Thus, Cys4p and Cdc28p are capable of interacting directly *in vitro*, in the absence of other "bridging factors."

Since we have shown the yeast Cdk and Cys4p to interact, and both human Cdk2 and hCBS can complement yeast cells lacking Cdc28p (114) or Cys4p (103), respectively, we wanted to see if these proteins might also physically interact. For this experiment we used purified recombinant human CBS (hCBS), yeast Cys4p, or yeast Cysp(1-353) with an N-terminal 6xHis fusion and commercially available recombinant Cdk2/cyclin E (from Enzo®) supplied as GST-fusions.

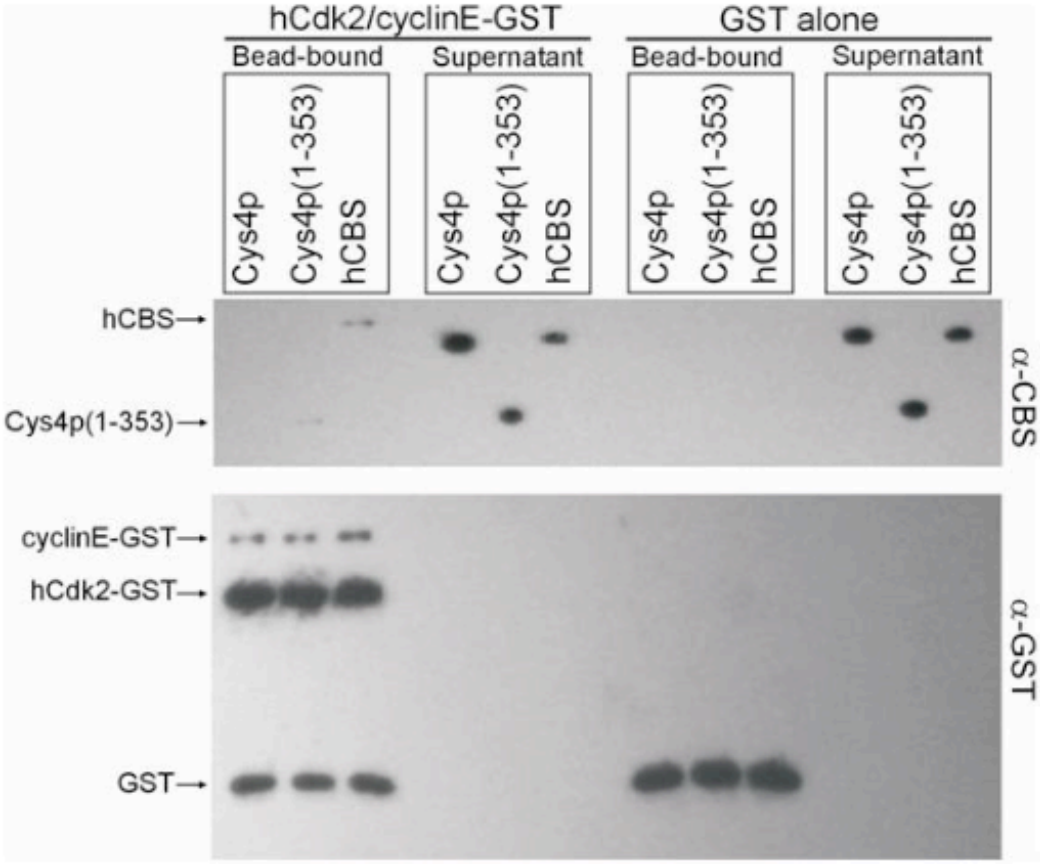

Fig. 4.4. hCBS and yeast Cys4p(1-353) interact with human Cdk2/cyclin E complex *in vitro*. Western blots of co-immunoprecipitation experiments using recombinant hCdk2/cyclin E complex and orthologs of Cys4p were performed by pulling down the GST tagged Cdk/cyclin complex and probing the bead bound and supernatant fractions to detect the presence of yeast Cys4p or the human ortholog. As a negative control free GST was added to the beads along with the Cys4p orthologs. The membrane was re-probed with an anti-GST antibody to detect the presence of the Cdk2/cyclin E complex and free GST.

We first allowed the Cdk2/cyclin E complex to bind glutathione beads, washed the beads, blocked with BSA, and then added Cys4p or hCBS protein in 10-fold molar excess that of the Cdk2/cyclin E complex. As a negative control, an additional set of samples was processed, but free GST was added to the reaction as opposed to the Cdk2/cyclin E complex. The beads were washed a final time and both the supernatant and bead bound fractions analyzed by western blotting. Fig. 4.4 shows binding of hCBS to the Cdk2/cyclin E complex, as detected by an anti-CBS antibody. A faint but detectable signal was also discernible in the yeast Cys4p(1-353) lane. Re-probing of the membrane with an anti-GST antibody showed the presence of the free GST used as a negative control and the Cdk2 and cyclin E proteins. The ratio of Cdk2:cyclin E from the commercially available complex was not 1:1, and this may have decreased CBS binding if the Cdk2/cyclin E complex is required for CBS to bind. Nonetheless, these results show the conservation of the Cys4p/Cdk interaction *in vitro* from yeast to humans.

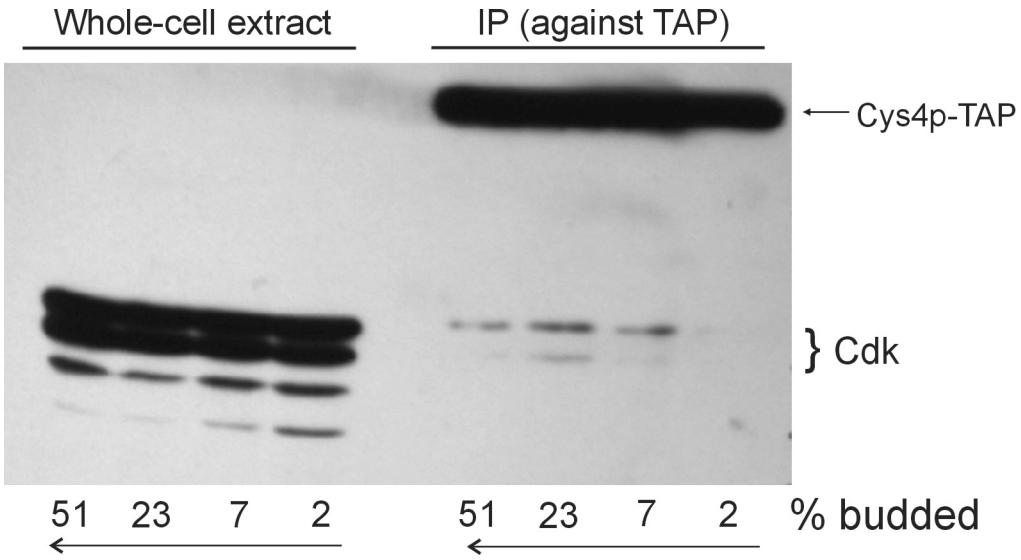

Fig. 4.5. Regulation of the Cys4p/Cdc28p interaction. Cells expressing Cys4p-TAP were synchronized by starvation, then washed and re-suspended in fresh YPD media containing 0.5% glucose. Aliquots were collected at the indicated budding indices. For each aliquot collected, a co-immunoprecipitation experiment was performed as in Fig. 4.2. As a loading control, whole cell extracts were run in parallel with the immunoprecipitated fractions. The protein A portion of the TAP tag cross reacts with the anti-Cdc28p antibody, and this serves as a control to ensure Cys4p was pulled down equally at all timepoints.

Regulation of the Cys4p/Cdc28p interaction

To determine if the interaction of Cys4p and Cdc28p varies as a function of the cell cycle, co-immunoprecipitation experiments were performed at different timepoints on a synchronous culture of cells as they advanced through the cell cycle. Cells were synchronized by starvation, washed in PBS, and resuspended in fresh YPD media. Samples were taken immediately upon resuspension in fresh media and at three additional timepoints with the indicated budding indices. Co-immunoprecipitation experiments identical to the one shown in Fig. 4.2 were performed on the aliquot collected at each timepoint (Fig. 4.5). Virtually no Cdc28p was detected by pulling down Cys4p-TAP at the timepoint when the cells were in a G_o starved state (budding index of 2%). Cdc28p was detected at each of the remaining three timepoints, with a possible peak when the cells were 23% budded. This result points toward regulation of the Cys4p/Cdc28p interaction and even suggests that binding may reach a maximum as the cells are going through the G1/S transition. More experiments need to be performed, however, before making a definitive statement on the temporal versus nutrient dependent regulation of this complex formation.

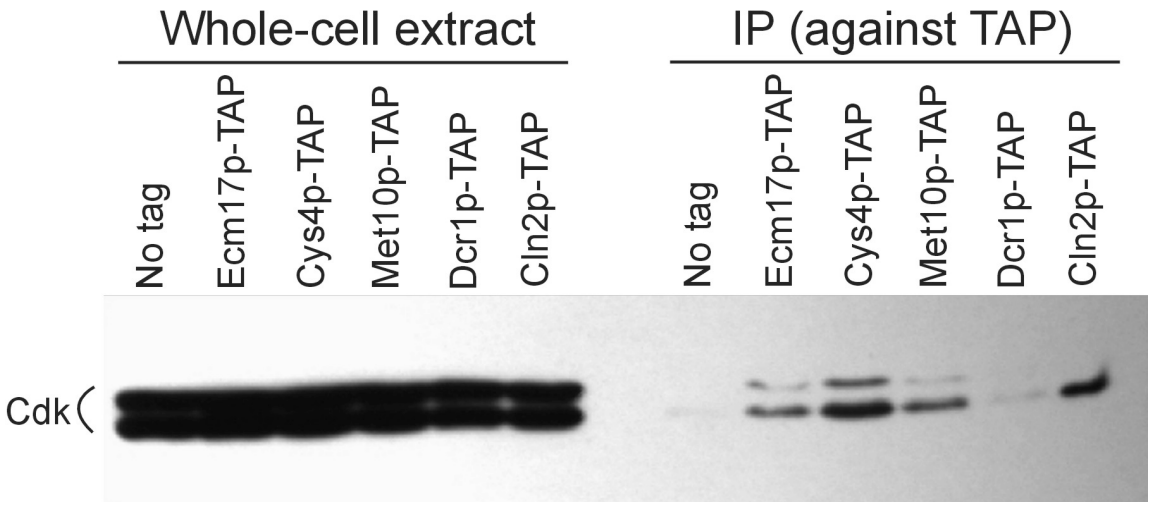

Fig. 4.6. Both subunits of sulfite reductase, Met10p and Ecm17p, interact with Cdc28p *in vivo*. A western blot performed as in Fig. 4.2, but with two additional proteins.

The phenomenon examined here, of a metabolic enzyme binding to a Cdk, may not be unique to Cys4p. I also examined the interaction of sulfite reductase with Cdc28p. Sulfite reductase consists of an alpha and beta subunit, Met10p and Ecm17p, respectively. Met10p was identified in two genome-wide proteomic studies to bind to Cdc28p (37, 38), and our co-immunoprecipitation analysis, performed the same as in Fig. 4.2, also showed an interaction of both sulfite reductase subunits with Cdc28p (Fig. 4.6).

The finding that two different metabolic enzymes physically interact with Cdc28p, and that at least *in vitro*, the Cys4p/Cdk interaction is conserved from yeast to humans, warrants further investigation of what could be a broader mechanism of metabolism affecting the cell cycle. Because of the conservation of the Cys4p/Cdk interaction, we will focus on separating the catalytic activity of Cys4p versus its ability to form a complex with Cdc28p. This type of analysis will allow us to draw conclusions about the effect of Cys4p binding on the interaction of the Cdk with its cyclins as well as what binding does do the catalytic activity of Cys4p and Cdc28p.

Materials and Methods

Strains and plasmids

To introduce a *CYS4(1-353)-13MYC::KANMX* allele in the standard BY4742 (*MATα; his3Δ1; leu2Δ0; lys2Δ0; ura3Δ0*); strain, we followed a single-step PCR replacement protocol as described (76), to generate strain SCMSP179. The corresponding wild-type isogenic strain carrying a full-length *CYS4-13MYC::KANMX*

was also constructed (strain SCMSP178). Both strains were genotyped by PCR and tested for protein expression of the corresponding alleles.

For recombinant expression of Cys4p and Cys4p(1-353) as N-terminal 6xHis fusions, DNA fragments encoding these proteins were generated by PCR and inserted into the NheI and XhoI sites of pET-28 (Novagen), to allow for T7-driven protein expression in *E.coli*. The proteins of interest were purified using TALON® Co^{2+} beads according to the manufacturer's instructions (Clontech), and analyzed for their kinetic parameters as described in (104).

For recombinant expression of Cdc28p GST, we used a Cdc28 HA construct cloned into the BamHI-EcoRI sites of pGEX-2T (115) and transformed into NEB Express I^q competent *E. Coli* (New England Biolabs, Inc.) according to the manufacturer's instructions. 10 ml LB containing amplicillin at 100 mg/ml and 0.5 M NaCl were inoculated and grown overnight at 37°C. The overnight culture was used to inoculate a 500 ml culture at 1:500 in LB containing ampicillin at 100 mg/ml and 0.5 M NaCl. Cells were grown at 37°C with shaking at 200 rpm, until the OD_{600} reached 0.5-0.7. IPTG was added to 0.4 mM and the cells were shifted to 23°C with shaking at 200 rpm to grow overnight.

Cells were harvested by centrifuging at 4,000 rpm for 30 min at 4°C. The supernatant was removed and cells frozen at -80°C for 3-4 hr. The frozen pellets were re-suspended in B-PER® reagent from Pierce containing lysozyme (0.1 mg/ml), DNaseI (5U/ml), β-mercaptoethanol (1mM), and protease inhibitor (Roche Complete Mini, EDTA-free, used according to manufacturer's instructions). 25 ml B-PER® reagent was

used per cell pellet obtained from the original 1 L culture. The re-suspended cell pellets were placed at room temperature, with rocking, for 15-20 min, then centrifuged for 30 min at 10,000 rpm. The supernatant was filtered through a 0.22 μm disk and applied to a 1.5 ml column packed with immobilized glutathione (Pierce) equilibrated with GST buffer (see below).

The column was washed with 20-30 bed volumes of GST buffer and eluted with 10 bed volumes of GST buffer containing 10 mM reduced glutathione, collected in 10-12 fractions. The A280 for each fraction was measured and a small aliquot analyzed by SDS-PAGE and Coomassie staining. The fractions containing the highest levels of the GST fusion protein were pooled and concentrated using a Vivaspin concentrator.

Yeast cultivation and cell cycle analysis

For batch cultures we followed established yeast protocols (69). Sporulation was carried out in 1% potassium acaetate, rotating at room temperature for 6 days. Tetrads were dissected onto non-selective plates, then colonies re-plated on selective plates to determine mating type and allele of *CYS4*. Centrifugal elutriation conditions, DNA content, "growth rate" and "critical size" analyses were done as we have described (46).

Yeast cell lysates

Cells were grown to log phase in YPD containing 0.5% glucose unless otherwise noted. Cells were washed twice in ice cold PBS and either processed immediately or frozen at -80^{o}C for further use. An equal volume of buffer (10mm K-HEPES, pH 7.9, 10mM KCl, 1.5mM MgCl2, and protease inhibitor (Roche Complete Mini, EDTA-free, used according to manufacturer's instructions) was added to the cell pellet. Cells were

then run twice through a French press and spun for 15min at 5,000rpm at 4°C. The supernantant was removed and spun again for 3min at 5,000rpm at 4°C. To this supernatant, the following were added to achieve the following final concentrations: Tris-Cl, pH 8.0, 10mM; NaCl, 150mM; and NP40, 0.1%.

Co-immunoprecipitation experiments

For *in vivo* assays, 1mL of cell lysate was added to 50uL of washed rabbit IgG agarose couple beads (Sigma A2909). The lysate/bead slurry was incubated for 2 hours at 4°C, rotating. Beads were washed 7x in buffer (Tris-Cl, pH 8.0, 10mM; NaCl, 150mM; and NP40, 0.1%) and 1x in PBS. Beads were then re-suspended in SDS loading buffer.

For the *in vitro* co-immunoprecipitations using human recombinant cyclin/Cdk, approximately 50uL of glutathione beads were pre-washed in GST buffer (150mM NaCl, 20mM Tris, pH 8.0, 1mM MgCl2, 0.1% NP40, 10% glycerol, protease inhibitor (Roche Complete Mini, EDTA free, used according to the manufacturer's instructions), and 1mM β-mercaptoethanol, added fresh). 1μg of cyclin/Cdk complex or 0.25μg free GST was added to the beads and incubated, rotating, for 1 hr at room temperature. Beads were then washed 3x, 5-10 min rotating each wash. Beads were then blocked with 5% BSA in GST buffer, made fresh and filtered, for 1 hour at RT. Beads were washed 3x as before, and 10x molar excess (compared to the cyclin/Cdk complex) of purifed Cys4 or hCBS was added to the beads in GST buffer. Beads were washed 3x as before and re-suspended in SDS loading buffer.

For the *in vitro* co-immunoprecipitation of the yeast Cdk with the truncated form of Cys4p, beads were pre-washed as described above. Cdc28p GST or free GST (final 16μg/ml) recombinant protein and Cys4p(1-353) (final 5.8 μg/ml) was added to the beads in GST buffer. Incubation was overnight, 4^{o}C, rotating. Beads were washed 3x as described above and re-suspended in SDS loading buffer.

Samples were analyzed by SDS-PAGE and transferred to a PVDF membrane. For immunoblotting we used an antibody against the PSTAIR motif of Cdc28p (Cat#: ab10345) from Abcam Inc., and a secondary antibody from Pierce, at the recommended dilutions. Yeast Cys4p and hCBS was detected using an anti-CBS antibody (Cat#: sc-46830) from Santa Cruz Biotechnology, and a secondary antibody from Pierce, at the recommended dilutions. GST and the GST fusion proteins were detected using an anti GST antibody (Cat#: 30001) from Pierce, and a secondary antibody from Pierce, at the recommended dilutions. The immunoblots were processed with reagents from Pierce.

CHAPTER V

CONCLUSION

Metabolism has generally been thought of as a continuous process operating in the background of cells, a process known to be *required* for cell division to take place but not thought to actively *promote* division. We hypothesized that metabolism and growth play a causal role in determining when cells divide, a topic that has gone largely unstudied. In order to address the question of whether or not metabolism can actively promote cellular division, we first needed to identify a unique type of mutant that was both a gain-of-function metabolic mutant and an accelerator of cell proliferation. We found this in cells that over-express Abf2p, leading to increased levels of mtDNA.

Cells with more mtDNA displayed an over-proliferation phenotype and were able to outcompete wild type cells when grown under carbon limiting conditions. Careful analysis of progression through the cell cycle demonstrated increased growth rates that allowed these cells to reach their critical budding size sooner than their wild type counterparts. These same cells also displayed physical changes at the chromatin level, with less Sir2p and increased acetylation at nuclear origins of DNA replication.

To further examine how metabolism was affected in our over-proliferating mutant, we examined the metabolic cycle of these cells and found the reductive phase to be expanded compared to wild type cells. Several sulfur metabolites were known to peak during this phase, which led us to examine sulfur metabolism in cells with more mtDNA. Sulfur flux in *3xABF2*$^{+}$ cells was up-regulated, and adding exogenous sulfur

sources to wild type cells caused them to phenocopy the enhanced growth rate and accelerated initiation of DNA replication seen in *3xABF2*$^{+}$ cells.

We next examined a key enzyme of sulfur metabolism, Cys4p in yeast or CBS in humans. Expression of a hypermorphic allele of *CYS4*$^{+}$ caused accelerated initiation of DNA replication. The *CYS4(1-353)* mutation acts recessively to *CYS4*$^{+}$, however; thus, the phenotype we saw is likely due to roles of Cys4p not related to its enzymatic activity in sulfur metabolism. Investigation of other possibilities for how Cys4p(1-353) might be exerting its affect to cause START acceleration showed a physical interaction of Cys4p with the yeast Cdk, Cdc28p. *In vitro*, the interaction appears to be conserved in humans, with the Cdk2/Cyclin E complex shown to bind to hCBS.

This project began with identification of a gain-of-function metabolic mutant that proliferated better than wild type cells. From that initial strain, we have been able to not only identify that sulfur metabolism specifically affects START, but also a physical link of two sulfur metabolic enzymes with the yeast Cdk. This physical interaction of a metabolic enzyme with a Cdk by co-immunoprecipitation techniques is the first of its kind to be shown. Because we detected the Cys4p/Cdk interaction with the human orthologs, this may indicate a broader mechanism for how metabolic signals are transmitted to the cell division machinery to help cells determine when to divide.

This work has focused on the sulfur metabolic pathways of yeast, where an eventual direct interaction with an evolutionary conserved enzyme, cystathionine-β-synthase, was shown to interact with the core yeast cell division machinery, also highly conserved. *In vitro*, the interaction was also identified using the homologous human

proteins. Cystathionine-β-synthase has been most often studied on the basis of its kinetic activity in sulfur metabolic pathways. Yet here we find a metabolic enzyme binding to core cell division machinery, a property that seems far away from its traditionally studied role. Much more work for the future lies ahead to determine the functional significance of this interaction. Some questions to answer include: how is the interaction regulated—by nutrient conditions or temporally throughout the cell cycle, how does the interaction affect the activity of both CBS and the cyclin dependent kinase, can the metabolic activity of CBS be separated from its function in binding the cyclin dependent kinase?

A single protein with two distinct functions is certainly not unprecedented in the literature, with more and more moonlighting proteins being identified. In order to function as a moonlighting protein, the protein must be able to switch between functions. Mechanisms for doing this include (but are not limited to nor mutually exclusive): being at two different cellular locations, differential expression by different cell types, binding of cofactors, oligomerization, complex formation, containing multiple binding sites, changes in the cellular concentration of a ligand or product, and change in redox status of the cell (116, 117).

CBS is a good candidate for a moonlighting protein. Besides its known role in sulfur metabolism and its possible effect on the cell division machinery we have uncovered, it displays many properties that would potentially allow for the functional "switch" to operate. For starters, CBS in humans is known to be sumoylated, leading to a nuclear localization of the protein (101). Secondly, the oligomerization state of CBS is

known to vary on the basis of whether or not the protein contains the inhibitory C-terminal tail (85).

Our *in vitro* co-IP data already provide preliminary evidence that in the absence of additional proteins, it is the truncated form of the enzyme that seems to bind the cdk. Perhaps a structural change involving loss of the C-terminal tail or the change in oligomerization state affects its binding to the cell division machinery. Lastly, CBS lies at a critical juncture in metabolism that ultimately leads to the production of glutathione. Glutathione is the cell's main redox buffer, and CBS activity *in vitro* and flux through the glutathione synthesis pathway *in vivo* (85), can be enhanced by changing the oxidation state of the cell. A redox switch could also provide the mechanism that allows CBS to have two distinctive functional roles.

How plausible is it for a protein to function dually in both a metabolic pathway and in conjunction with the cell division machinery? The moonlighting proteins identified are very diverse in their function, and certainly do not rule out the possibility of CBS also impinging upon cell division. Existing evidence indicates that metabolic enzymes may be good moonlighting enzymes. For example, aconitase functions in animals as both a Krebs cycle enzyme in the mitochondrial and as an iron responsive protein in the cytosol, regulating the translation of of certain proteins involved in iron metabolism (118). Aconitase in yeast similarly acts as a both a Krebs cycle enzyme and also functions in mtDNA maintenance (119).

Since we were able to recapitulate the CBS/Cyclin-Cdk interaction *in vitro* with human proteins, it is interesting to speculate on how this type of interaction may function

within the context of a multi-cellular organism with different tissue types. A large body of evidence already exists for the role of amino acids in general acting to regulate metabolic pathways (120). There is a smaller, but growing, body of evidence suggesting that sulfur amino acids in particular may play a role in signaling (120), including the activation of intracellular kinases by methionine, expression of a fibroblast ubiquitin ligase by methionine, and increased activity of transcription factor NFκB via cysteine levels (120).

Evidence already exists showing that manipulating sulfur metabolism through diet or as a consequence of disease affects different tissues to varying degrees, so it seems plausible that our model of CBS binding to the Cdk could work well in a multicellular organism as well. Because sulfur compounds play a role in combating oxidative stress, it is also possible that redox status may play a role in how sulfur metabolism exerts its effect on signaling. This is especially interesting in the context of mammals, where the CBS enzyme contains a redox responsive heme group. Combined with existing data that cells with higher reduction potentials show increased response to cell proliferation and cell survival, while more oxidized cells respond stronger to signals of differentiation and death, the possibilities for how CBS could be made responsive to the needs of the cell and its capacity to divide are endless (121). This type of regulation also provides one model where the CBS/Cdk interaction can be regulated differently and have different effects in various tissue types.

This type of regulation may not just be limited to the sulfur pathways. While Lafaye, *et al*. (94) showed no rate-limiting step for the sulfur metabolic pathways in

yeast, this may be more common to other pathways than initially thought. For several decades, manipulating metabolism in an organism has focused on a "rate limiting step." Criteria for being one of these key enzymes included things such as location in the pathway (at the beginning or a branch point), enzymes that are susceptible to regulation by compounds found in other metabolic pathways, such as NADH/NAD^+, and ATP/ADP, and having a low maximal rate (V_{max}). Once accepted as a rate limiting step, researchers often focus solely on that particular enzyme and its substrates, ignoring other possible sources of control. However, attempts to control overall metabolic flux via one rate limiting step have often proved unsuccessful (122).

As people began to see flaws in the traditional approaches to the control of metabolism, other ways of analyzing the importance of an enzyme to the overall metabolic pathway were developed. One of these approaches is Metabolic Control Analysis (MCA). It does away with the notion of a rate-limiting step, and instead deals with determining *how* both overall metabolic flux and metabolite concentrations vary with enzyme activity (122). These types of analyses have shown that even for well-studied pathways such as glycolysis, control of flux often resides equally between more than one enzyme or even an enzyme that was not traditionally considered a rate-limiting step (122). This type of scenario seems to better mimic what occurs under physiologic conditions in the cell (122), and it is highly probable that more metabolic pathways will be found to act similarly to the sulfur metabolic pathway in that there is no one enzyme that is controlling overall flux of that particular pathway.

The data presented in this dissertation examine for the first time an interaction of a metabolic enzyme with a Cdk via co-immunoprecipitation. Because both CBS and the cell division machinery are well-conserved proteins, we expect this interaction might be found in many eukaryotes, including humans, where we have shown preliminary data supporting this. Due to the properties of cystathionine-β-synthase, and the role that amino acids and particularly sulfur amino acids play in regulation, the link of CBS with a Cdk as a way to integrate metabolic signals with cell division is not only exciting, but plausible based on the properties of the enzyme and of sulfur metabolism in general. As more data becomes available through Metabolic Control Analysis and other approaches of various metabolic pathways, we may find a general trend where flux can be increased through these pathways and cause signaling to the cell division machinery in a manner similar to that of CBS.

Signal integration between metabolism and the cell division machinery must exist, but little is known about how it might occur. The data presented here provide at least one possible mechanism whereby metabolic signals are tied in with the cell division cycle. Based on the properties of both cystathionine-β-synthase and the Cdk, this type of mechanism, though still unexplored, should be a promising avenue of future study. Even more importantly, a growing body of evidence suggests no reason this type of mechanism is limited to only the sulfur metabolic pathway or could not work in higher eukaryotic organisms.

REFERENCES

1. Raina AK, Zhu X, Smith MA (2004) Alzheimer's disease and the cell cycle. *Acta Neurobiol Exp (Wars)* 64:107-112.

2. Hartwell LH, Culotti J, Reid B (1970) Genetic control of the cell-division cycle in yeast. I. Detection of mutants. *Proc Natl Acad Sci USA* 66:352-359.

3. Hartwell LH, Culotti J, Pringle JR, Reid BJ (1974) Genetic control of the cell division cycle in yeast. *Science* 183:46-51.

4. Hartwell LH (1973) Synchronization of haploid yeast cell cycles, a prelude to conjugation. *Exp Cell Res* 76:111-117.

5. Nurse P, Thuriaux P, Nasmyth K (1976) Genetic control of the cell division cycle in the fission yeast Schizosaccharomyces pombe. *Mol Gen Genet* 146:167-178.

6. Nurse P, Thuriaux P (1980) Regulatory genes controlling mitosis in the fission yeast Schizosaccharomyces pombe. *Genetics* 96:627-637.

7. Beach D, Durkacz B, Nurse P (1982) Functionally homologous cell cycle control genes in budding and fission yeast. *Nature* 300:706-709.

8. Lee MG, Nurse P (1987) Complementation used to clone a human homologue of the fission yeast cell cycle control gene cdc2. *Nature* 327:31-35.

9. Masui Y, Markert CL (1971) Cytoplasmic control of nuclear behavior during meiotic maturation of frog oocytes. *J Exp Zool* 177:129-145.

10. Guerrier P, Moreau M, Doree M (1977) Hormonal control of meiosis in starfish: stimulation of protein phosphorylation induced by 1-methyladenine. *Mol Cell Endocrinol* 7:137-150.

11. Maller J, Wu M, Gerhart JC (1977) Changes in protein phosphorylation accompanying maturation of Xenopus laevis oocytes. *Dev Biol* 58:295-312.

12. Doree M, Peaucellier G, Picard A (1983) Activity of the maturation-promoting factor and the extent of protein phosphorylation oscillate simultaneously during meiotic maturation of starfish oocytes. *Dev Biol* 99:489-501.

13. Wagenaar EB (1983) The timing of synthesis of proteins required for mitosis in the cell cycle of the sea urchin embryo. *Exp Cell Res* 144:393-403.

14. Gerhart J, Wu M, Kirschner M (1984) Cell cycle dynamics of an M-phase-specific cytoplasmic factor in Xenopus laevis oocytes and eggs. *J Cell Biol* 98:1247-1255.

15. Picard A, Peaucellier G, le Bouffant F, Le Peuch C, Doree M (1985) Role of protein synthesis and proteases in production and inactivation of maturation-promoting activity during meiotic maturation of starfish oocytes. *Dev Biol* 109:311-320.

16. Evans T, Rosenthal ET, Youngblom J, Distel D, Hunt T (1983) Cyclin: a protein specified by maternal mRNA in sea urchin eggs that is destroyed at each cleavage division. *Cell* 33:389-396.

17. Doree M, Hunt T (2002) From Cdc2 to Cdk1: when did the cell cycle kinase join its cyclin partner? *J Cell Sci* 115:2461-2464.

18. Labbe JC, Picard A, Peaucellier G, Cavadore JC, Nurse P*, et al.* (1989) Purification of MPF from starfish: identification as the H1 histone kinase p34cdc2 and a possible mechanism for its periodic activation. *Cell* 57:253-263.

19. Schmidt EV (2004) Coordination of cell growth and cell division. *Cell growth: control of cell size*, eds Hall MN, Raff MC, & Thomas G (Cold Spring Harbor Laboratory Press, New York), pp 101-137.

20. Jorgensen P, Tyers M (2004) How cells coordinate growth and division. *Curr Biol* 14:R1014-1027.

21. Epstein CJ (1967) Cell size, nuclear content, and the development of polyploidy in the mammalian liver. *Proc Natl Acad Sci USA* 57:327-334.

22. Gregory TR (2001) Coincidence, coevolution, or causation? DNA content, cell size, and the C-value enigma. *Biol Rev Camb Philos Soc* 76:65-101.

23. Pardee AB (1974) A restriction point for control of normal animal cell proliferation. *Proc Natl Acad Sci USA* 71:1286-1290.

24. de Bruin RA, Kalashnikova TI, Chahwan C, McDonald WH, Wohlschlegel J*, et al.* (2006) Constraining G1-specific transcription to late G1 phase: the MBF-associated corepressor Nrm1 acts via negative feedback. *Mol Cell* 23:483-496.

25. Polymenis M, Schmidt EV (1997) Coupling of cell division to cell growth by translational control of the G1 cyclin CLN3 in yeast. *Genes Dev* 11:2522-2531.

26. Verges E, Colomina N, Gari E, Gallego C, Aldea M (2007) Cyclin Cln3 is retained at the ER and released by the J chaperone Ydj1 in late G1 to trigger cell cycle entry. *Mol Cell* 26:649-662.

27. Porro D, Martegani E, Ranzi BM, Alberghina L (1988) Oscillations in continuous cultures of budding yeast: a segregated parameter analysis. *Biotechnol Bioeng* 32:411-417.

28. Richard P (2003) The rhythm of yeast. *FEMS Microbiol Rev* 27:547-557.

29. Klevecz RR, Bolen J, Forrest G, Murray DB (2004) A genomewide oscillation in transcription gates DNA replication and cell cycle. *Proc Natl Acad Sci USA* 101:1200-1205.

30. Lloyd D, Murray DB (2005) Ultradian metronome: timekeeper for orchestration of cellular coherence. *Trends Biochem Sci* 30:373-377.

31. Tu BP, Kudlicki A, Rowicka M, McKnight SL (2005) Logic of the yeast metabolic cycle: temporal compartmentalization of cellular processes. *Science* 310:1152-1158.

32. Chen Z, Odstrcil EA, Tu BP, McKnight SL (2007) Restriction of DNA replication to the reductive phase of the metabolic cycle protects genome integrity. *Science* 316:1916-1919.

33. Tu BP, Mohler RE, Liu JC, Dombek KM, Young ET*, et al.* (2007) Cyclic changes in metabolic state during the life of a yeast cell. *Proc Natl Acad Sci USA* 104:16886-16891.

34. Huxtable R (2000) Expanding the Circle 1975-1999; Sulfur Biochemistry and Insights on the biological functions of tauring. *Taurine 4: taurine and excitable tissues,* Advances in experimental medicine and biology, eds Della Corte L, Huxtable R, Sgaragli G, & Tipton K (Kluwer Academic/Plenum Publishers, New York), pp 1-6.

35. Brosnan JT, Brosnan ME (2006) The sulfur-containing amino acids: an overview. *J Nutr* 136:1636S-1640S.

36. Unger MW, Hartwell LH (1976) Control of cell division in *Saccharomyces cerevisiae* by methionyl-tRNA. *Proc Natl Acad Sci USA* 73:1664-1668.

37. Gavin AC, Aloy P, Grandi P, Krause R, Boesche M*, et al.* (2006) Proteome survey reveals modularity of the yeast cell machinery. *Nature* 440:631-636.

38. Ho Y, Gruhler A, Heilbut A, Bader GD, Moore L*, et al.* (2002) Systematic identification of protein complexes in *Saccharomyces cerevisiae* by mass spectrometry. *Nature* 415:180-183.

39. Chen XJ, Butow RA (2005) The organization and inheritance of the mitochondrial genome. *Nat Rev Genet* 6:815-825.

40. Zelenaya-Troitskaya O, Newman SM, Okamoto K, Perlman PS, Butow RA (1998) Functions of the high mobility group protein, Abf2p, in mitochondrial DNA segregation, recombination and copy number in *Saccharomyces cerevisiae*. *Genetics* 148:1763-1776.

41. Sia RA, Carrol S, Kalifa L, Hochmuth C, Sia EA (2009) Loss of the mitochondrial nucleoid protein, abf2p, destabilizes repetitive DNA in the yeast mitochondrial genome. *Genetics* 181:331-334.

42. Kang D, Kim SH, Hamasaki N (2007) Mitochondrial transcription factor A (TFAM): roles in maintenance of mtDNA and cellular functions. *Mitochondrion* 7:39-44.

43. Parisi MA, Xu B, Clayton DA (1993) A human mitochondrial transcriptional activator can functionally replace a yeast mitochondrial HMG-box protein both *in vivo* and *in vitro*. *Mol Cell Biol* 13:1951-1961.

44. Kucej M, Kucejova B, Subramanian R, Chen XJ, Butow RA (2008) Mitochondrial nucleoids undergo remodeling in response to metabolic cues. *J Cell Sci* 121:1861-1868.

45. Ferea TL, Botstein D, Brown PO, Rosenzweig RF (1999) Systematic changes in gene expression patterns following adaptive evolution in yeast. *Proc Natl Acad Sci USA* 96:9721-9726.

46. Blank HM, Li C, Mueller JE, Bogomolnaya LM, Bryk M*, et al.* (2008) An increase in mitochondrial DNA promotes nuclear DNA replication in yeast. *PLoS Genet* 4:e1000047.

47. Pringle JR, Hartwell L (1981) The *Saccharomyces cerevisiae* cell cycle. *The molecular biology of the yeast saccharomyces, life cycle and inheritance,* Cold Spring Harbor monograph series, eds Strathern JN, Jones EW, & Broach JR (Cold Spring Harbor Laboratory, Cold Spring Harbor, NY), pp 97-142.

48. MacAlpine DM, Perlman PS, Butow RA (1998) The high mobility group protein Abf2p influences the level of yeast mitochondrial DNA recombination intermediates *in vivo*. *Proc Natl Acad Sci USA* 95:6739-6743.

49. Okamoto K, Shaw JM (2005) Mitochondrial morphology and dynamics in yeast and multicellular eukaryotes. *Annu Rev Genet* 39:503-536.

50. Bonawitz ND, Clayton DA, Shadel GS (2006) Initiation and beyond: multiple functions of the human mitochondrial transcription machinery. *Mol Cell* 24:813-825.

51. Diffley JF, Stillman B (1991) A close relative of the nuclear, chromosomal high-mobility group protein HMG1 in yeast mitochondria. *Proc Natl Acad Sci USA* 88:7864-7868.

52. Friddle RW, Klare JE, Martin SS, Corzett M, Balhorn R*, et al.* (2004) Mechanism of DNA compaction by yeast mitochondrial protein Abf2p. *Biophys J* 86:1632-1639.

53. Stigter D (2004) Packaging of single DNA molecules by the yeast mitochondrial protein Abf2p: reinterpretation of recent single molecule experiments. *Biophys Chem* 110:171-178.

54. Blander G, Guarente L (2004) The Sir2 family of protein deacetylases. *Annu Rev Biochem* 73:417-435.

55. Dutnall RN, Pillus L (2001) Deciphering NAD-dependent deacetylases. *Cell* 105:161-164.

56. Rusche LN, Kirchmaier AL, Rine J (2003) The establishment, inheritance, and function of silenced chromatin in *Saccharomyces cerevisiae*. *Annu Rev Biochem* 72:481-516.

57. Bryk M, Banerjee M, Murphy M, Knudsen KE, Garfinkel DJ*, et al.* (1997) Transcriptional silencing of Ty1 elements in the RDN1 locus of yeast. *Genes Dev* 11:255-269.

58. Li C, Mueller JE, Bryk M (2006) Sir2 represses endogenous polymerase II transcription units in the ribosomal DNA nontranscribed spacer. *Mol Biol Cell* 17:3848-3859.

59. Smith JS, Boeke JD (1997) An unusual form of transcriptional silencing in yeast ribosomal DNA. *Genes Dev* 11:241-254.

60. Pasero P, Bensimon A, Schwob E (2002) Single-molecule analysis reveals clustering and epigenetic regulation of replication origins at the yeast rDNA locus. *Genes Dev* 16:2479-2484.

61. Pappas DL, Jr., Frisch R, Weinreich M (2004) The NAD(+)-dependent Sir2p histone deacetylase is a negative regulator of chromosomal DNA replication. *Genes Dev* 18:769-781.

62. Weinreich M, Palacios DeBeer MA, Fox CA (2004) The activities of eukaryotic replication origins in chromatin. *Biochim Biophys Acta* 1677:142-157.

63. Vogelauer M, Rubbi L, Lucas I, Brewer BJ, Grunstein M (2002) Histone acetylation regulates the time of replication origin firing. *Mol Cell* 10:1223-1233.

64. Baganz F, Hayes A, Farquhar R, Butler PR, Gardner DC*, et al.* (1998) Quantitative analysis of yeast gene function using competition experiments in continuous culture. *Yeast* 14:1417-1427.

65. O'Rourke TW, Doudican NA, Mackereth MD, Doetsch PW, Shadel GS (2002) Mitochondrial dysfunction due to oxidative mitochondrial DNA damage is reduced through cooperative actions of diverse proteins. *Mol Cell Biol* 22:4086-4093.

66. Chelstowska A, Butow RA (1995) RTG genes in yeast that function in communication between mitochondria and the nucleus are also required for expression of genes encoding peroxisomal proteins. *J Biol Chem* 270:18141-18146.

67. Epstein CB, Waddle JA, Hale Wt, Dave V, Thornton J*, et al.* (2001) Genome-wide responses to mitochondrial dysfunction. *Mol Biol Cell* 12:297-308.

68. Spencer F, Gerring SL, Connelly C, Hieter P (1990) Mitotic chromosome transmission fidelity mutants in *Saccharomyces cerevisiae*. *Genetics* 124:237-249.

69. Kaiser C, Michaelis S, Mitchell A (1994) *Methods in Yeast Genetics* (Cold Spring Harbor Laboratory Press, Cold Spring Harbor, NY).

70. Nash P, Tang X, Orlicky S, Chen Q, Gertler FB*, et al.* (2001) Multisite phosphorylation of a CDK inhibitor sets a threshold for the onset of DNA replication. *Nature* 414:514-521.

71. Murray DB, Beckmann M, Kitano H (2007) Regulation of yeast oscillatory dynamics. *Proc Natl Acad Sci USA* 104:2241-2246.

72. Anderson RM, Latorre-Esteves M, Neves AR, Lavu S, Medvedik O*, et al.* (2003) Yeast life-span extension by calorie restriction is independent of NAD fluctuation. *Science* 302:2124-2126.

73. Huang J, Moazed D (2003) Association of the RENT complex with nontranscribed and coding regions of rDNA and a regional requirement for the replication fork block protein Fob1 in rDNA silencing. *Genes Dev* 17:2162-2176.

74. Aggarwal BD, Calvi BR (2004) Chromatin regulates origin activity in Drosophila follicle cells. *Nature* 430:372-376.

75. Poloumienko A, Dershowitz A, De J, Newlon CS (2001) Completion of replication map of *Saccharomyces cerevisiae* chromosome III. *Mol Biol Cell* 12:3317-3327.

76. Longtine MS, McKenzie A, 3rd, Demarini DJ, Shah NG, Wach A*, et al.* (1998) Additional modules for versatile and economical PCR-based gene deletion and modification in *Saccharomyces cerevisiae*. *Yeast* 14:953-961.

77. Brachmann CB, Davies A, Cost GJ, Caputo E, Li J*, et al.* (1998) Designer deletion strains derived from *Saccharomyces cerevisiae* S288C: a useful set of strains and plasmids for PCR-mediated gene disruption and other applications. *Yeast* 14:115-132.

78. Ghaemmaghami S, Huh WK, Bower K, Howson RW, Belle A*, et al.* (2003) Global analysis of protein expression in yeast. *Nature* 425:737-741.

79. Bogomolnaya LM, Pathak R, Guo J, Cham R, Aramayo R*, et al.* (2004) Hym1p affects cell cycle progression in *Saccharomyces cerevisiae*. *Curr Genet* 46:183-192.

80. Guo J, Bryan BA, Polymenis M (2004) Nutrient-specific effects in the coordination of cell growth with cell division in continuous cultures of *Saccharomyces cerevisiae*. *Arch Microbiol* 182:326-330.

81. Pathak R, Bogomolnaya LM, Guo J, Polymenis M (2004) Gid8p (Dcr1p) and Dcr2p function in a common pathway to promote START completion in *Saccharomyces cerevisiae*. *Eukaryot Cell* 3:1627-1638.

82. Cross FR, Archambault V, Miller M, Klovstad M (2002) Testing a mathematical model of the yeast cell cycle. *Mol Biol Cell* 13:52-70.

83. Bryk M, Briggs SD, Strahl BD, Curcio MJ, Allis CD*, et al.* (2002) Evidence that Set1, a factor required for methylation of histone H3, regulates rDNA silencing in *S. cerevisiae* by a Sir2-independent mechanism. *Curr Biol* 12:165-170.

84. Castrillo JI, Zeef LA, Hoyle DC, Zhang N, Hayes A*, et al.* (2007) Growth control of the eukaryote cell: a systems biology study in yeast. *J Biol* 6:4.1-4.25.

85. Banerjee R, Evande R, Kabil O, Ojha S, Taoka S (2003) Reaction mechanism and regulation of cystathionine beta-synthase. *Biochim Biophys Acta* 1647:30-35.

86. Thomas D, Surdin-Kerjan Y (1997) Metabolism of sulfur amino acids in *Saccharomyces cerevisiae*. *Microbiol Mol Biol Rev* 61:503-532.

87. Giaever G, Chu AM, Ni L, Connelly C, Riles L*, et al.* (2002) Functional profiling of the *Saccharomyces cerevisiae* genome. *Nature* 418:387-391.

88. Kim HS, Fay JC (2007) Genetic variation in the cysteine biosynthesis pathway causes sensitivity to pharmacological compounds. *Proc Natl Acad Sci USA* 104:19387-19391.

89. Fowler B (2005) Homocysteine: overview of biochemistry, molecular biology, and role in disease processes. *Semin Vasc Med* 5:77-86.

90. Kraus JP, Janosik M, Kozich V, Mandell R, Shih V*, et al.* (1999) Cystathionine beta-synthase mutations in homocystinuria. *Hum Mutat* 13:362-375.

91. Shan X, Kruger WD (1998) Correction of disease-causing CBS mutations in yeast. *Nat Genet* 19:91-93.

92. Maclean KN, Janosik M, Kraus E, Kozich V, Allen RH*, et al.* (2002) Cystathionine beta-synthase is coordinately regulated with proliferation through a redox-sensitive mechanism in cultured human cells and *Saccharomyces cerevisiae*. *J Cell Physiol* 192:81-92.

93. Porro D, Martegani E, Ranzi BM, Alberghina L (1988) Oscillations in continuous cultures of yeast: a segragated parameter analysis. *Biotechnol Bioengin* 32:411-417.

94. Lafaye A, Junot C, Pereira Y, Lagniel G, Tabet JC*, et al.* (2005) Combined proteome and metabolite-profiling analyses reveal surprising insights into yeast sulfur metabolism. *J Biol Chem* 280:24723-24730.

95. Fauchon M, Lagniel G, Aude JC, Lombardia L, Soularue P*, et al.* (2002) Sulfur sparing in the yeast proteome in response to sulfur demand. *Mol Cell* 9:713-723.

96. Gauthier BR, Wiederkehr A, Baquie M, Dai C, Powers AC*, et al.* (2009) PDX1 deficiency causes mitochondrial dysfunction and defective insulin secretion through TFAM suppression. *Cell Metab* 10:110-118.

97. Hayashi Y, Yoshida M, Yamato M, Ide T, Wu Z*, et al.* (2008) Reverse of age-dependent memory impairment and mitochondrial DNA damage in microglia by

an overexpression of human mitochondrial transcription factor a in mice. *J Neurosci* 28:8624-8634.

98. Spellman PT, Sherlock G, Zhang MQ, Iyer VR, Anders K*, et al.* (1998) Comprehensive identification of cell cycle-regulated genes of the yeast *Saccharomyces cerevisiae* by microarray hybridization. *Mol Biol Cell* 9:3273-3297.

99. Bitterman KJ, Anderson RM, Cohen HY, Latorre-Esteves M, Sinclair DA (2002) Inhibition of silencing and accelerated aging by nicotinamide, a putative negative regulator of yeast sir2 and human SIRT1. *J Biol Chem* 277:45099-45107.

100. Landry J, Slama JT, Sternglanz R (2000) Role of NAD(+) in the deacetylase activity of the SIR2-like proteins. *Biochem Biophys Res Commun* 278:685-690.

101. Kabil O, Zhou Y, Banerjee R (2006) Human cystathionine beta-synthase is a target for sumoylation. *Biochemistry* 45:13528-13536.

102. Jhee KH, McPhie P, Miles EW (2000) Domain architecture of the heme-independent yeast cystathionine beta-synthase provides insights into mechanisms of catalysis and regulation. *Biochemistry* 39:10548-10556.

103. Kruger WD, Cox DR (1994) A yeast system for expression of human cystathionine beta-synthase: structural and functional conservation of the human and yeast genes. *Proc Natl Acad Sci USA* 91:6614-6618.

104. Belew MS, Quazi FI, Willmore WG, Aitken SM (2009) Kinetic characterization of recombinant human cystathionine beta-synthase purified from *E. coli*. *Protein Expr Purif* 64:139-145.

105. Vido K, Spector D, Lagniel G, Lopez S, Toledano MB*, et al.* (2001) A proteome analysis of the cadmium response in *Saccharomyces cerevisiae*. *J Biol Chem* 276:8469-8474.

106. Dang AQ, Cook DE (1977) The transsulfuration pathway in *Tetrahymena pyriformis*. *Biochim Biophys Acta* 496:264-271.

107. Caspi R, Foerster H, Fulcher CA, Kaipa P, Krummenacker M*, et al.* (2008) The MetaCyc Database of metabolic pathways and enzymes and the BioCyc collection of Pathway/Genome Databases. *Nucleic Acids Res* 36:D623-631.

108. Shimizu S, Yamada H (1989) Adnosylmethionine, adenosylhomocysteine and related nucleotides. *Biotechnology of pigments, vitamins, and growth factors,* Elseiver applied biotechnology series, ed Vandamme E (Elsevier Science Publishing Co., Inc., New York, NY), pp 351-372.

109. Loenen WA (2006) S-adenosylmethionine: jack of all trades and master of everything? *Biochem Soc Trans* 34:330-333.

110. Refsum H, Smith AD, Ueland PM, Nexo E, Clarke R*, et al.* (2004) Facts and recommendations about total homocysteine determinations: an expert opinion. *Clin Chem* 50:3-32.

111. Wang L, Chen X, Tang B, Hua X, Klein-Szanto A*, et al.* (2005) Expression of mutant human cystathionine beta-synthase rescues neonatal lethality but not homocystinuria in a mouse model. *Hum Mol Genet* 14:2201-2208.

112. Mendenhall MD, Hodge AE (1998) Regulation of Cdc28 cyclin-dependent protein kinase activity during the cell cycle of the yeast *Saccharomyces cerevisiae*. *Microbiol Mol Biol Rev* 62:1191-1243.

113. Simmons Kovacs LA, Nelson CL, Haase SB (2008) Intrinsic and cyclin-dependent kinase-dependent control of spindle pole body duplication in budding yeast. *Mol Biol Cell* 19:3243-3253.

114. Elledge SJ, Spottswood MR (1991) A new human p34 protein kinase, CDK2, identified by complementation of a cdc28 mutation in *Saccharomyces cerevisiae*, is a homolog of Xenopus Eg1. *EMBO J* 10:2653-2659.

115. Kaldis P, Sutton A, Solomon MJ (1996) The Cdk-activating kinase (CAK) from budding yeast. *Cell* 86:553-564.

116. Jeffery CJ (2009) Moonlighting proteins--an update. *Mol Biosyst* 5:345-350.

117. Jeffery CJ (1999) Moonlighting proteins. *Trends Biochem Sci* 24:8-11.

118. Rouault TA (2006) The role of iron regulatory proteins in mammalian iron homeostasis and disease. *Nat Chem Biol* 2:406-414.

119. Chen XJ, Wang X, Kaufman BA, Butow RA (2005) Aconitase couples metabolic regulation to mitochondrial DNA maintenance. *Science* 307:714-717.

120. Metayer S, Seiliez I, Collin A, Duchene S, Mercier Y*, et al.* (2008) Mechanisms through which sulfur amino acids control protein metabolism and oxidative status. *J Nutr Biochem* 19:207-215.

121. Noble M, Mayer-Proschel M, Proschel C (2005) Redox regulation of precursor cell function: insights and paradoxes. *Antioxid Redox Signal* 7:1456-1467.

122. Moreno-Sanchez R, Saavedra E, Rodriguez-Enriquez S, Olin-Sandoval V (2008) Metabolic control analysis: a tool for designing strategies to manipulate metabolic pathways. *J Biomed Biotechnol* 2008:597913.

APPENDIX A

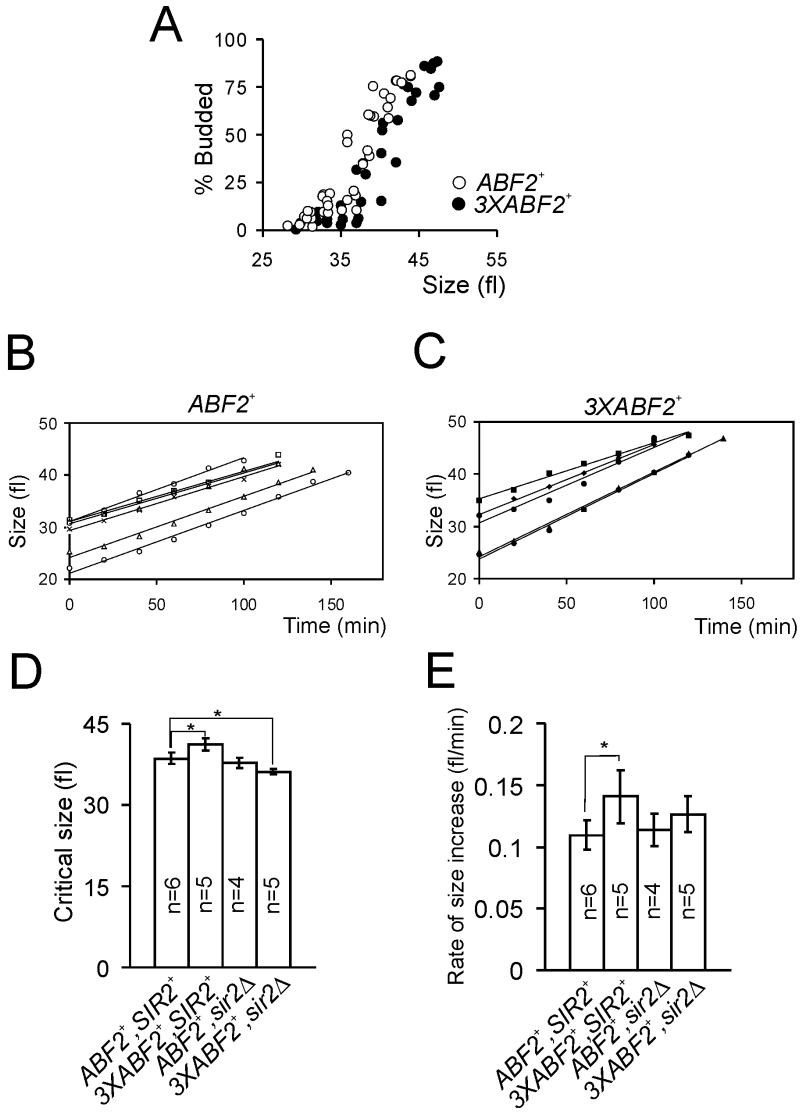

Fig. A-1. Summary of data from elutriation experiments with ρ^+ strains. *(A)* The raw data points showing the percent of budded cells as a function of cell size, from separate independent elutriation experiments with *ABF2*$^+$ and *3XABF2*$^+$ strains. The data points shown were from the linear portion of each experiment, when the percentage of budded cells began to increase, and they were used to determine the critical budding size as described in Materials and Methods. *(B,C)* The rate of cell size increase for each elutriation experiment of the indicated strains (*ABF2*$^+$ and *3XABF2*$^+$) is shown. From these graphs we calculated the rate of size increase as described in Materials and Methods. *(D)* The critical size for budding of the indicated strains is shown. Where marked with an asterisk (*), the difference is statistically significant, based on 2-tailed Student's *t* tests. *E*, The rate of cell size increase of the indicated strains is shown. Where marked with an asterisk (*), the difference is statistically significant, based on 2-tailed Student's *t* tests.

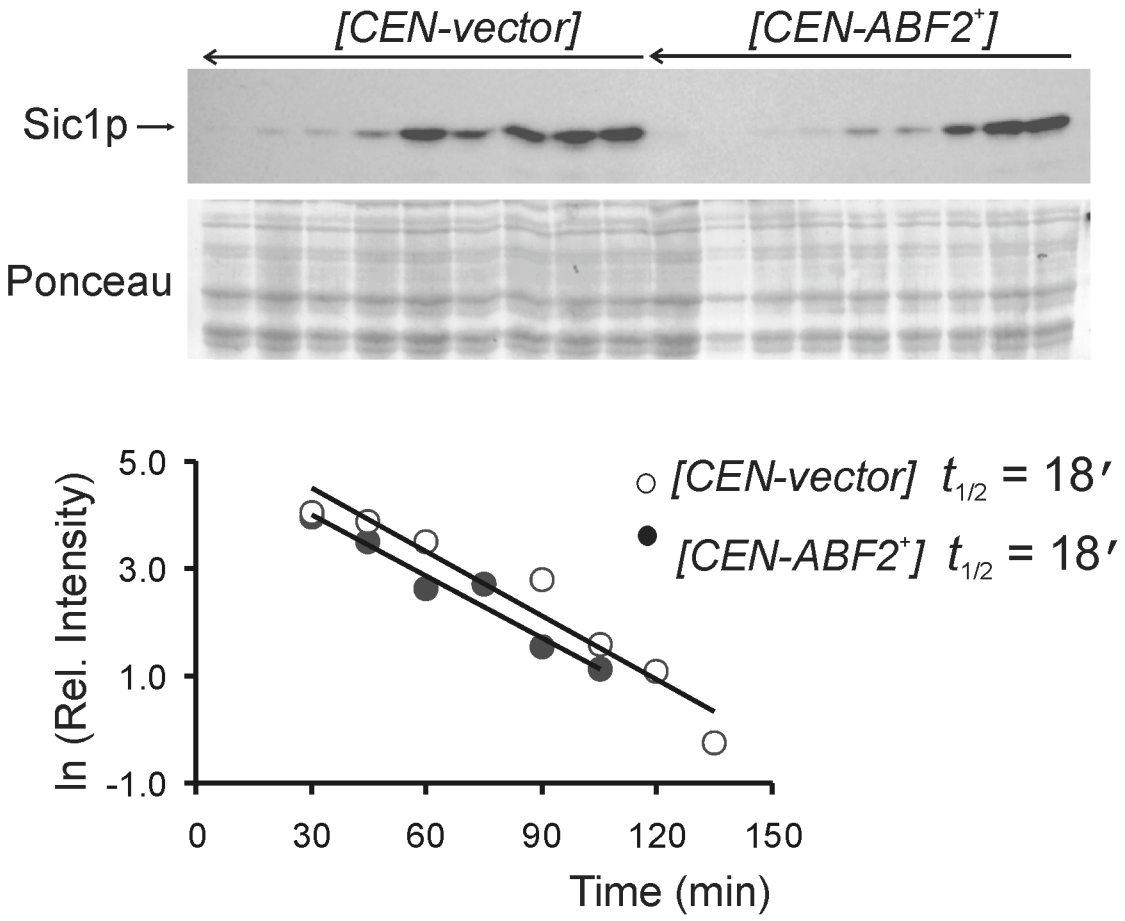

Fig. A-2. Sic1p stability and Abf2p. A separate experiment, similar to the one described in Fig. 2.5, is shown, except that loading was estimated from the Ponceau-stained blot.

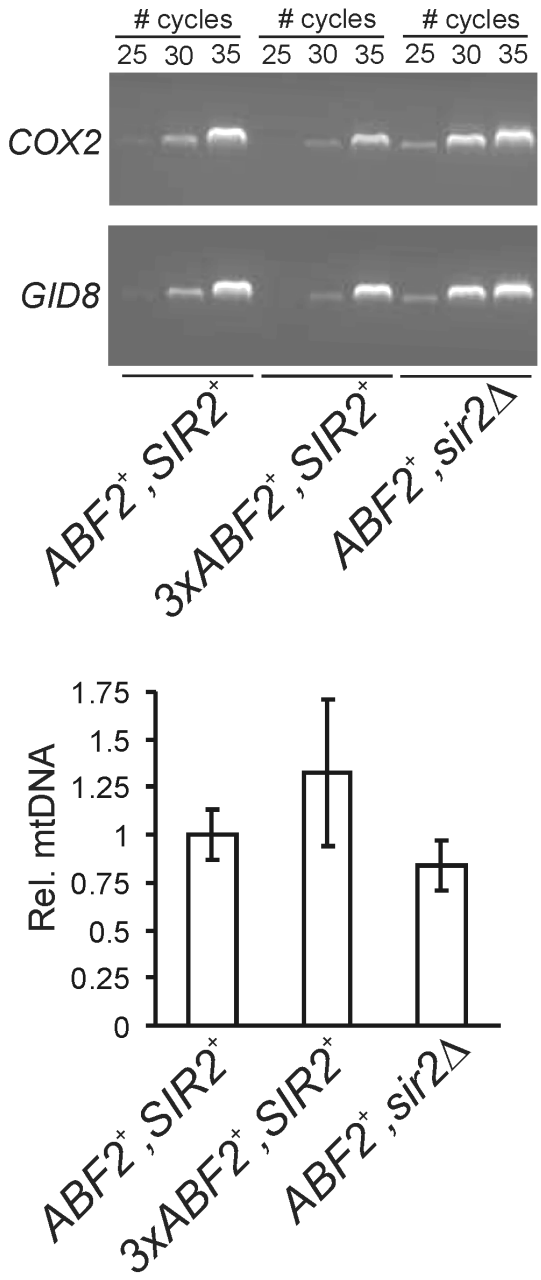

Fig. A-3. mtDNA abundance is not increased in cells lacking Sir2p. To estimate the mtDNA abundance of the indicated strains we used PCR (*Top*), as described in Materials and Methods. The ratio between the *COX2* and the *GID8* product was determined to normalize for differences in initial DNA concentration and reaction efficiencies. The ratio for each strain relative to *ABF2*$^{+}$ cells is shown (*Bottom*). Graph represents average data from two independent experiments (+/- range). As a control, we also performed this analysis on *3xABF2*$^{+}$ cells, which are known to have higher mtDNA levels.

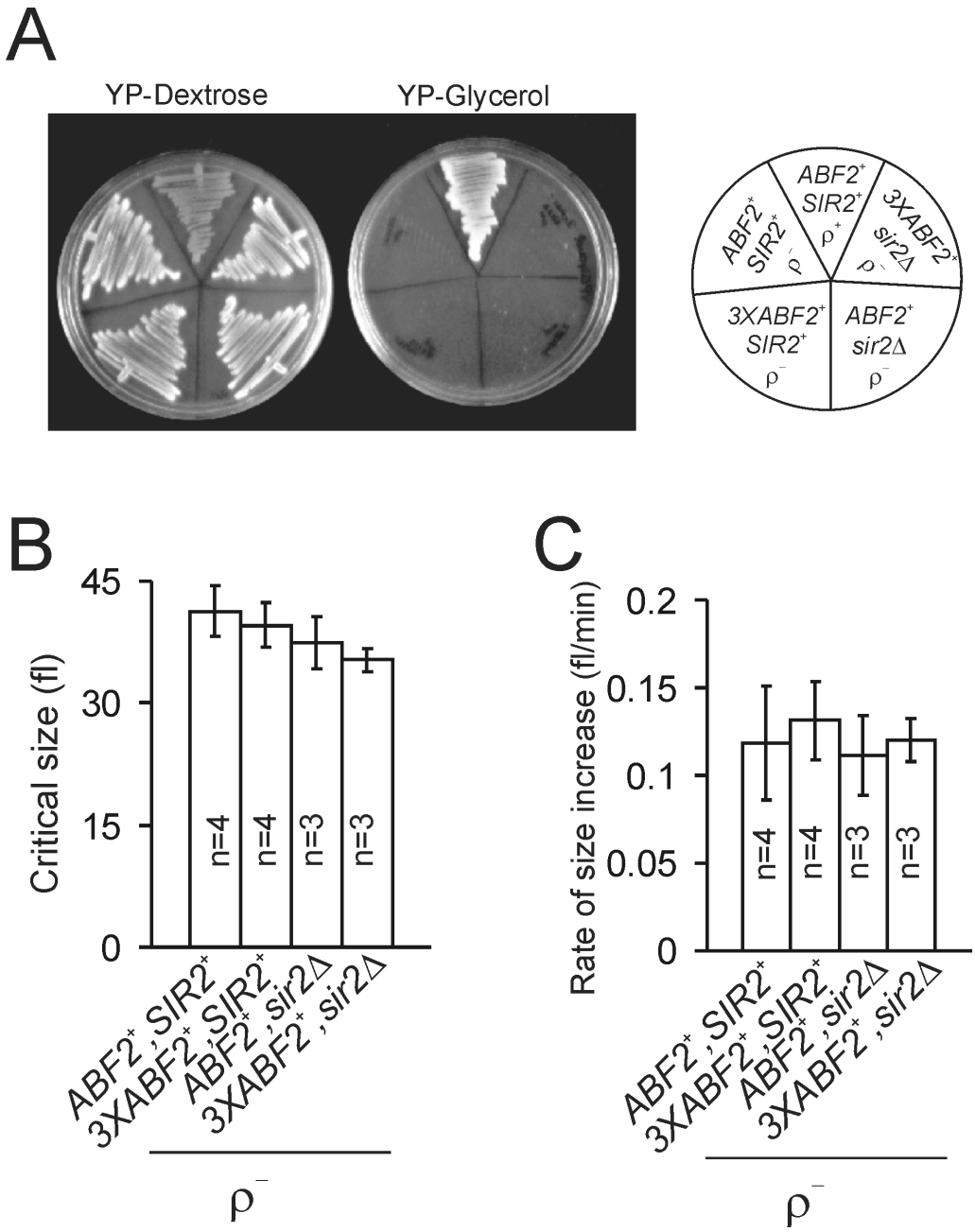

Fig. A-4. Cell cycle progression of ρ$^-$ strains. (*A*) The strains used were respiratory-incompetent and they could not proliferate on plates with glycerol as a carbon source. The critical size for budding (*B*), and the rate of cell size increase *(C)*, of the indicated strains was determined as in Fig. A-1.

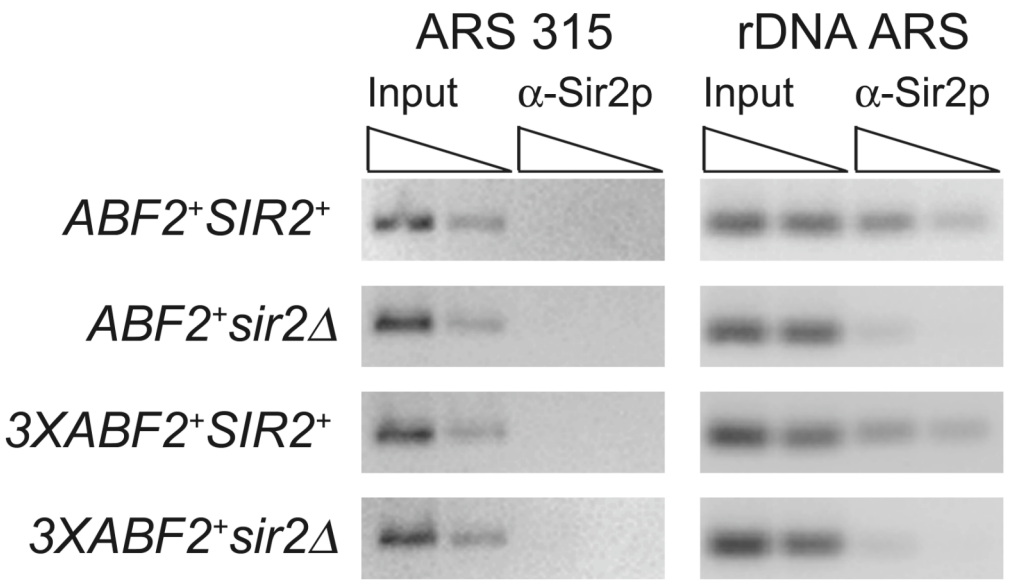

Fig. A-5. ChIP experiments from the indicated strains analyzed by PCR do not detect Sir2p bound to ARS315 (left panel). As a control, we also performed this analysis on rDNA ARS using primer pair 21 and detected Sir2p association with the rDNA ARS (right panel). PCR products from input and IP samples were subjected to agarose gel electrophoresis and analyzed by ethidium bromide staining. The open triangles represent serial dilution of template DNA in the PCR reaction. Other labels as in Fig. 2.9*B*.

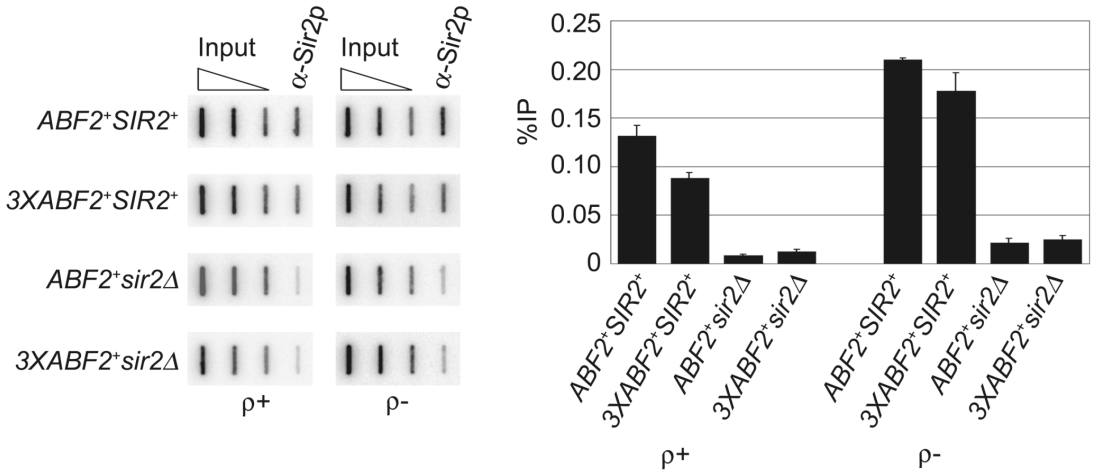

Fig. A-6. Sir2p ChIP to rDNA ARS in ρ^+ and ρ^- cells. ChIP experiments from the indicated strains analyzed by slot blot to detect Sir2p bound to rDNA ARS. Note that applying slot blot methodology to the rDNA ARS reproduced the reduced Sir2p levels bound to the rDNA ARS in *3xABF2*$^+$ cells that we observed with the real-time PCR analysis shown in Fig. 2.9*B*. Graph represents average data from two independent experiments (+/- range). Other labels as in Fig. 2.9.

APPENDIX B

Fig. B-1. *A*, The rate of cell size increase for each elutriation experiment of the indicated strains and metabolite treatments is shown. From these graphs we determined the rate of size increase reported in Fig. 3.3, calculated as described in (46). *B*, Graphs showing the percent of budded cells as a function of cell size, from separate independent elutriation experiments with the indicated strains and metabolite treatments. The data points shown were from the linear portion of each experiment, when the percentage of budded cells began to increase, and used to determine the critical size for division, as described in (46). The average (± SD) is shown in each case. The graphs shown in (*A*) and (*B*) for the *ABF2*$^{+}$ and *3xABF2*$^{+}$ strains (without added metabolites), incorporate not only new experiments, but also earlier ones we had described in (46).

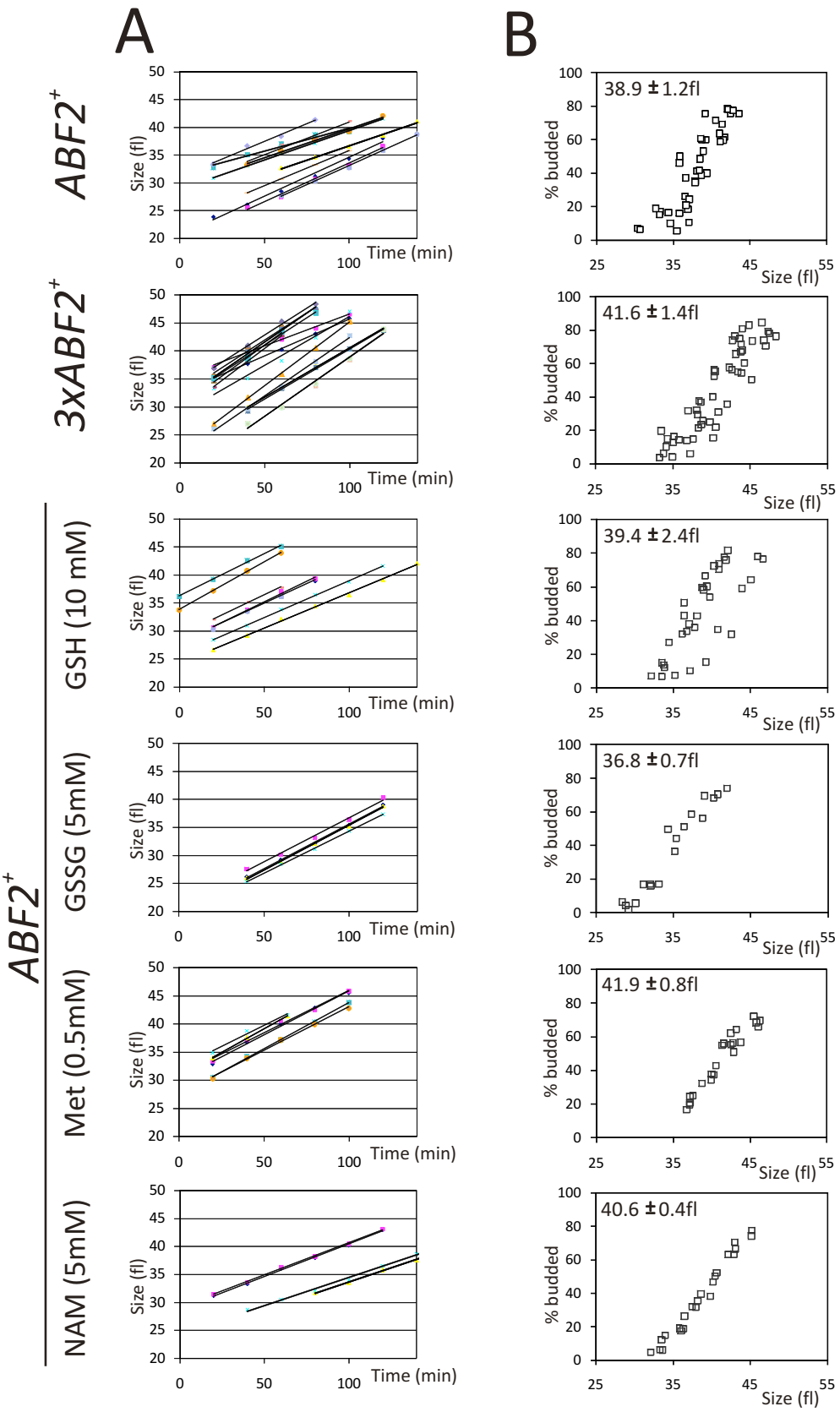
A
B
ABF2+
3xABF2+
ABF2+
GSH (10 mM)
GSSG (5mM)
Met (0.5mM)
NAM (5mM)
Size (fl)
Time (min)
% budded
Size (fl)
38.9 ±1.2fl
41.6 ±1.4fl
39.4 ±2.4fl
36.8 ±0.7fl
41.9 ±0.8fl
40.6 ±0.4fl

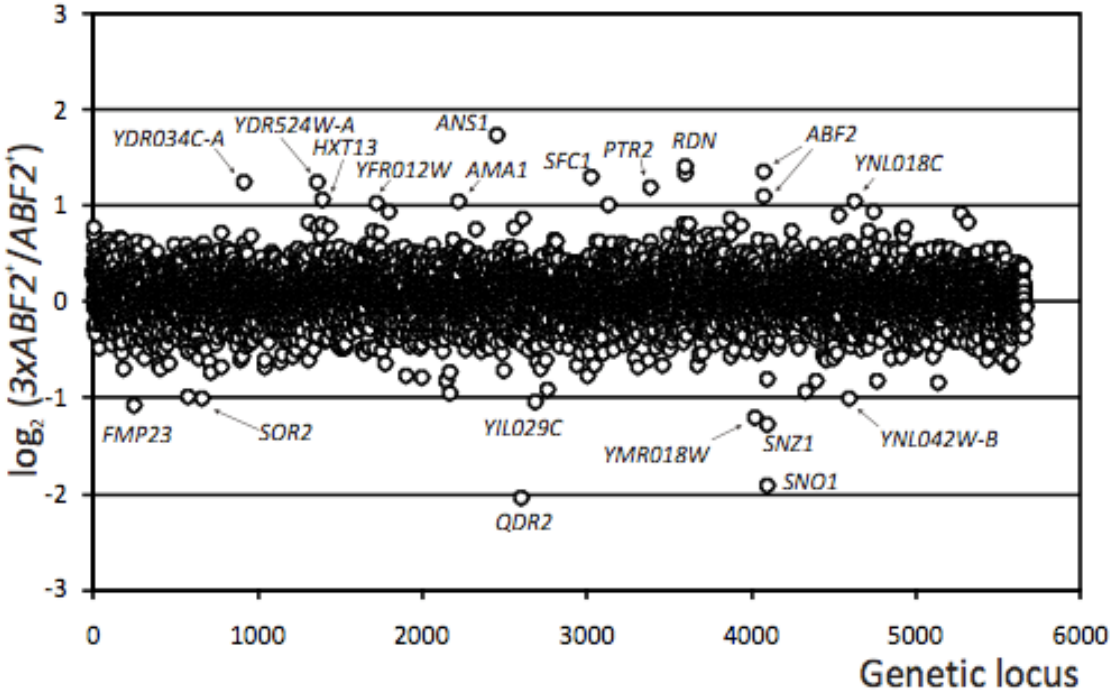

Fig. B-2. Microarray expression profile of cells with more mtDNA (*3xABF2*$^{+}$) vs. wild type (*ABF2*$^{+}$). The genes that showed ≥ 2-fold change in their steady-state mRNA levels between the two strains are indicated. In addition to *ABF2* and the *RDN* locus, which were up-regulated in *3xABF2*$^{+}$ cells as expected, there were some additional changes that were anticipated. For example, the increased transcription of *SNZ1* and *SNO1* in wild type (*ABF2*$^{+}$) cells was expected because expression of these genes is increased in strains auxotrophic for tryptophan and uracil, such as the wild-type (*ABF2*$^{+}$) strain. The *3xABF2*$^{+}$ strain is not auxotrophic for tryptophan and uracil. Furthermore, up-regulation of *SFC1* is consistent with up-regulation of mitochondrial processes in *3xABF2*$^{+}$ cells, because *SFC1* encodes a mitochondrial transporter, which transports succinate into and fumarate out of the mitochondrion.

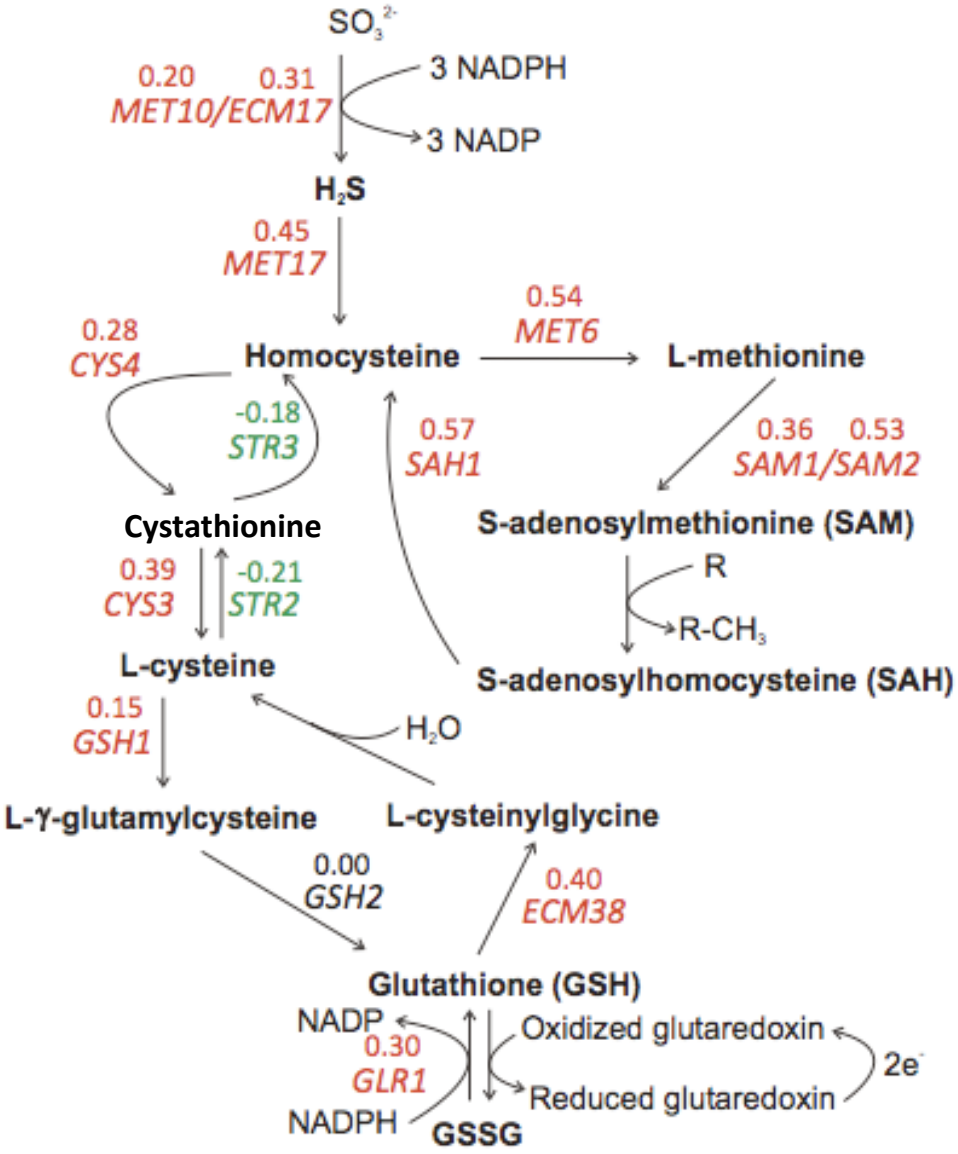

Fig. B-3. Sulfur metabolic pathways and expression profile in cells with more mtDNA (*3xABF2*$^+$) vs. wild type (*ABF2*$^+$). The genes encoding enzymes with increased expression are shown in red, while those with reduced expression are shown in green, while for one gene (*GSH2*), there was no change. The numbers above each gene indicate the corresponding $\log_2$(*3xABF2*$^+$/*ABF2*$^+$) values.

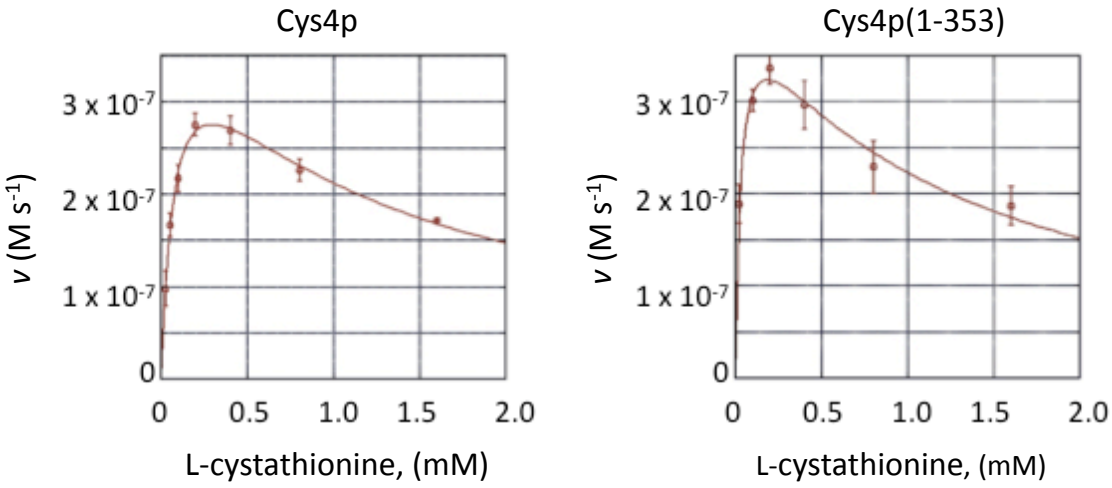

	Cys4p	Cys4p(1-353)
k_{cat} (s^{-1})	1.10±0.06	1.14±0.08
K_M (mM)	0.080±0.009	0.032±0.007
k_{cat}/K_M (M^{-1} s^{-1})	14,000±2,000	36,000±8,000

Fig. B-4. Kinetic parameters of recombinant Cys4p and Cys4p(1-353). Rate-dependence of the yeast full-length Cys4p and Cys4p(1-353) enzymes on the concentration of cystathionine is shown. Cystathionine-β-synthase activity was measured using a spectrophotometric assay (104), where the reverse-physiological hydrolysis of L-cystathionine to L-Ser and L-homocysteine was detected as absorbance changes at 412 nm, through the reaction of 5,5′-dithiobis-(2-nitrobenzoic acid) (DTNB) with the free thiol of the L-homocysteine product. The enzymes displayed strong substrate inhibition above 0.4 mM, and this was accounted for when we plotted the data using the non-linear regression function of KaleidaGraph™ (Synergy Software) to obtain the average (± SEM) kinetic parameters shown, from at least four independent experiments in each case. (Experiment in Fig. B-4 performed by Andrey Belyanin.)

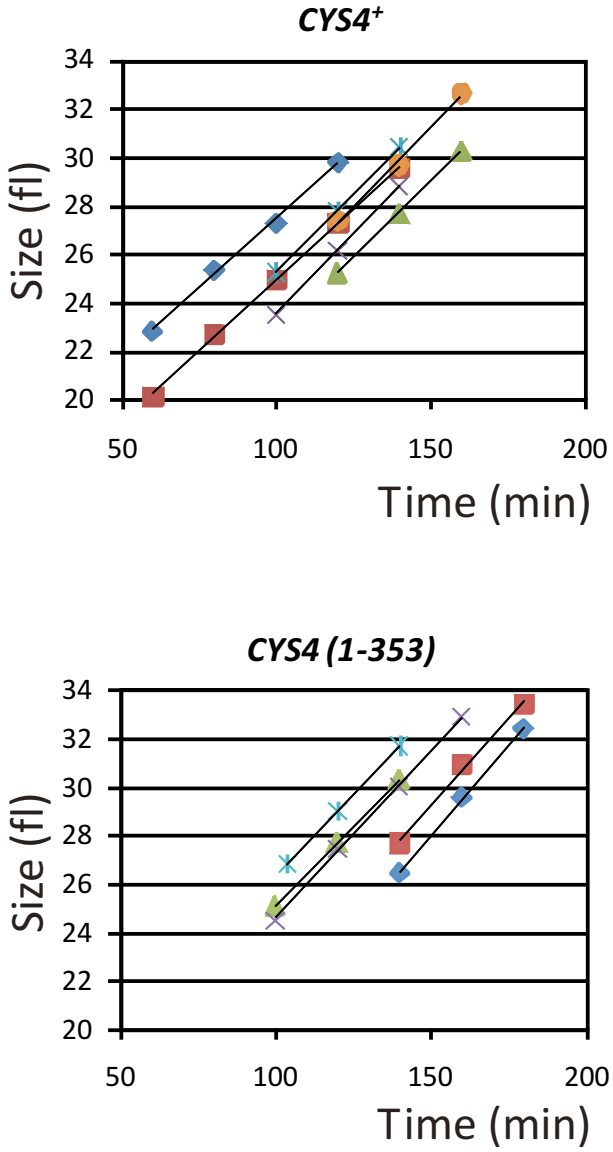

Fig. B-5. The rate of cell size increase for each elutriation experiment of the *CYS4*$^{+}$ and *CYS4(1-353)* strains is shown. From these graphs we determined the rates reported in Fig. 3.4, calculated as described in (46).

APPENDIX C

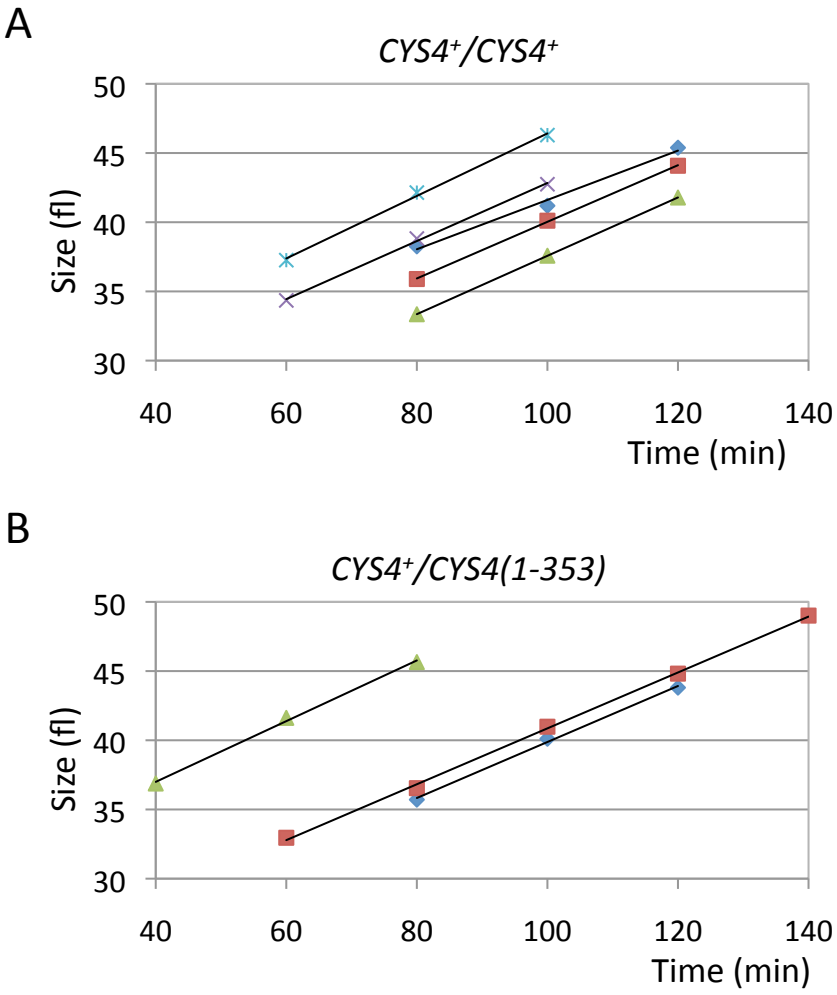

Fig. C-1. The rate of cell size increase for each elutriation experiment of the indicated strains is shown. From these graphs we determined the rate of size increase reported in Fig. 4.1*C*, calculated as described in (46).

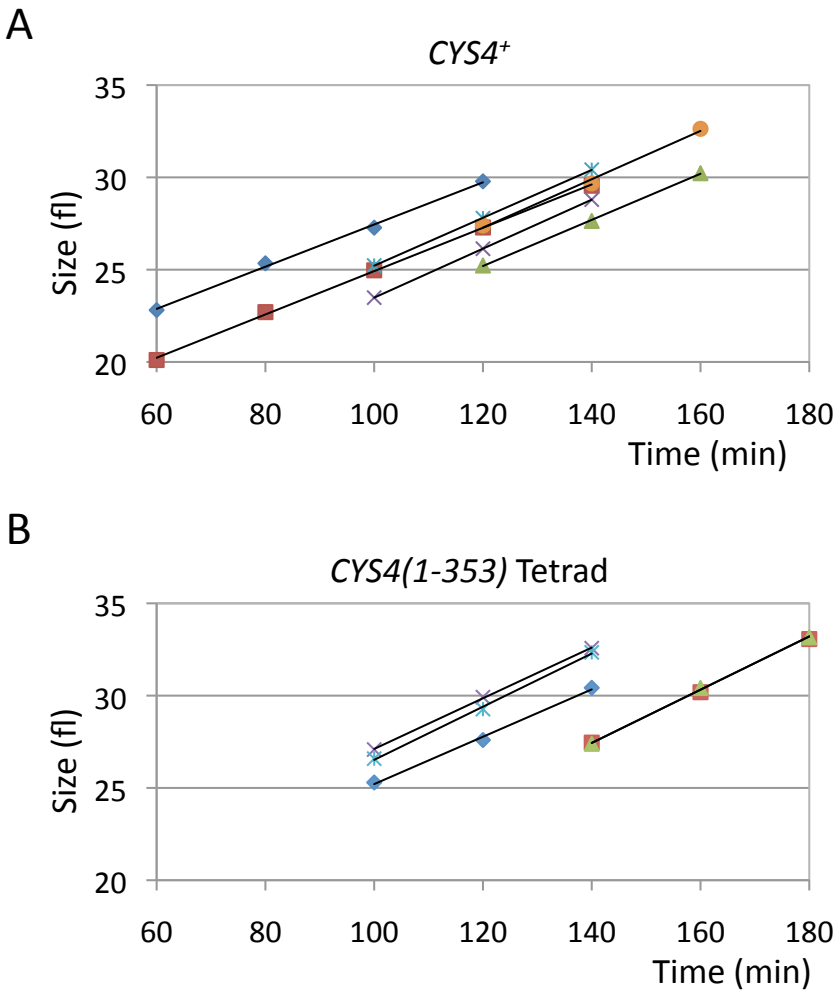

Fig. C-2. The rate of cell size increase for each elutriation experiment of the indicated strains is shown. From these graphs we determined the rate of size increase reported in Fig. 4.1*C*, calculated as described in (46).

VITA

Name: Heidi Marie Blank

Address: Department of Biochemistry & Biophysics
103 Biochemistry/Biophysics Building
Texas A&M University
2128 TAMU
College Station, TX 77843-2128

Email Address: h_finke@yahoo.com

Education: B.S., Environmental Engineering,
Southern Methodist University, 2001

Ph.D., Biochemistry,
Texas A&M University, 2009